**İSTANBUL TECHNICAL UNIVERSITY ★ INSTITUTE OF SCIENCE AND TECHNOLOGY**

# NUMERICAL MODELLING OF COMPLEX CHANNEL SYSTEMS



**MSc Thesis by**
**Civil Engineer Davut KOCA**

**(501001460)**

**Date of submission:** **2 January 2002**

**Date of defence examination:** **17 January 2002**

**Supervisor (Chairman):** **Prof. Dr. Sedat KABDAŞLI**

**Members of the Examining Committee:** **Prof. Dr. Necati AĞIRALİOĞLU (İTÜ.)**

**Prof. Dr. Yalçın YÜKSEL (YTÜ.)**

**JANUARY 2002**

İSTANBUL TEKNİK ÜNİVERSİTESİ ★ FEN BİLİMLERİ ENSTİTÜSÜ

# KOMPLEKS KANAL SİSTEMLERİNİN NÜMERİK MODELLENMESİ



YÜKSEK LİSANS TEZİ

İnşaat Müh. Davut KOCA
(501001460)

Tezin Enstitüye Verildiği Tarih : 2 Ocak 2002
Tezin Savunulduğu Tarih : 17 Ocak 2002

Tez Danışmanı : Prof.Dr. Sedat KABDAŞLI
Diğer Jüri Üyeleri : Prof.Dr. Necati AĞIRALİOĞLU (İTÜ.)
Prof.Dr. Yalçın YÜKSEL (YTÜ.)

OCAK 2002

**PREFACE**

In this study the theories and the finite element numerical solution methods of surface flow and transport phenomena of complex systems are explained with the numerical flow and transport models of Köyceğiz Dalyan Lagoon System.

The numerical models of Köyceğiz Lake and Dalyan Channel are generated with Aquasea and Aquadyn commercial software packages, which solve the flow and transport equations with Galerkin finite element method on triangular mesh.

The theoretical equations of flow and transport equations with parameters and boundary conditions are given in the 2$^{nd}$ section.

Before the numerical model applications of Köyceğiz Lake and Dalyan Channel, general principles of mesh generation are explained clearly with the appropriate terminology.

The finite element numerical method is explained in the 3$^{rd}$ section. General information about mesh generation and the numerical codes that were used in this study are also explained in this section.

Information about the study area, Köyceğiz-Dalyan Lagoon System, and the numerical models set up are given in the 4$^{th}$ section.

The numerical models results are discussed and compared with the previous field measurements data in the 5$^{th}$ section.

I would like to thank my supervisor Prof. Dr. Sedat Kabdaşlı, and Research Assistant MSc. Dilek Eren Mercan for advises and supports on this study.

I would also like to thank my family for their continuous supports during this study.

January 2001 Davut KOCA

**INDEX**

## ABBREVIATIONS

| | |
|---|---|
| **CFD** | : Computational Fluid Dynamics |
| **FEM** | : Finite Element Method |
| **FDM** | : Finite Difference Method |
| **FVM** | : Finite Volume Method |
| **CN** | : Courant Number |
| **Pe** | : Peclet Number |
| **DSI** | : Devlet Su İşleri (State Water Works) |
| **ESA** | : European Space Agency |

**LIST OF TABLES**

## LIST OF FIGURES

## LIST OF SYMBOLS

| | |
|---|---|
| **A** | : Cross sectional area |
| **V** | : Sectional velocity |
| **Q** | : Flow quantity |
| **u** | : Water velocity component in x direction |
| **v** | : Water velocity component in y direction |
| **H** | : Water depth |
| **dx** | : Distance |
| **t** | : Time |
| $\eta$ | : Change in water level |
| **P** | : Pressure |
| **F** | : Total force |
| **Fx** | : Total force components in x directions |
| **Fy** | : Total force components in y directions |
| **a** | : Acceleration |
| $\mathbf{a_x}$ | : Acceleration component in x direction |
| $\mathbf{a_y}$ | : Acceleration component in y direction |
| $\rho$ | : Density |
| **m** | : Mass |
| **X** | : Mass forces acting in x direction |
| **Y** | : Mass forces acting in y direction |
| $\nu_T$ | : Kinematic viscosity |
| **g** | : Acceleration due to gravity |
| **f** | : Coriolis parameter |
| **C** | : Chezy coefficient |
| **k** | : Wind stress parameter |
| **W** | : Horizontal wind velocity |
| **Wx** | : Wind velocity component in x direction |
| **Wy** | : Wind velocity component in y direction |
| **Q** | : Injected water |
| $\mathbf{u_0}$ | : Injected water velocity component in x direction |
| $\mathbf{v_0}$ | : Injected water velocity component in y direction |
| **w** | : Settling velocity |
| **c** | : Concentration |
| **Dx** | : Longitudinal dispersion coefficient |
| **Dy** | : Transversal dispersion coefficient |
| **S** | : Mass flux |
| $\mathbf{c_0}$ | : Injected water concentration |
| $\lambda_V$ | : Volumetric decay parameter |
| $\mathbf{T_{90}}$ | : Time in which 90 percent of the population is no longer detectable |
| $\lambda_A$ | : Areal decay parameter |
| **Cp** | : Specific heat of water |
| **K** | : Atmospheric cooling factor |

| | |
|---|---|
| **T** | : Reference temperature |
| $\mathbf{c_t}$ | : Excess temperature |
| $\mathbf{S_1}$ | : Deposition flux term |
| $\mathbf{S_2}$ | : Erosion flux term |
| $\tau_b$ | : Bottom shear stress |
| $\tau_d$ | : Critical deposition shear stress |
| $\tau_e$ | : Critical erosion shear stress |
| **E** | : Erosion rate coefficient |
| **Re** | : Reynolds number |
| **Fr** | : Froude number |
| **n** | : Manning coefficient |
| $\mathbf{k_s}$ | : Roughness coefficient |
| $\Omega$ | : Earths' rotational speed |
| $\varphi$ | : Angle of latitude |
| $\rho_A$ | : Density of air |
| $\mathbf{C_D}$ | : Wind drag coefficient |
| **I** | : Slope of channel |
| **B** | : Width of channel |
| **u*** | : Shear velocity |
| **Un** | : Normal velocity component |
| $\Delta$ | : Triangular element |
| $\partial\Delta$ | : Boundary of triangular element |
| $\partial\Delta_A$ | : Boundary edge *BC,* opposite to node A |
| $\lvert\Delta\rvert$ | : The area of triangular element |
| **n** | : General outward unit normal vector on boundary edge |
| **a, b, c** | : Outward normal vectors on boundary edges |
| $\mathbf{a_x}$, $\mathbf{a_y}$ | : Components of outward normal vector |
| **z** | : The unit vector on z direction |
| **N** | : The element divergence matrix |
| **M** | : The element matrix |
| $\mathbf{M_l}$ | : The lumped element matrix |
| **Kx** | : The element x-stiffness matrix |
| **Ky** | : The element y-stiffness matrix |
| **K** | : The element stiffness matrix |
| **Lx** | : The element x-derivative matrix |
| **Ly** | : The element y-derivative matrix |
| **h** | : Approximate water level at nodes |
| $\mathbf{h_m}$ | : Average water level within element |
| **Sx** | : Wind stress vector in x direction |
| **Sy** | : Wind stress vector in y direction |
| **s** | : Decay vector |
| **Va** | : Approximate velocity within the adjacent element |
| $\psi$ | : Weight function |
| **q** | : Boundary normal outflow |
| **Pd** | : Boundary normal mass outflow |
| **Pe** | : Peclet number |
| **CN** | : Courant number |
| $\Delta l$ | : Space interval |
| $\Delta t$ | : Time interval |

## KOMPLEKS KANAL SİSTEMLERİNİN NÜMERİK MODELLENMESİ

## ÖZET

Bu çalışmada, nümerik analiz yöntemi ile iki bilgisayar yazılımı kullanılarak Köyceğiz-Dalyan Lagün Sistemi'nin hidrodinamik özellikleri modellenmiştir. Hidrodinamik özellikler akım ve taşıma denklemleri ile ayrı ayrı çözülmüş ve kullanılan temel denklemlerin çıkarılışı, parametrelerin özellikleri ve sınır koşullar açıklanmıştır. Kullanılan nümerik model yöntemi ile ilgili bilgiler ve model oluşturma konusundaki temel hususlar da bu çalışmada yer almaktadır.

Çalışma alanı Köyceğiz Gölü ve Dalyan Kanalı olmak üzere iki ayrı kısımda iki ayrı bilgisayar yazılımı ile modellenmiştir. Her iki model alanının özellikleri ve kompleks kanal sistemlerinin modellenmesi konusunda bilgiler çalışmada yeralmaktadır. Köyceğiz Gölü, Aquasea yazılımı ile Dalyan Kanalı, ise Aquadyn yazılımı ile modellenmiştir. Her iki yazılım da akım ve taşıma denklemlerini Galerkin sonlu elemanlar yöntemi ile üçgen elemanlar ağı üzerinden çözümlemektedir. Modellerin hazırlanması öncesinde, modelin kurulması ve kalibrasyonu için gerekli olan çalışma alanının fiziksel özellikleri ile model sonuçlarını mukayese etmekte kullanılacak olan daha önce yapılmış saha ölçümleri temin edilmiştir. Köyceğiz Gölü modeli için akım ve tuzluluk dağılımı ile Dalyan Kanalı modeli için akım ve oksijen dağılımı, nümerik method ile bu çalışmada elde edilmiştir.

Bu çalışma sonucunda, elde edilen nümerik model sonuçları ile daha önce yapılmış olan saha ölçüm değerlerinin paralel olduğu görülmüştür. Oluşturulan Köyceğiz Gölü modeli, gölde hidrodinamik özelliklerin büyük ölçüde Dalyan Kanalı girişinde görülen gelgit hareketine bağlı olduğunu göstermiştir; gölde aşırı rüzgar kuvvetinin oluşması halinde kanalın uzak olduğu kuzey kesimlerinde rüzgar doğrultusunda akıntıların oluştuğu görülmüştür. Ayrıca nehir ağızlarında akım ve tuzluluk konsantrasyonunun nehir akımının etkisiyle kısa mesafeli bir geçiş alanı oluşturduğu da gözlenmiştir. Kanal modelinde elde edilen sonuçlar, Dalyan Kanalı'nda akımın gelgit peryodu sırasında deniz göl etkileşimini başarılı bir şekilde yansıtmaktadır. Kanalda oksijen konsantrasyon dağılımının ise gelgit süresince en fazla kanalın alt kısmı ile orta kısmı arasına kadar ulaştığı görülmüştür.

**NUMERICAL MODELLING OF COMPLEX CHANNEL SYSTEMS**

**SUMMARY**

In this study hydrodynamic properties of Köyceğiz-Dalyan Lagoon System were modeled with numerical methods by using two computer code. Hydrodynamic properties were solved with flow and transport equations and the governing equations, parameters, and boundary conditions were explained in this study. Informations about the numerical method used in this study and basic principles of model generation were also given in this study.

The study area was modelled in two parts as Köyceğiz Lake and Dalyan Channel with two different commercial computer programs. Informations about both of the two parts of study area and modelling complex channel systems were also given in this study. Köyceğiz Lake was modeled with Aquasea computer program and Dalyan Channel was modeled with Aquadyn computer program. Before modelling the lagoon system, the physical properties of study area were obtained for model setup and calibration, and in order to compare the numerical results previous field measurements data were obtained. In this study flow and salinity trasnport of Köyceğiz Lake and flow and oxygen values of Dalyan Channel were obtained with numerical methods.

Comparing the results of two numerical model with previous field measurements shows that numerical model values are similar to field study data. The Köyceğiz Lake model shows that the hydrodynamic properties of lake highly depends on tidal wave force acting on Dalyan Channel inlet at lake. Lake model also shows that if strong winds act on surface of lake, there will be currents in wind direction at the northern part of lake. Additionally at river mouths as a result of river inflows, currents and salinity concentration change in a short transition region. The results of Dalyan Channel succesfully shows the sea lake interaction during the tidal wave period. Results of transport model shows that concentration of oxygen can reachs a part of channel at downstream.

# 1. INTRODUCTION

## 1.1 Evolution of Fluid Mechanics

The development of fluid mechanics was occured at three main terms. In the first term, by the beginning of 17th century theoretical developments at fluid mechanics were accelerated. The theories of basic equations were available at the end of the 18th century. The equations that are used today were first developed in this term (Figure 1.1).

In order to solve the fluid flows, heat and mass transport, these equations must be stated with methods. The methods that are used today were first developed in the second half of 20th century. The numerical and experimental methods were developed in this period (Durst, 2000).

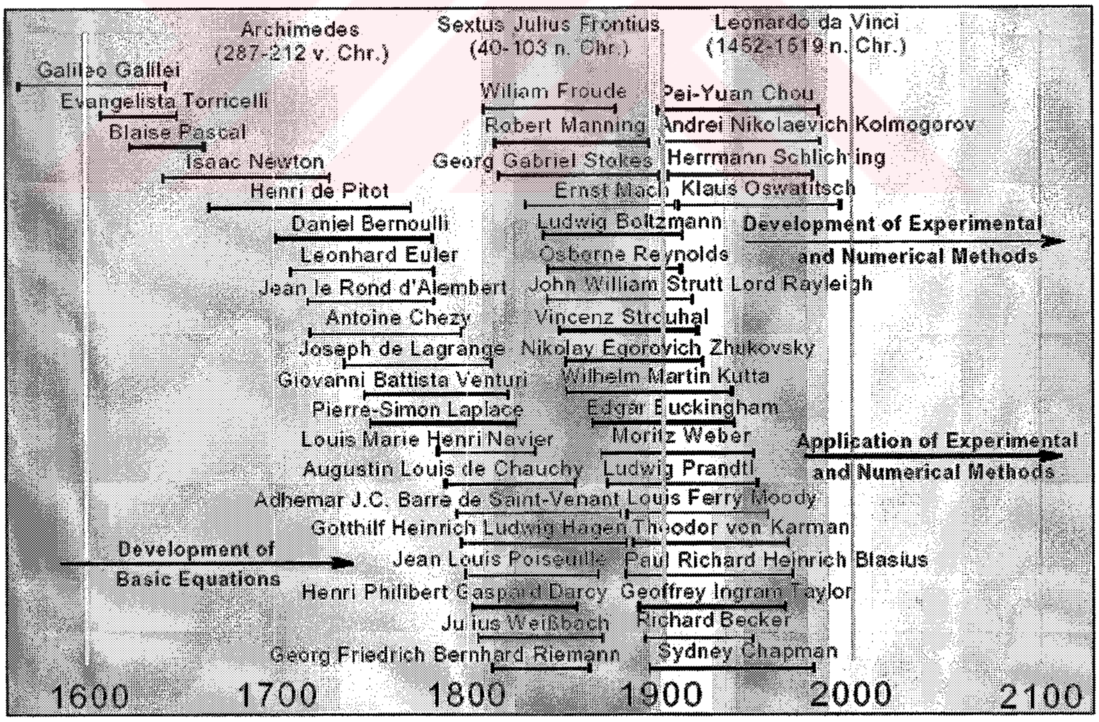


Figure 1.1 Historical developments of fluid mechanics (Durst, 2000).

The methods developed at this term were available by the end of the 20th century. This is the present term of fluid mechanics and numerical methods which are the results of mathematical studies at early years of century and improvements of computer technology. The cronological summary of fluid mechanics and important scientist are shown in Figure 1.1.

In the future with technological developments and new approachs for numerical methods will be applied at fluid mechanics to obtain better convergency and visualisation.

## 1.2 Flow and Transport Phenomena

There are several reasons that cause an increase on fluid mechanics popularity. The environmental pollution is the main reason, which includes the discharges of pollutants to lakes, rivers, and estuaries. By the end of $20^{th}$ century numerical methods allow us to compute the complex flow and transport equations with computers. The scenarios of pollution in rivers, lakes, and estuaries can be calculated with computer programs. By this way the potential damages can be prevented before they occur.

Another important reason is flooding of rivers, which causes great damages on structures over rivers such as dams and bridges.

In order to solve the problems there are several solution methods.

## 1.3 Solution Methods in Fluid Mechanics

The methods that are used in fluid mechanics are generally based on four primary groups:

- field measurements
- analytical solutions
- numerical methods
- physical models

Any of these methods, or combinations can be applied in fluid mechanics. Usually two different methods are applied to the problem and then the results of applied methods are compared. Choosing the solution method requires knowledge and experience about the phenomena (U.S. Army Corps of Engineers, 1991).

### 1.3.1 Field Measurements

In the field measurements, effects of variables can be estimated by skillful scheduling of data, careful analysis, and luck. The field measurements demonstrate the behavior of study area with the effects of several forces such as tide, wind, river discharge, coriolis, and others. The data collected in field are also indispensable element in verification of numerical and analytical methods results. Field measurement with spatial and temporal variation is formidable and expensive task.

### 1.3.2 Analytical Solutions

Analytical solutions are mathematical expressions of physical phenomena. The terms which aren't complex such as manning coefficient can be obtained directly with mathematical expressions. The analytical solutions combine complex problems into coefficient termed form that are determined empirically. The degree of simplification of analytical model depends on its solution. If the term is quite complex, it must be simplified in several steps with other methods especially numerical methods. If the values of mathematical expression are independent, the solution will be modified for each step by hand or computer. The advantages of analytical methods are speed and simplicity. The complexity of geometry is important in analytical solution for obtaining the desired results. If the area has got a regular geometry, the solution can easily applied to the model.

### 1.3.3 Numerical Methods

Numerical methods are computational models of mathematical expressions for physical phenomena. The difference between numerical methods and analytical solutions is the convergence value, which depends several parameters and concepts of each method. The numerical methods that are generally used in hydraulics are finite difference method (FDM), finite volume method (FVM), and finite element method (FEM). In any of three methods the governing equations are used to solve the unknown values at special points, which are generated with any mesh generation method. In order to solve the equations quickly with the desired accuracy high-speed computers are used. There are a lot of different numerical codes in use. The numerical solutions can be classified with the number of spatial dimensions over which variables are permitted to define and change.

- One-dimensional, usually in longitudinal direction with width-depth averaged

- Two-dimensional, depth averaged
- Two-dimensional, width averaged
- Three-dimensional with a hydrostatic pressure assumption
- Fully three-dimensional

The advantages of numerical methods are more accurate and detailed results than analytical methods. In order to solve the complex models with very small convergence values large computers with significant environmental properties should be necessary. Therefore the disadvantages of this method are long modeling and iteration time, and cost of modeling. Numerical methods results can be compared with analytical solutions and field measurements.

Today's hydraulic engineering mostly use numerical methods with field measurements in flow and transport models. This is a reason of rapid developments in computer technology. The numerical methods that are used in fluid mechanics are a part of Computational Fluid Dynamics.

### 1.3.4 Physical Models

This method has been used since 19$^{th}$ century. In order to obtain reliable model careful observance of appropriate scaling. Physical models of water resources can reproduce tides and other long waves, short period waves, longshore currents, freshwater inflows, pollutant discharges, sedimentation, and three-dimensional variation in salinity, current, density, and pollutant concentration. If there is a geometric distortion at short period wave model, reproduction of refraction and diffraction will not be available.

### 1.3.5 Hybrid Method

The methods that are described above have advantages and disadvantages. For better approximation two or more methods are used jointly. Each method is applied to that part of problem for which it is best suited. If physical modeling and numerical method are applied together to provide results not obtainable any other way, the method is called hybrid solution method and combining them in a closely coupled fashion that permits feedback between the models is termed an integrated hybrid solution. Judicious selection of solution methods in a hybrid approach can greatly improve accuracy and detail of the results.

## 1.4 Purpose of This Study

Complex systems are the physical combinations of different systems that should be lakes, channels, seas, and oceans. In these combinations, effects of larger systems such as seas' over smaller systems such as channels and/or lakes are complicated that is why we named these systems as *complex systems*. The results of these effects cause flow and transport phenomena.

In this study Köyceğiz Lake, and Dalyan Channel are modelled with numerical methods in order to analyse the flow and tranport process. This area is a Special Protected Area in southwest part of Turkey in the province of Muğla. The Köyceğiz Lake is about 55 $km^2$ and connected to the Mediterranean Sea with Dalyan Channel which is 10 km long natural water channel. The arae was first designated as Special Protected Area in 12.6.1988 by Turkish Authority. The protection area was modified and extended in 2.3.1990. The area which is about 385 $km^2$ declared as protection area in order to protect it against enviromental pollution and destruction (ESA, 2000).

There are number of field studies about this area, therefore numerical model results can be compared with field measurements. The water level variations and velocities at lake with the effects of various forces such as tides, wind, rivers, and coriolis force are obtained with numerical code. The Aquasea numerical code was used to solve the model. The code was developed for circulation in lake and esturies. The two dimensional depth averaged flow and transport equations are solved with Galerkin FEM on unstructured triangular mesh form.

The water level variations, velocities, and salinity transport at channel with the effects of tide and bed slope are obtained with numeric code. The Aquadyn numerical code was used to solve the model in two dimensional form. The code was developed for open channel flows. The two dimensional depth averaged flow and transport equations are solved with Galerkin FEM on unstructured triangular mesh.

The numerical methods results are compared with field measurements of special coordinates at lake and channel.

## 2. THEORETICAL APPROACH

In this study two essential problem surface flow model and transport model are reviewed. Therefore theoretical equations, and parameters are explained in two groups:

- Surface flow model
- Transport model

### 2.1 Governing Equations

Governing equations of hydraulic models are based on conservation laws. Flow model is consisted on equations of:

- Continuity law
- Momentum law

The equations represent mass conservation, and momentum balance for each of the two coordinate directions.

#### 2.1.1 Flow Model Equations

The basic equations that govern the flow of a fluid were laid in 1750 by Euler as the conservation law of momentum for a mass point and by applying it in integrated form to a fluid continuum. He also generalized d'Alembert's differential equation of continuity. Hence, the presently accepted form of these equations originates from him. Friction within the fluid has been highly debated at that time, but promising results for practical and tractable use were not given before the 19th century.

Attraction and repulsion between molecules was considered by Navier (1822) in a purely theoretical treatise about the motion of a fluid. However, even though Navier gave the complete equation of motion for a fluid with internal friction, he could not attach a particular physical significance to the essential parameter today known as viscosity. As it is noted the approach of Navier does not fulfill the continuum assumption of the fluid.

The problem was successfully re-analyzed by de Saint-Venant (1843), who considered internal stresses instead of collisions of molecules. His assumptions for the stresses of a continuum fluid are similar to those given earlier by Cauchy (1828) for an elastic continuum. The form given to these stresses is the only extension possible of Newton's hypotheses of fluids with internal frictional shear.

The assumption that the stresses are linear functions of the rates of distortion, and not like the pressure uniform in all directions, allowed Saint-Venant to distinguish tangential and normal stresses. His equations were not restricted to a specific flow like laminar flow but are valid for any flow involving stresses of the type he had assumed. The derivation implied that these stresses are proportional to the local formation and destruction of eddies i.e. the stress tensor does not change when molecular scales or even large scales are considered.

Eleven years later the derivation of the fundamental equation was obtained for a second time by Stokes (1845) who also gave a physical interpretation of the parameter inherent to his theory as dynamic viscosity. He also confirmed the theory by experiments (Sander, 1998).

#### 2.1.1.1 Continuity Equation

Conservation of mass can be described by *continuity equation*. In order to explain the continuity equation, we assume some considerations that flow is steady and fluid is incompressible (ρ is constant).

Due to these assumptions we should define the constant volume equation for any section of flow layers.

In one dimensional space (Figure 2.1), the velocity variation in y direction should be neglected. So the velocity in all points is a constant V averaged sectional velocity value (Güney, 1995).

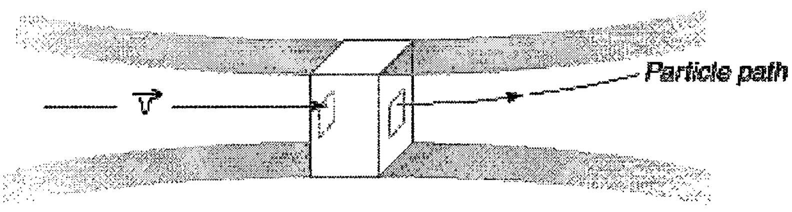


Figure 2.1 Particle path of fluid on cross sectional area with velocity.

The volume of fluid that pass from a section at unit time is named as *flow* and formulated in Eq. (2.1).

$$Q = V_1 A_1 = V_2 A_2 = V_3 A_3 = \ldots \tag{2.1}$$

In this equation A is the cross sectional area of flow layer in $m^2$, V is the sectional averaged velocity of fluid in m/s, and Q is the flow quantity in $m^3/s$.

The theory of unsteady and incompressible flow shows that water depth changes with time as it is seen in Fig. (2.2). In this figure, u is the water velocity component in x direction in m/s, H is the water level in m, dx is the distance of longitudinal profile.

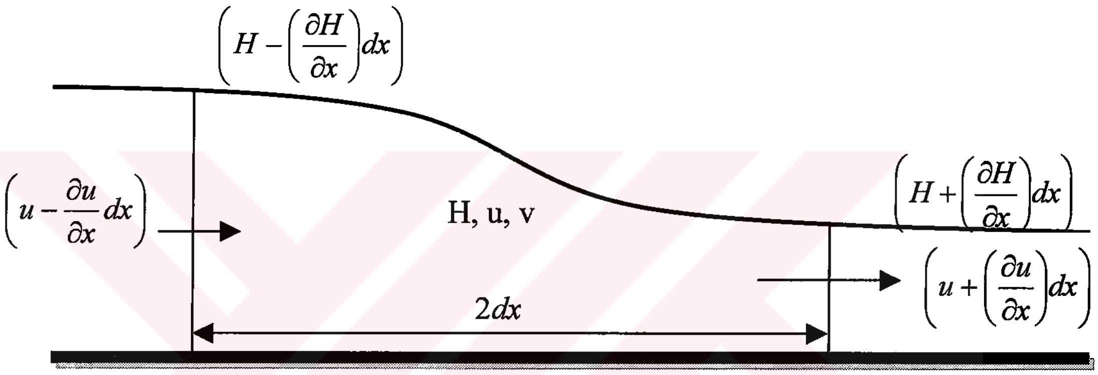


Figure 2.2 Longitudinal profile of unsteady flow.

According coservation of mass, rate of accumulation is expressed Eq. (2.2) and with local time (t) derivation in Eq. (2.3).

$$\textit{Rate of accumulation} = \textit{flux incoming- flux outgoing} \tag{2.2}$$

$$\text{Rate of accumulation} = \frac{\partial H}{\partial t} 2dx \tag{2.3}$$

The flux incoming and outgoing are expressed in Eq. (2.4) and (2.5).

$$\text{Flux incoming} = \left(u - \frac{\partial u}{\partial x} dx\right)\left(H - \frac{\partial H}{\partial x} dx\right) \tag{2.4}$$

$$\text{Flux outgoing} = \left(u + \frac{\partial u}{\partial x} dx\right)\left(H + \frac{\partial H}{\partial x} dx\right) \tag{2.5}$$

The rate of accumulation and net flux with incoming and outgoing fluxes are expressed in Eq. (2.6)

$$\frac{\partial H}{\partial t}2dx = \left(u - \frac{\partial u}{\partial x}dx\right)\left(H - \frac{\partial H}{\partial x}dx\right) - \left(u + \frac{\partial u}{\partial x}dx\right)\left(H + \frac{\partial H}{\partial x}dx\right) \tag{2.6}$$

From Eq. (2.6), one dimensional time dependent continuity equation (Eq. 2.7) can form.

$$\frac{\partial(uH)}{\partial x} + \frac{\partial H}{\partial t} = 0 \tag{2.7}$$

Equation (2.8) shows the relation in change and depth with time and x space. The two dimensional form of with the water velocity componenet v in direction y is shown in Eq. (2.8) (Dalziel and others, 1999).

$$\frac{\partial(uH)}{\partial x} + \frac{\partial(vH)}{\partial y} + \frac{\partial H}{\partial t} = 0 \tag{2.8}$$

If there is an injection between the two section, the injected water will be stated at the right side of the equation with the term Q in $m^3/s$ (Eq. 2.9)

$$\frac{\partial(uH)}{\partial x} + \frac{\partial(vH)}{\partial y} + \frac{\partial \eta}{\partial t} = Q \tag{2.9}$$

#### 2.1.1.2 Momentum Equations

The Figure (2.3) below describes the flow in two dimensional x-y form in unit z dimension. The mass of the figure below is defined as $m = \rho dxdy$ and $P$ is pressure on surface (Güney, 1995).

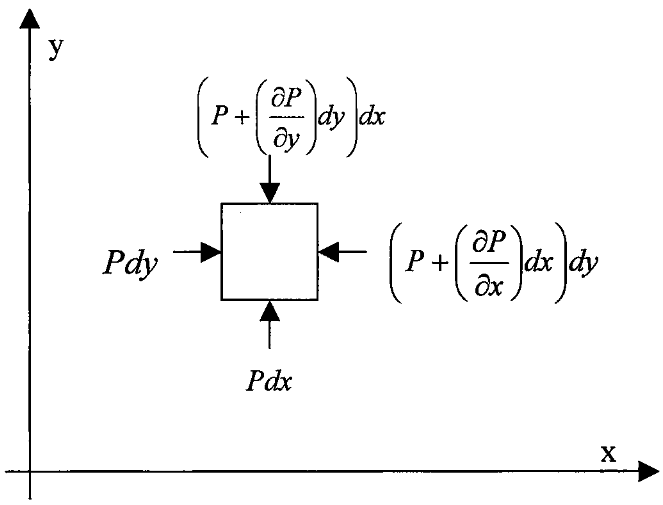


Figure 2.3 Motion for ideal fluids in two dimensional form.

As the fluid is assumed as ideal, frictional forces do not act on its surfaces and the forces only act on it are surface pressures.

The forces that acts on the square are Fx and Fy pressure forces that are described with Newton's Second Law in Eq. (2.10), (2.11), (2.11), (2.12), (2.13), (2.17), and (2.18).

The X and Y terms are the mass forces acting on particle. The derivation of total acceleration components ($a_x$, $a_y$) are given in Eq. (2.14), (2.15), (2.16), (2.16), (2.19), (2.20), and (2.21).

$$Fx = a_x dm \tag{2.10}$$

$$Fy = a_y dm \tag{2.11}$$

$$Fx = Pdy - \left( P + \left( \frac{\partial P}{\partial x} \right) dx \right) dy + X\rho dxdy \tag{2.11}$$

$$Fx = \left( -\frac{1}{\rho} \right) \left( \frac{\partial P}{\partial x} \right) dm + Xdm \tag{2.12}$$

$$a_x dm = \left( -\frac{1}{\rho} \right) \left( \frac{\partial P}{\partial x} \right) dm + Xdm \tag{2.13}$$

$$a_x = \frac{du}{dt} \tag{2.14}$$

$$a_x = \frac{\partial u}{\partial t} + \left( \frac{\partial u}{\partial x} \right) \frac{dx}{dt} + \left( \frac{\partial u}{\partial y} \right) \frac{dy}{dt} \tag{2.15}$$

$$a_x = \frac{\partial u}{\partial t} + \left( \frac{\partial u}{\partial x} \right) u + \left( \frac{\partial u}{\partial y} \right) v \tag{2.16}$$

$$Fy = Pdx - \left( P + \left( \frac{\partial P}{\partial y} \right) dy \right) dx + Y\rho dxdy \tag{2.17}$$

$$Fy = \left( -\frac{1}{\rho} \right) \left( \frac{\partial P}{\partial y} \right) dm + Ydm \tag{2.18}$$

$$a_y = \frac{dv}{dt} \tag{2.19}$$

$$a_y = \frac{\partial v}{\partial t} + \left(\frac{\partial v}{\partial x}\right)\frac{dx}{dt} + \left(\frac{\partial v}{\partial y}\right)\frac{dy}{dt} \tag{2.20}$$

$$a_y = \frac{\partial v}{\partial t} + \left(\frac{\partial v}{\partial x}\right)u + \left(\frac{\partial v}{\partial y}\right)v \tag{2.21}$$

$\partial v/\partial t$ and $\partial u/\partial t$ are local accelarations as a result of temporal variation of velocity.

$u(\partial v/\partial x)$; $v(\partial v/\partial y)$; $u(\partial u/\partial x)$ and $v(\partial u/\partial y)$ are general convective accelarations as a result of spatial variation of velocity.

If the force and the acceleration equations are combined, the conservation of momentum will be formed. The equations, which are known as Eulers Momentum Equations, are seen in Eq. (2.22) and (2.23) (Güney, 1995).

$$\overbrace{\underbrace{\frac{\partial u}{\partial t}}_{local} + \underbrace{\left(\frac{\partial u}{\partial x}\right)u + \left(\frac{\partial u}{\partial y}\right)v}_{convective}}^{accelerations} = \overbrace{\underbrace{\left(-\frac{1}{\rho}\right)\left(\frac{\partial P}{\partial x}\right)}_{pressure} + \underbrace{X}_{mass}}^{forces} \tag{2.22}$$

$$\overbrace{\underbrace{\frac{\partial v}{\partial t}}_{local} + \underbrace{\left(\frac{\partial v}{\partial x}\right)u + \left(\frac{\partial v}{\partial y}\right)v}_{convective}}^{accelerations} = \overbrace{\underbrace{\left(-\frac{1}{\rho}\right)\left(\frac{\partial P}{\partial y}\right)}_{pressure} + \underbrace{Y}_{mass}}^{forces} \tag{2.23}$$

The momentum equations of fluid dynamics, were originally derived by Navier (1827), Poisson (1831), Saint Venant (1843), and Stokes (1845). In the older classical literature, they are called the Navier-Stokes equations. In the recent computational literature, the term Navier-Stokes equations includes the continuity and energy equations, as well as the momentum equations (Orkwis and Wolff, 2001).

As it was mentioned before, the frictional forces acting on particle are neglected with ideal fluid assumption. Navier-Stokes equations (Eq. 2.24 and 2.25) improved Eulers' equations by adding frictional forces $\nu_T(\partial^2 u / \partial^2 x + \partial^2 u / \partial^2 y)$.

$$\frac{\partial u}{\partial t}+\left(\frac{\partial u}{\partial x}\right)u+\left(\frac{\partial u}{\partial y}\right)v=\left(-\frac{1}{\rho}\right)\left(\frac{\partial P}{\partial x}\right)+X+\underbrace{\upsilon_T\left(\frac{\partial^2 u}{\partial x^2}+\frac{\partial^2 v}{\partial y^2}\right)}_{viscosity} \tag{2.24}$$

$$\frac{\partial v}{\partial t}+\left(\frac{\partial v}{\partial x}\right)u+\left(\frac{\partial v}{\partial y}\right)v=\left(-\frac{1}{\rho}\right)\left(\frac{\partial P}{\partial y}\right)+Y+\underbrace{\upsilon_T\left(\frac{\partial^2 u}{\partial x^2}+\frac{\partial^2 v}{\partial y^2}\right)}_{viscosity} \tag{2.25}$$

*Saint Venant Equations*

Saint Venant equations are obtained from Navier-Stokes equations (Eq. 2.7 and 2.8) by averaging the horizontal velocities along the depth of the water body. The pressure variable *P* is replaced with the water height *H* using the hydrostatic pressure distribution assumption. The Saint Venant equations in two dimensional form with are given in Eq. (2.26) and Eq. (2.27).

$$\underbrace{\frac{\partial u}{\partial t}}_{local}+\underbrace{\left(\frac{\partial u}{\partial x}\right)u+\left(\frac{\partial u}{\partial y}\right)v}_{convective}=\underbrace{(-g)\left(\frac{\partial H}{\partial x}\right)}_{pressure}+\underbrace{fv}_{corolis}\underbrace{-gu\left(\frac{\sqrt{(u^2+v^2)}}{HC^2}\right)}_{friction}+\underbrace{kW_x|W|}_{wind}+\underbrace{\frac{Q(u-u_0)}{H}}_{source/sink} \tag{2.26}$$

$$\underbrace{\frac{\partial v}{\partial t}}_{local}+\underbrace{\left(\frac{\partial v}{\partial x}\right)u+\left(\frac{\partial v}{\partial y}\right)v}_{convective}=\underbrace{(-g)\left(\frac{\partial H}{\partial y}\right)}_{pressure}+\underbrace{fu}_{coriolis}\underbrace{-gv\left(\frac{\sqrt{(u^2+v^2)}}{HC^2}\right)}_{friction}+\underbrace{kW_y|W|}_{wind}+\underbrace{\frac{Q(v-v_0)}{H}}_{source/sink} \tag{2.27}$$

In these equations the variables are explained below:

u: water velocity components in x direction, m/s

v: water velocity components in y direction, m/s

t: time, s

g: acceleration due to gravity, $m^2/s$

H: total water depth, m

η: change in water level, m

f: coriolis parameter

C: chezy friction coefficient, $m^{1/2}/s$

k: wind stress parameter

W: horizontal wind velocity, m/s

Wx: wind velocity component in x direction, m/s

Wy: wind velocity component in y direction, m/s

Q: injected water, $m^3/s$

$u_0$: injected water velocity component in x direction, m/s

$v_0$: injected water velocity component in y direction, m/s

### 2.1.2 Transport Model

#### 2.1.2.1 Convection Diffusion Equation

The movement of sediments, temperature or a pollutant in water can be described by convection-diffusion equation. The convection-diffusion equation for steady flows is expressed in Eq. (2.28) (Olsen, 2000).

$$\underbrace{u\frac{\partial c}{\partial x}+w\frac{\partial c}{\partial z}}_{convection}=\underbrace{\frac{\partial}{\partial x}\left(D_X\frac{\partial c}{\partial x}\right)}_{diffusion} \tag{2.28}$$

The transport model expressed in Eq. (2.28) is based on two main process named as convection and diffusion. Convection is the movement of particle by water. Particles vertical movement $w\partial c/\partial z$ should also be defined as convective term. The term is similar to the navier stokes equation term and should be described as spatial variation of transport process.

The second term diffusion is explained as turbulent diffusion of particle due to the turbulent mixing and concentration gradients. Here $D_x$ and $D_y$ are the dispersivity coefficients in $m^2/s$. In two dimensional space the conservation of concentration for unsteady sediment transport process the equation is expressed in Eq. (2.29) (Olsen, 2000).

$$v\frac{\partial c}{\partial y}+u\frac{\partial c}{\partial x}+w\frac{\partial c}{\partial z}+\frac{\partial c}{\partial t}=\frac{\partial}{\partial x}\left(D_X\frac{\partial c}{\partial x}\right)+\frac{\partial}{\partial y}\left(D_y\frac{\partial c}{\partial y}\right) \tag{2.29}$$

As it was mentioned in continuity equation, the flow model is assumed as unsteady. Therefore H must be expressed in transport equations. Additionally the injected water flux difference to the conservation of concentration as $S=Q(c_0-c)$ in equation form.

Q is the flow quantity of discharge in $m^3/s$, $c_o$ is the concentration of discharge in $kg/m^3$, and S is the flux term is expressed for pollutant, heat and sediment in different forms (Vatnaskil, 1998).

i. In pollutant transport process, the flux term is expressed in Eq. (2.30).

$$S = \lambda_V Hc \tag{2.30}$$

In this equation λv is the volumetric decay parameter and is calculated from Eq. (2.31).

$$\lambda_V = \frac{\ln 10}{T_{90}} \tag{2.31}$$

In this $T_{90}$ is the time in which 90 percent of the population are no longer detectable.

ii. In heat transport process, the flux term is expressed in Eq. (2.32).

$$S = \lambda_A c \tag{2.32}$$

In this equation $\lambda_A$ is the areal decay parameter and calculated from Eq. (2.33).

$$\lambda_A = \frac{K}{\rho C_P} \tag{2.33}$$

In Eq. (2.33) $\rho$ is the density of water in $kg/m^3$, Cp is the specific heat of water in J/kg°C, and K which can be calculated from Eq. (2.34) is the atmospheric cooling factor in J/ $m^2$°Cs.

$$K = 0.2388(4.6 - 0.09(T + c) + 4.06|W|)\exp(0.033(T + c_t)) \tag{2.34}$$

In equation above, T is the reference temperature in °C, |W| is the wind speed at 2 m elevation in m/s, $c_t$ is the excess temperature °C.

iii. In sediment transport process, the flux term is expressed in Eq. (2.35).

$$S = \underbrace{S_1}_{deposition} + \underbrace{S_2}_{erosion} \tag{2.35}$$

Deposition of sediment on bed is calculated with Eq. (2.36) or (2.37).

If $\tau_b < \tau_d$, then $S_1 = wc\left(1 - \frac{\tau_b}{\tau_d}\right)$ (2.36)

If $\tau_b > \tau_d$, then $S_1 = 0$ (2.37)

w is the settling velocity, $\tau_b$ is the bottom shear stress, and $\tau_d$ is the critical deposition shear stress.

Erosion of sediment from bed is calculated with Eq. (2.38) or (2.39).

If $\tau_b > \tau_e$, then $S_2 = E\left(\frac{\tau_b}{\tau_d} - 1\right)$ (2.38)

If $\tau_b < \tau_e$, then $S_2 = 0$ (2.39)

E is the erosion rate coefficient, and $\tau_e$ is the critical shear stress for erosion. According to the assumptions the general form of transport equation is seen in Eq. (2.40) (Vatnaskil, 1998).

$$\frac{\partial(Hc)}{\partial t} + \left(\partial\frac{(Hvc)}{\partial y}\right) + \left(\partial\frac{(Huc)}{\partial x}\right) = \frac{\partial}{\partial x}\left(HDx\left(\frac{\partial c}{\partial x}\right)\right) - \frac{\partial}{\partial y}\left(HDy\left(\frac{\partial c}{\partial y}\right)\right)$$

$$+ S - Q(c_0 - c) \qquad (2.40)$$

## 2.2 Parameters

### 2.2.1 Flow Model Parameters

The flow equations include different terms about gravitational, frictional, viscous and inertial forces that are acting on surface flow system. In order to describe the relationship between these forces, some parameters are used. The parameters that are used in equations are described below.

#### 2.2.1.1 Reynolds Number

Turbulence arises from the non linear terms in the momentum equation. Reynolds number describes the importance of these terms and it is the ratio of non-linear terms to the viscous terms (Equation 2.41 and 2.42).

$$\mathrm{Re} = \frac{Non-Linear-Terms}{Viscous-Terms} = \frac{\left(\dfrac{u\partial u}{\partial x}\right)}{\left(\dfrac{\upsilon_T \partial^2 u}{\partial x}\right)} \approx \frac{U\dfrac{U}{L}}{\upsilon_T \dfrac{U}{L^2}} \tag{2.41}$$

$$\mathrm{Re} = \frac{H\sqrt{\left(u^2+v^2\right)}}{\upsilon_T} \tag{2.42}$$

According to this term, if the speed is small, the flow is smooth. This is called *laminar flow*. At higher speeds, the flow becomes irregular and turbulent. The transition occured at $\mathrm{Re} = VD/\upsilon_T \approx 2000$, where V is average speed, D is diameter, and $\upsilon_T$ is the kinematic viscosity fluid. As Reynolds number increases, the flow becomes more turbulent (Stewart, 1998).

#### 2.2.1.2 Froude Number

The value of froude number determines the type of the flow. If the froude number is smaller than 1, then the flow is determined as *subcritical* or *fluvial flow*. If the froude number is greater than 1, then the flow is determined as *supercritical* or *torrential flow*. And if the froude is equal to 1, then the flow is critical. Froude number is expressed in Eq. (2.43) (Stewart, 1998).

$$Fr = \frac{\sqrt{\left(u^2+v^2\right)}}{gH} \tag{2.43}$$

In this equation u, v are the velocity components of water in m/s, g is gravitational acceleration in $m^2/s$, and H is the water depth in m.

#### 2.2.1.3 Molecular Viscosity

Molecules in a fluid close to a solid boundary can strike to the boundary and transfer momentum to the boundary. The transferred momentum is called molecular viscosity. Molecular viscosity is the ratio the stress $T_x$ tangential to the boundary of a fluid and the shear of the fluid at the boundary. The stress term expression is given in Eq. (2.44).

$$T_x = \rho\upsilon\frac{\partial u}{\partial z} \tag{2.44}$$

Some values for viscosity are seen in Table 2.1 (Stewart, 1998).

Table 2.1 Viscosity values of water.

| | |
|---|---|
| $v_{water}$ | $=10^{-6}$ m$^2$/s |
| $v_{tar}$ at 15 °C | $=10^{6}$ m$^2$/s |
| $v_{glacier\ ice}$ | $=10^{10}$ m$^2$/s |

### 2.2.1.4 Manning Coefficient

Manning coefficient describes the roughness of water bed. It is an emprical measured effect of roughness between natural surface, wall, bed configuration and fluid. The roughness creates friction and resistance that causes losses on velocity, elevation, energy and other related terms

Table 2.2 Values of coefficient n for different categories of rivers (Hydrosoft, 1999).

| River Category | Category Definitions | Manning Coefficient |
|---|---|---|
| 1 | Small mountain flow with very irregular bottom, 10 to 30 m wide | 0.038-0.043 |
| 2 | Large mountain flow from 30 to 50 m wide, with a gradient exceeding 0.002 and a rough gravel bottom (many stones 10 to 20 cm in diameter) | 0.034-0.037 |
| 3 | Similar or larger rivers, with a gradient between 0.000 and 0.002 and a gravel bottom with pebbles whose maximum diameters generally do not exceed 8 to 10 cm (Rhine in Basel) | 0.030-0.033 |
| 4 | Gradient ranging from 0.0006 and 0.0008; pieces of gravel from 4 to 8 cm in diameter (Rhône in Lyons) | 0.027-0.029 |
| 5 | Same gradient with smaller gravel (Rhône near Scex, Lake Geneva) | 0.025-0.026 |
| 6 | Gradient less than 0.0006 but over 0.00025, very small stones or sand (Danube in Vienna) | 0.023-0.024 |
| 7 | Low-turbulence river, gradients between 0.00012 and 0.00025, sand and mud bottom (Seine, Saône, Lower Rhine) | 0.022-0.023 |
| 8 | Very large river, very low gradient (less than 0.00012) and very smooth bottom | 0.020-0.021 |

Manning coefficient should be estimated by the following expression in Eq. (2.45)

$$n = \frac{26}{k_S^{\frac{1}{6}}} \qquad (2.45)$$

In this equation *ks* is roughness coefficient. The relation between the roughness and the grain size distribution for bed material is defined by Van Rijn (1982) in Eq. (2.46) (Olsen, 2001).

$$k_S = 3d_{90} \tag{2.46}$$

In this equation $d_{90}$ is grain size sieve that 90 % of the material is finer. It shows that manning coefficient depends on the grain size of bed material. In Table 2.2 various categories of rivers and definitions of bottom with manning values are listed.

#### 2.2.1.5 Chezy Coefficient

The chezy is expressed with manning coefficient in Eq. (2.47) (Vatnaskil, 1998).

$$C = \left(\frac{1}{n}\right) H^{1/6} \tag{2.47}$$

In this equation n is the manning coefficient, H is the water level in m.

#### 2.2.1.6 Coriolis Coefficient

Coriolis force becomes evedent due to Earth rotation and deflects fluid motion to the right in the Northern Hemisphere. Figure (2.4) shows the deflections of motion with the effect of Coriolis force.

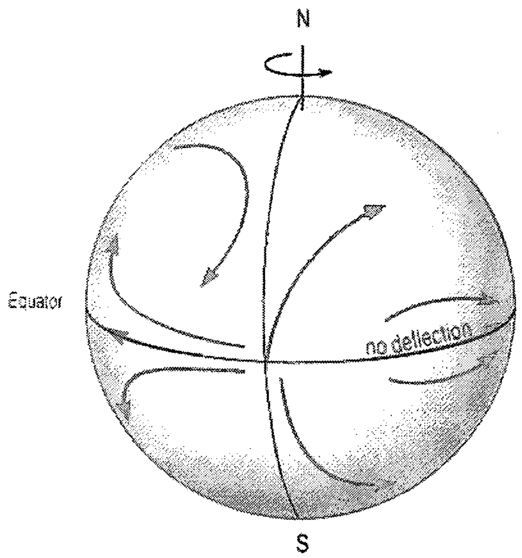


Figure 2.4 Coriolis force effect on fluid motion.

Coriolis coefficient is depends on latitude and earth's rotational speed which is equal to $7.27 \times 10^{-5}$ rad/s. Coriolis parameter is expressed in Eq. (2.48) (Vatnaskil, 1998).

$$f = 2\Omega Sin\phi \tag{2.48}$$

In equation (2.48) $\Omega$ is earth's rotational speed in 1/s, $\varphi$ is the latitude in degrees.

#### 2.2.1.6 Wind Stress Parameter

It is an empirical coefficient depending on which elevation the wind speed measured. There are number of different formulas about it. According to Bengtsson the wind stress coefficient should be taken as $1.1\times10^{-3}$ (Olsen, 2001). Another empirical formula is seen in Eq. (2.49) (Vatnaskil, 1998).

$$k = \frac{(\rho_A C_D)}{\rho} \tag{2.49}$$

In expression above, $\rho_A$ is density of air in kg/m$^3$, $\rho$ is density of fluid in kg/ m$^3$, and $C_D$ is the wind drag coefficient which is an emprical parameter.

### 2.2.2 Transport Model Parameters

In this study the transport model is obtained to solve the salinity and oxygen, therefore the necessary parameters for appropriate transport process are described below.

#### 2.2.2.1 Longitudinal Dispersivity

The dispersivity coefficient is effective parameter in transport process. It regulates the concentration distribution in fluid. There are several empirical formulas about heat and pollutant transport dispersivity coefficients. According to McQuivey and Keefer (1974) the longitudinal dispersion coefficient should be found with the following empirical formula in Eq. (2.50) (Olsen, 2001).

$$D_X = 0.058\frac{Q}{IB} \tag{2.50}$$

Q is the water discharge in m$^3$/s, I is slope, B is width in m. As longitudinal dispersion coefficients are a function of stream velocity, and Fisher developed an empirical formula for dispersivity coefficient in 1979 as seen in Eq. (2.51) (Olsen, 2001).

$$D_X = 0.011\frac{(UB)^2}{Hu^*} \qquad (2.51)$$

Here U is the water velocity in x direction in m/s, $u^*$ is the shear velocity in m/s. Typical values of longitudinal dispersivity for small streams are 0.05 to 0.3 $m^2/s$ and large rivers can be > 1000 $m^2/s$.

#### 2.2.2.2 Transversal Dispersivity

In previous section, longitudinal dispersivity coeffient was expressed. The difference between these two coefficents is the directions. If the point of inmjection source is not uniform across for instance a single near a bank, contaiminant must travel before it becomes uniformly mixed in cross section which is called *transverse mixing zone.* Transversal dispersivity is used to calculate the transverse mixing zone.

Transverse mixing is responsible for the lateral movement and this only occurs as a result of turbulence. Transversal dispersivity coefficient can be estimated with Eq. (2.52) and (2.53).

- $D_y = 0.15Hu^*$ for straight channels (2.52)

- $D_y = 0.60Hu^*$ for natural channels (2.53)

Here H is the water level in m, and $u^*$ is the shear velocity in m/s. Measured transversal dispersivity cofficient has got a range of 0.0014 to 3.1 $m^2/s$.

#### 2.2.2.3 Shear Velocity

Turbulence is due to shear velocity and is given in Eq. (2.54).

$$u^* = \sqrt{(gHI)} \qquad (2.54)$$

In this equation g is the earth's gravitational acceleration in $m^2/s$, H is water level in m, and I is the the slope of bottom topography.

### 2.3 Boundary Conditions

These conditions are required on physical boundaries to solve the flow and transport equations. The most used types of boundary conditions are:

- Zero gradient
- Dirichlet

In the first type of boudary condition, the derivative of the variable at the boundary is zero. The value at the boundary is the same as the value in the element closest to the boundary. In iterative solutions, this is straightforward. This boundary condition gives good results at outflow open section. It can also be used at wall boundaries. This boundary condition is a type of Neumann boundary condition which is defined as a given gradient prescribed on the boundary.

Dirihclet boundary conditions are defined as given values of variables at boundaries. This type of boundary condition is usually used at inflow open sections. For example H water level, concentration at upstream open section are Dirichlet boundary contions (Olsen, 2001).

Boundaries are defined at internal and external boundaries. Internal boundaries are the islads, blocks other structures at inner parts of flow field. These are also known as physical boundaries.

If a part of physical boundary is an open section which means there is an interaction with another water body, that part of boundary will be defined as open section with water level, flow quantity or normal water velocity.

Boundaries should be external or internal and defined as wall or open. The special conditions for wall and open sections are defined under in flow and transport conditions.

Additionally source/sink can be defined at any point with flow quantity and concentration values.

### 2.3.1 Flow Model

Wall boundaries are also known as solid and closed boundary. In these types of boundaries, two main condition can be defined as:

- Free slip condition, Un = 0.
- No slip condition, U = V = 0.

In the first type the normal water velocity is defined as 0 as a reasult of assumption that the particle can't pass through the boundary.

In the second type the water velocity components are defiened as 0 without the assumption mentioned above.

The selection of boundary condition depends on several reasons such as geometry of study area, bottom topography. Comparing the results with field measurements in studies shows that usually free slip boundary condition gives better results.

In open sections, boundary conditions should be defined as:

- Water level
- Flow quantity

Any of these conditions defined at a part of physical boundary can be time dependent boundary. Each of the time interval values are defined as boundary condition.

### 2.3.2 Transport Model

In open sections, two main condition can be defined as:

- Specified concentration, $c \neq 0$.
- Zero concentration gradient, indicating convective transport through the boundary, $c = 0$.

The first type of boundary condition can be time dependent. Each of the time interval values are defined as boundary condition.

## 3. NUMERICAL MODELLING METHODS

By the beginning of twentieth century, scientific studies on numerical methods were accelerated. Although the computer technology hadn't begun yet, the numerical methods by different engineers were developed. In order to solve the environmental problems especially river and lake pollutions, numerical methods have applied in different forms. By this way the problems effects should be viewed successfully before they occur.

After the invention of computer, numerical algorithms were developed and applied in scientific studies. At hydraulic engineering numerical methods for flow problems weren't available as the computers were too slow. Later in 1980's previously developed methods were carried out with new integrated computers.

The numerical methods are based on known as boundaries and unknowns and operators and iteration parameters. The most important point in this structure for analyse is iteration parameters control the stability and accuracy of iteration. At this point to have better convergence should not be easy sometimes, therefore the CPU time has an important role in iteration process. By the evolution of computer technology enough CPU time with significant enviromental properties have been using in hydraulic engineering (Olsen, 1999).

The numerical codes that are used today have easy understanding structure. The outputs of the models can be understood easily with minimum knowledge of the user. The main problem at using these models is based on two points: a.) model setup b.) decision about output files.

Model setup process is dominant for the results. The results that have been modeled is completely created by the input data and the parameters. The inserted data are the boundaries restrict the unknown data and the initial values for iteration start up.

The results that are generated by model can easily be viewed by user. The important point at this process is that the results are expected or not. If the results aren't realistic, there must be a problem with model setup or numeric code.

Todays numerical methods may not include all the processes occuring at hydraulic system. It is also possible to neglect some of the processes in numerical method with personal expect.

To have better approximation the user needs to be aware of numerical methods parameters such as courant number and peclet number.

The conversion of the continuous partial differential equation to its discrete algebraic counterpart, the process of discretization can be done in various ways. Well-known methods are

- The Finite Difference Method (FDM); this method approximates the partial differential equations using Taylor series expansions, thus creating a system of algebraic equations.
- The Finite Volume Method (FVM); this method takes the integral form of the conservation laws as a starting point and uses discrete approximations to the surface and boundary integrals appearing in the integral formulation.
- The Finite Element Methods (FEM); this method defines in each cell, in this methodology called elements a set of basis functions and the solution is expanded in terms of these basis functions. The unknown coefficients in this expansion become the unknowns in FEM. Usually a weighted residual strategy is employed to set up the system of algebraic equations (Gerritsma and Koren, 2000).

Before explaninig the finite element method, some concepts of grids and mesh generation for numerical models will be explained in next part.

## 3.1 Grids and Mesh Generation

An important part when working in the field of numerical models is concerned with the generation of meshes. Numerical mesh generation arose from the need to compute solutions to the partial differential equations of fluid mechanics on physical regions with complex geometries.

Mesh generation method depends on the numerical method which will be used to solve the domain. Therefore there are number of different mesh generation methods appropriate to the using numerical method. For instance in finite difference numerical method the structured grid is generally used.

Assuming that the numerical method was chosen for the model, the domain geometry must be defined with an appropriate grid method. The domain bounded by the object and the outer boundaries is then covered by a so called *mesh* or *grid* (Figure 3.1).

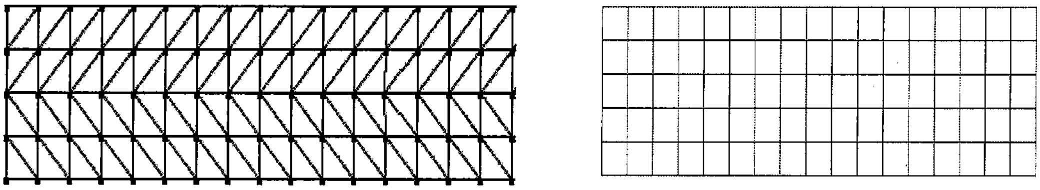

Figure 3.1 Examples of triangular and rectangular mesh generation.

Grids can be classified according to several characteristics:

a) Shape
b) Orthogonality
c) Structure
d) Blocks
e) Position of variable
f) Grid movements

a) The shape of grid is usually triangular or quadrilateral (Figure 3.2).

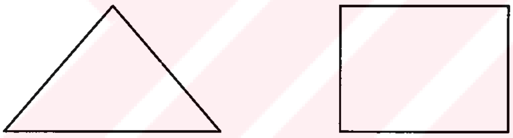

Figure 3.2 Triangular and quadrilateral elements.

b) The orthogonolity of element is defined with the angle between the links of element. If the angle is 90', the element is defined as orthogonal. Other wise the grid is defined as non-orthogonal (Figure 3.3).

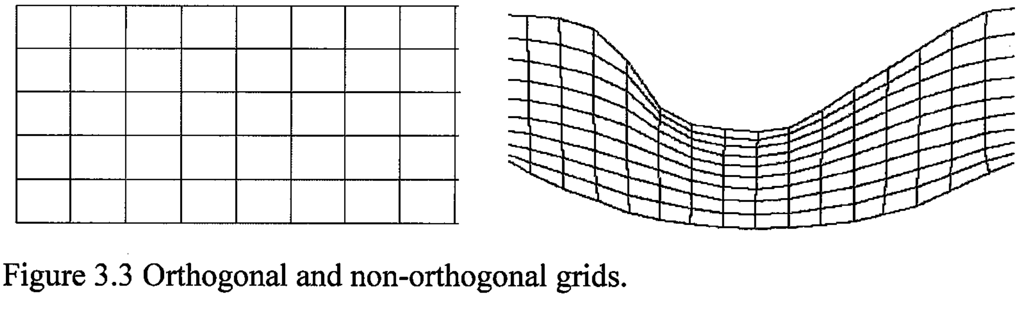

Figure 3.3 Orthogonal and non-orthogonal grids.

c.) The shape of grid should be defined as structured if it is possible to make two dimensional array indexing the grid cells. If it is not possible then the grid will be named as unstructured (Figure 3.4).

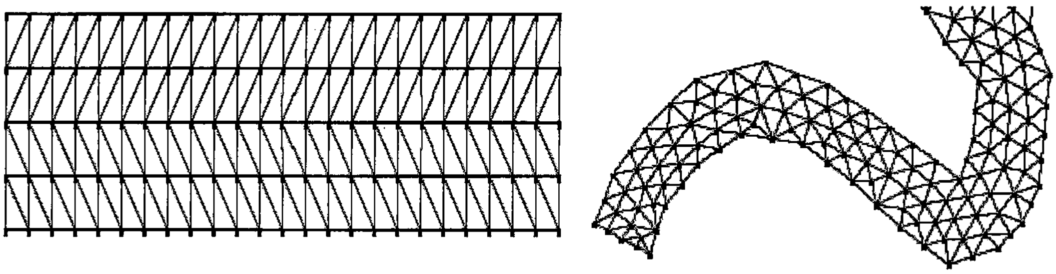

Figure 3.4 Structured and unstructured grids.

d.) A structured grid is named as block grid. If more than two structured grid generated, the grid will be named as multiblock grid (Figure 3.5).

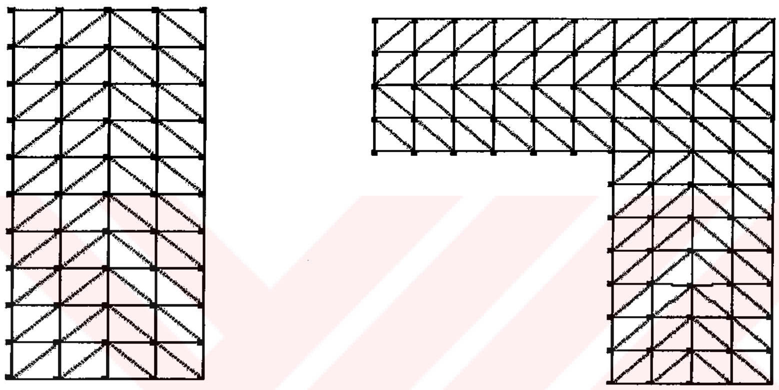

Figure 3.5 Block and multi-block grids.

e.) If all the variables of cell or element are calculated in the same location such as on link, or node, then the grid will be named as staggered grid. If the calculation of variables is occured at different locations, grid will be named as unstaggered (Figure 3.6) (Olsen, 1999).

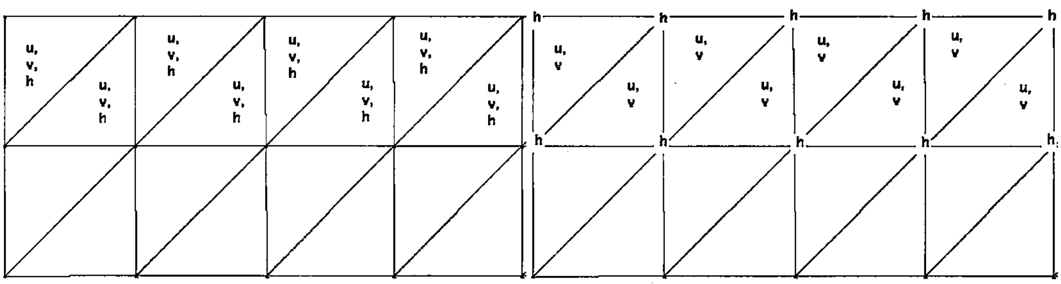


Figure 3.6 Staggered and unstaggered grids.

Note that in finite element methods the variables can be calculated at nodes and center.

f.) If the grid moves during the iteration process, the grid will be named as adaptive. Adaptive grids give better results as the grid regenerated with the effect of water level, bed level changes.

It is well known that the error of approximations of the hosted equations depends not only on the derivatives of the solution of the hosted equations and the grid spacing, but also on the rate of change of grid spacing and the departure of the grid from orthogonality. For a given grid spacing, smooth, orthogonal grids usually result in the smallest error in simple problems. Thus another major goal of grid-generation algorithms is to produce smooth grids, that is grids where the spacing varies smoothly and the angles between the grid lines do not become too small. It turns out that it is not possible to generate orthogonal grids for a wide class of problems.

If the solution of the hosted equation varies rapidly in some part of the physical region,then is reasonable to choose a finer grid in that part of the region to reduce the error in the numerical simulation. Such a grid is called solution adapted; it is important to be able to generate solution adapted grids.

The main advantage of modern grid generation algorithms is that these algorithms can be used to efficiently generate large grids, containing tens of thousands to a few million points, and the resulting grids allow the reduction of error and simplified treatment of boundary conditions.

As a summary for accuracy and convergency the quality of grid can be generated with the following informations:

- Defining the necessary elements for grid. Element numbers is the most important parameter at iteration process. If it is so high, iteration process will take much more time.
- Drawing the geometry is important as the external boundaries define over it. The inflow and outflow areas must be defined carefully. At these areas the flow direction and the dispertion of concentration generally depend on these definitions.
- Grid lines should follow the stream lines as much as possible.
- Grid aspect ratio should not be greater than 2.
- Grid expansion ratio should not be greater than 1.5.
- Higher densities should be necessary at areas with higher velocities and concentrations.
- Higher densities should be necessary at areas where water depth fast varies.

## 3.2 Finite Element Method

Primary advantage of finite element method is that it allows us to accurately model irregular geometries.

The finite element method minimizes the error in the solution to the underlying mathematical equations in a global sense whilst finite volume minimizes it in a local sense. This means that a finite volume method will always conserve mass at each time step and throughout a simulation.

A finite element method will only have true mass conservation once the grid is refined to a level where further refinement makes no further change to the solution. In river modeling this level is difficult to achieve as refinement of the mesh effectively redefines the bathymetry and sets up a different problem and in work published so far there is little evidence that mesh independence has been achieved.

A finite element method often uses an unstructured mesh. This means that the matrix A is sparse. To solve the system of equations, the matrix needs to be inverted. This is a fairly time-consuming procedure. A good solver is therefore essential in the finite element method.

The finite element method gives similar problems with stability as the finite volume method. Implicit solvers, high-order upstream schemes etc. are more difficult to formulate with the finite element method than the finite volume method. This especially applies to an unstructured grid, where it is difficult to derive an implicit high-order upstream procedure.

Many finite element programs have employed various techniques to try to overcome these problems, with varying degree of success (Wright, 2001).

## 3.3 Galerkin Finite Element Method

The finite element method can be formulated in different ways. Often a weighed residual method is used. Then the basic equations are multiplied with a weighting function, W, and integrated over the element A.

Galerkin formulation is used if the weighting functions are equal to the interpolation functions. The result of the integration is a residual, which is minimized. The equation with the residual is called the *residual equation.*

A term often encountered in the finite element method is the *weak formulation*. This means that when formulating the equation system, there are no restrictions that the derivative of the unknown need to exist on the surface between elements, as opposed to the original differential equations. The Galerkin formulation is a weak formulation. The main effect of the weak formulation is that mass continuity need nnot be satisfied automatically in the satisfied solution procedure (Olsen, 1999).

### 3.3.1 Finite Element Notation

In order to define the finite element notation, we need the triangular mesh element to describe some procedures (Figure 3.7).

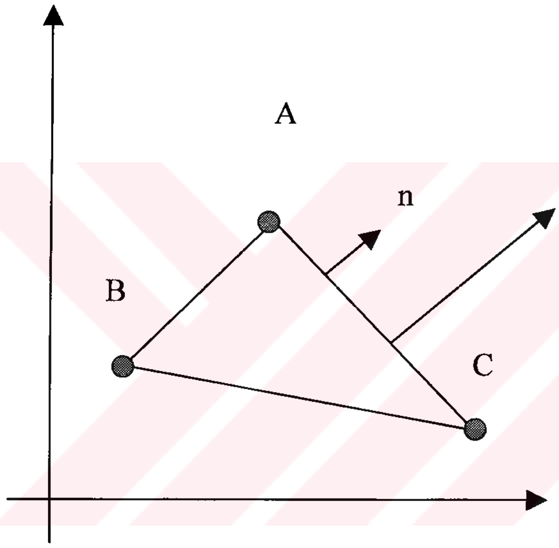


Figure 3.7 Triangular hydrodynamic element.

| | |
|---|---|
| A, B, C: | Nodes of triangular element. |
| $A_x$, $A_y$: | X, Y coordinates of nodes |
| $\Delta$ : | Triangular element. |
| $\partial\Delta$ : | Boundary of triangular element $\Delta$. |
| $\partial\Delta_A$ : | Boundary edge *BC*, opposite link to *A*. Similarly $\partial\Delta_B$, $\partial\Delta_C$ are the boundary edges of appropriate nodes. |
| $\lvert\Delta\rvert$ : | The area of the triangular element. |
| n: | General outward unit normal vector on boundary edge. |
| a, b, c: | Outward normal vectors on boundary edges. The outward normal vector between *B* and *C* is named as *a* and equal to the distance between these nodes. Similarly *b* and *c* are the outward normal vectors of appropriate nodes. |

a = ($a_x$, $a_y$): Components of the outward normal vector in x, y directions. $a = ((B_x - C_x),(B_y - C_y))$. Similarly the other outward normal vectors components are depends on the coordinates of the appropriate nodes.

z: The unit vector on z direction (Vatnaskil, 1998).

We need to define the element matrices:

1. The element divergence matrix;

$$N = \left(\frac{1}{2}\right)\begin{bmatrix} a_x & a_y \\ b_x & b_y \\ c_x & c_y \end{bmatrix}$$

2. The element matrix;

$$M = \left(\frac{|\Delta|}{12}\right)\begin{bmatrix} 2 & 1 & 1 \\ 1 & 2 & 1 \\ 1 & 1 & 2 \end{bmatrix}$$

3. The lumped element matrix;

$$M_1 = \left(\frac{|\Delta|}{3}\right)\begin{bmatrix} 1 & 0 & 0 \\ 0 & 1 & 0 \\ 0 & 0 & 1 \end{bmatrix}$$

4. The element x-stiffness matrix;

$$K_X = \left(\frac{1}{4|\Delta|}\right)\begin{bmatrix} a_x^2 & a_x b_x & a_x c_x \\ a_x b_x & b_x^2 & b_x c_x \\ a_x c_x & b_x c_x & c_x^2 \end{bmatrix}$$

5. The element y-stiffness matrix;

$$K_y = \left(\frac{1}{4|\Delta|}\right)\begin{bmatrix} a_y^2 & a_y b_y & a_y c_y \\ a_y b_y & b_y^2 & b_y c_y \\ a_y c_y & b_y c_y & c_y^2 \end{bmatrix}$$

6. The element stiffness matrix;

$$K = K_x + K_y = \left(\frac{1}{\Delta}\right) N N^T$$

7. The element x-derivative matrix;

$$L_x = -\left(\frac{1}{6}\right)\begin{bmatrix} a_x & b_x & c_x \\ a_x & b_x & c_x \\ a_x & b_x & c_x \end{bmatrix}$$

8. The element y-derivative matrix;

$$L_y = -\left(\frac{1}{6}\right)\begin{bmatrix} a_y & b_y & c_y \\ a_y & b_y & c_y \\ a_y & b_y & c_y \end{bmatrix}$$

The nodes and elements hydrodynamic properties are defined for unknowns with averaged values, approximations:

Approximate water level at nodes A,B and C: $h = (h_A, h_B, h_C)$
Approximate concentration or temperature at nodes A,B and C: $c = (c_A, c_B, c_C)$
Approximate velocity within the element: $V = (u, v)$
Approximate velocity within the adjacent element that a points into: $Va = (u_a, v_a)$
Average water level within the element: $h_m = 1/3(h_A + h_B + h_C)$
H, Hm, h and hm are defined similarly
Velocity of injected water: $V_o = (u_o, v_o)$
Wind stress vector: $S = (S_x, S_y)$
Decay vector $s = (s_a, s_b, s_c)$

### 3.3.2 Flow Model

#### 3.3.2.1 Finite Element Weak Formulation of Continuity Equation

The finite element weak formulation of continuity equation (2.9) is given in Eq. (3.1). $\psi i$ are the weight functions of nodes A,B, and C and taking the value 1 at node i and the value 0 on the opposite edge (Vatnaskil, 1998).

$$\int_{\partial\Delta}(HV)n\psi ds - \iint_{\Delta}(HV)\nabla\psi dxdy + \iint_{\Delta}\frac{\partial H}{\partial t}\psi dxdy = \iint_{\Delta}Q\psi dxdy \tag{3.1}$$

The resulting finite element approximation is given in Eq. (3.2).

$$q + H_m NV + M\frac{\partial H}{\partial t} = Q \tag{3.2}$$

Here Q is injected water and for $i = A, B, C$ expressed in Eq. (3.3), and Eq. (3.4). $q$ is the boundary normal outflow and for $i = A, B, C$ is expressed in Eq. (3.5), and (3.6).

$$Q = (Q_A, Q_B, Q_C) \tag{3.3}$$

$$Q_i = \iint_{\Delta}Q\psi_i dxdy \tag{3.4}$$

$$q = (q_A, q_B, q_C) \tag{3.5}$$

$$q_i = \int_{\partial\Delta}q\psi_i ds \tag{3.6}$$

#### 3.3.2.2 Finite Element Weak Formulations of Momentum Equations

The finite element weak formulation of momentum equations (2.26 and 2.27) are given in Eq. (3.7) and Eq. (3.8) (Vatnaskil, 1998).

$$\iint_{\Delta}\left[\frac{\partial u}{\partial t} + u\frac{\partial u}{\partial x} + v\frac{\partial u}{\partial y}\right]\psi dxdy + \int_{\partial\Delta_a}\left[\frac{1}{2}(V + V_A)a\right](u_a - u)\psi ds =$$

$$\iint_{\Delta}\left[-g\frac{\partial n}{\partial x} - \beta u + fv + \frac{1}{H}S_x - \frac{Q}{H}(u - u_0)\right]\psi dxdy \tag{3.7}$$

$$\iint_{\Delta}\left[\frac{\partial v}{\partial t} + u\frac{\partial v}{\partial x} + v\frac{\partial v}{\partial y}\right]\psi dxdy + \int_{\partial\Delta_a}\left[\frac{1}{2}(V + V_A)a\right](v_a - v)\psi ds =$$

$$\iint_{\Delta}\left[-g\frac{\partial H}{\partial y} - \beta v - fu + \frac{1}{H}S_y - \frac{Q}{H}(v - v_0)\right]\psi dxdy \tag{3.8}$$

The resulting finite element approximation of momentum equations is given in Eq. (3.9).

$$|\Delta|\frac{dV}{dt}+\left[\frac{1}{2}(V+V_a)a\right](V_a-V)=gN^T H-|\Delta|\left[\beta V+fkxV-\frac{1}{H}S+\frac{Q}{H}(V-V_0)\right] \quad (3.9)$$

### 3.3.3 Transport Model

#### 3.3.3.1 Finite Element Weak Formulation of Transport Equation

The finite element weak formulation of transport equation (2.40) is given in Eq. (3.10). The resulting finite element approximation of trasnport equation is given in Eq. (3.11) (Vatnaskil, 1998).

$$\int_{\partial\Delta} H\left(D_x\frac{\partial c}{\partial x},D_y\frac{\partial c}{\partial y}\right)n\psi ds-\iint_{\Delta} H\left(D_x\frac{\partial c}{\partial x}\frac{\partial \psi}{\partial x}+D_y\frac{\partial c}{\partial y}\frac{\partial \psi}{\partial y}\right)dxdy-\iint_{\Delta} Hu\frac{\partial c}{\partial x}\psi dxdy=$$

$$\iint_{\Delta}\left(H\frac{\partial c}{\partial t}+s-Q(c_0-c)\right)\psi dxdy \quad (3.10)$$

$$-P^d-H_m(D_xK_x+D_yK_y)c-H_m uL_x c=H_m M\frac{dc}{dt}+Ms-QM(c_0-c) \quad (3.11)$$

Here Pd is the boundary normal mass outflow and for $i=A,B,C$ expressed in Eq. (3.12) and Eq. (3.13).

$$P^d=(p_A^d,p_B^d,p_C^d) \quad (3.12)$$

$$p_i^d=\int_{\partial\Delta} p^d\psi_i ds \quad (3.13)$$

### 3.3.4 Grid Size and Iteration Time Step Adjustment

It is well known that the advective-dispersive transport equation is more difficult to solve numerically. The problems are particularly severe when advection dominates over dispersion. These numerical oscillations tend to be more severe as advection becomes more dominant.

#### 3.3.4.1 Peclet Number

Relationship between the advective and diffusive components of solute transport is expressed by *peclet number* as the ratio of the product of the average interstitial velocity and the characteristic length, divided by the dispersion coefficient (Eq. 3.14). Peclet number characterizes the oscillations that may occur in the numerical solution when this number is greater than 2. Small values indicate diffusion dominates; large values indicate advection dominates (Vatnaskil, 1998).

$$P_e = \frac{V(\Delta l)}{D} < 2 \tag{3.14}$$

#### 3.3.4.2 Courant Number

According to courant criteria, the timestep should be smaller that a water particle can pass from one section to another. If courant number is greater than 1, the iteration will be unstable. Therefore the timestep can be reviewed and adjusted as smaller time step. Courant number is expressed in Equation (3.15) below (Olsen, 2001).

$$CN = \frac{V(\Delta t)}{\Delta l} < 1 \tag{3.15}$$

## 3.4 AquaSea Numerical Modelling Code

Aquasea is a scientific software developed in 1983 by Vatnaskil Consulting Engineers to solve the two dimensional shallow water flow and transport equations using the Galerkin finite element method on triangular elements. The program consists of the following two models:

- Hydrodynamic flow model
- Transport-dispersion model

The hydrodynamic flow model can simulate water level variations and flows in response to various forcing functions such as corolis, gravity, wind, tide effects in lakes, estuaries, bays and coastal areas. The program can simulate waterlevels and flows for different times and different elements.

The basic equations program uses are continuity and momentum equations in x and y directions. The boundary conditions for flow model are no flow and H water level. Source and sink conditions can also be defined at physical boundary nodes.

The transport-dispersion model is divided into three main parts as faecal coliforms, heat, and suspended sediment. Transport of substances such as, conservative or nonconservative, inorganic or organic salt, heat suspended sediment, dissolved oxygen, inorganic phosphorus, nitrogen and other water quality parameters can be solved by proper selection of the parameters.

The basic equation for transport model is advection–diffusion equation that consists of transport by fluid flow and existing dispersion process. The boundary conditions for the transport model are zero concentration or temperature gradient, indicating just convective transport of mass or heat through the boundary and specified concentration or temperature at the boundary.

The program has automatic and manual mesh generation with local and global condensation property. The results of models are in contour, flow arrows and time series modules (Vatnaskil, 1998).

### 3.5 AquaDyn Numerical Modelling Code

Aquadyn is a software package developed by Hydro-Québec's environmental team and the Ministère de l'environnement et de la Faune of the province of Québec. The program solves two dimensional flow and transport equations with Galerkin finite element on triangular method.

- Hydrodynamic flow model
- Transport-dispersion model

The hydrodynamic flow model can simulate the dynamics of an open channel for steady and unsteady conditions in rivers, lakes and estuaries.
The flow model is based on continuity and St. Venant momentum equations in x and y directions. The boundary conditions for model are no slip (U = V = 0), free slip (Un = 0), discharge rate, water level or normal velocity of any constant or variable value at nodes or along cross-sections.

The transport model can solve mass and heat transport. The boundary conditions for tranport model are zero concentration or temperature and specified concentration or temperature (Hydrosoft, 1999).

# 4. NUMERICAL MODELS OF KÖYCEĞİZ-DALYAN LAGOON SYSTEM

## 4.1 Numerical Models of Lagoon Systems

Lagoons are lakes joining to the sea through a channel or a similar morphologic structure. The hydrodynamic interaction between two different systems controls the natural balance. The behaviour of natural balance depends on numerous parameters. The effective parameters of system are water circulation as convective terms and hydrodynamic properties of this circulation diffusive terms (Kabdaşlı, 2001).

The are several effects such as sea level variation, rivers flowing into lagoon, wind forces, and coriolis force cause spatial and temporal variation of water levels, velocities, and hydrodynamic characteristics. As a result of flow phenomena the changes in hydrodynamics of lagoon controls transport phenomena. The salinity, temperature, and sediment concentration dispersion are occured as a result of hydrodynamic circulation. Briefly the lagoon sea interaction changes with rivers draining into the lagoon and the wave climate acting near the coastal area on connection channel.

Todays hydraulic engineering is using all the capabilities of computer technology in hydrodynamic modelling studies. The numerical modelling in hydraulic engineering has been rapidly developed by the beginning of 1980's. Upto now a lot of succesfull projects are modelled with numerical methods.

Modelling of complex channel systems and lagoon and coupled systems is available by different computer codes. There are number of different models of lagoons and complex systems. Venice Lagoon is situated at Northern Adriatic Sea and covers an area about 500 $km^2$. Venice Lagoon is a complex system and the exchanges between the lagoon and the Adriatic Sea take place through three inlets. The finite element model of Venice Lagoon was developed at ISDGM-CNR to solve flow and transport process with different effects (Figure 4.1) (Umgiesser and Zampato, 1998).

with higher condensation. The large sized elements have been used for the shallower parts where hydrodynamic activity is reduced.

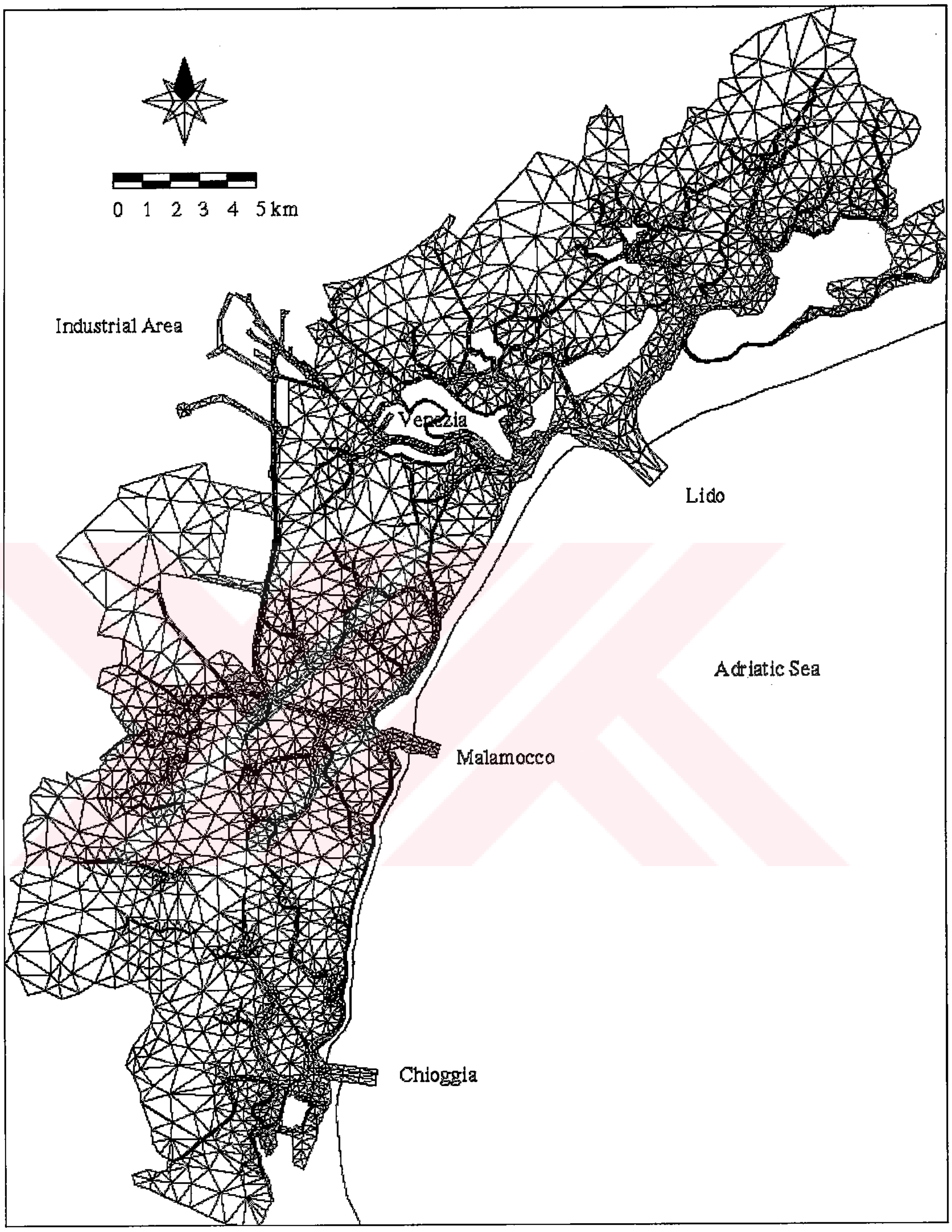


Figure 4.1 Unstructured triangular mesh of Venice Lagoon contains 4237 nodes and 7666 elements (Umgiesser and Zampato, 1998).

The method used in this model is FEM as the irregular geometry of lagoon and channel system can easily form with this method. The variable depth of water is another reason for using this method.

Due to fast and irregular varied bathymetry values, nodes of finite element mesh were inserted manually. This is a general problem of all numerical models. In order to solve this problem, nodes density should be increased, but as a result of increaing the condensation of nodes, model set up and iteration time increase. Therefore this is best way for irregular variable depth structures.

## 4.2 Köyceğiz-Dalyan Lagoon System

The Köyceğiz-Dalyan Protection Area is located at southwestern part of Turkey. It is in the province of Muğla. The area includes Köyceğiz Lake and Dalyan Channel which connects the lake to the Mediterranean Sea(Figure 4.2).

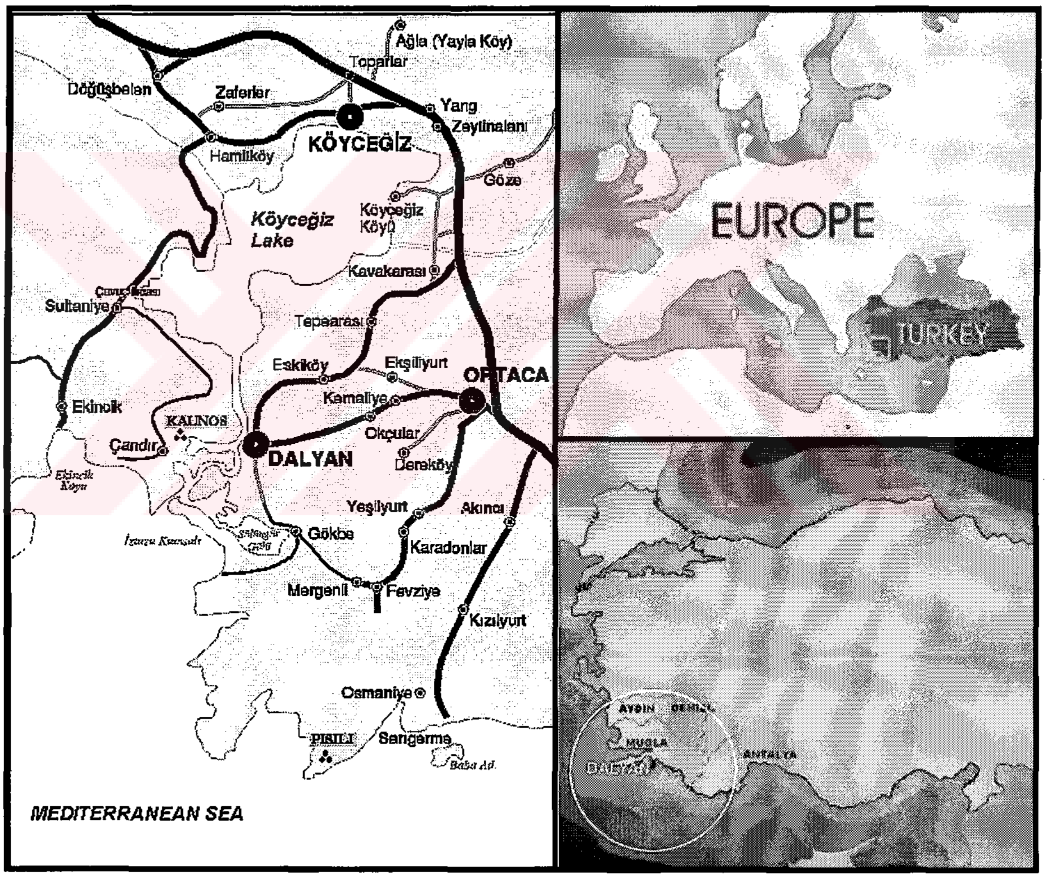


Figure 4.2 Location of Dalyan Wetland and an overview of Köyceğiz-Dalyan Lagoon System.

In 1998 the area, where the Köyceğiz Lake and the Dalyan Channel is located at was first designated as Special Protected Area. The protection area is about 385 km$^2$ and 55 km$^2$ of this area is Köyceğiz Lake. The area includes İztuzu Beach, which is extremely important for sea turtles Caretta Caretta (ESA, 2000).

Köyceğiz-Dalyan Lagoon System is consist of:

- Köyceğiz Lake
- Dalyan Channel

### 4.2.1 Köyceğiz Lake

Köyceğiz lake is located in southwestern part of Turkey in Muğla province very near to the county of Köyceğiz. Surface area of lake is about 55 $km^2$ and its drainage area is 2100 $km^2$. Lake is approximately 12 km long and 5 km wide and it has got 30 km shoreline. Its connection to the Mediterranean Sea is via 10 km long Dalyan Channel which allows interactions between sea and lake. Therefore Köyceğiz Lake is a type of lagoon (ESA, 2000).

The formation of lake is filled tectonic depression which is located between Akçakavak point and Babadağ Mountain. The connection between the depression and the sea was filled with silt which was carried by Dalaman River from east of lake.

There are three main freshwater sources coming from mountains. From west part of lake the largest freshwater source of lake, Namnam River drains into to lake with a flow volume of 9~2.4 $m^3/s$, from the east part of lake Yuvarlak River with a flow volume of 4 $m^3/s$ drain to lake. Additionally from north part of lake Kargıcık River drains into the lake. It is also known that lake is fed by groundwater sources.

The water of lake includes low oxygen rate and mainly fresh. Eastern coasts of lake are mostly covered with reeds which are approximately 2~3 m high from water surface.

### 4.2.2 Dalyan Channel

Dalyan channel is located between the Köyceğiz Lake and Mediterranean Sea. Its length is about 10 km in North-South direction. At the downstream of channel there are two main lakes located. On the east side of lake Iztuzu Lake and on the west side of the channel Sülüngür Lake is located. The channel has complex geometry at downstream part. The narrow connection of channel to the Mediterranean Sea is named as Dalyanağzı. The length of channel mouth is variational by water level and wave changes of sea. The formation of downstream section is named as Dalyan Delta which includes the Sülüngür Lake, İztuzu Lake and Dalyanağzı.

In this study the channel geometry isn't defined completely. The main reason for this reason is the long iteration time, and available data of whole area (ESA, 2000).

## 4.3 Numerical Models of Köyceğiz-Dalyan Lagoon System

The numerical model of Köyceğiz-Dalyan Lagoon System was developed in two parts. The lake was modeled with Aquasea FEM code, and channel was modeled with Aquadyn FEM code. Main reasons for using two codes in this study:

- Previous field studies shows that the downstream section of channel is not effective on hydrodynamic properties of channel. Additionally the study area has got an unstructured and complex geometry, which causes too many nodes in finite element mesh of model. For these reasons the study area divided into two parts as lake and channel model.
- Both of the parts could be modeled with any of two codes. As Aquasea is mostly recommended for lake circulation, the lake was modeled with it. Similarly as Aquadyn is mostly recommended for open channel flows, the channel was modeled with it.

### 4.3.1 Model of Köyceğiz Lake

Numerical model of Köyceğiz Lake was developed with Aquasea software package. Before the finite element model constitude, mesh of lake was generated with an automatic mesh generation property of aquadyn in unstructured triangular form. External boundary nodes inserted at a distance smaller than the density of the mesh. This is a preliminary decision. The generated mesh is consist of 12.000 elements and condensation is higher at shorelines of lake (Figure 4.3).

The generated mesh isn't not available to solve as the node number is very high to solve the equations and complete the iteration. Therefore model has to be regenerated by inserting the nodes manully. By this way the total node and element number should be decreased and as a result of it the model will run in a reduced iteration time.

- The final lake model was developed at aquasea. The finite element mesh of lake was generated by inserting nodes manually. Several criterias are taken into consideration while creating the mesh.

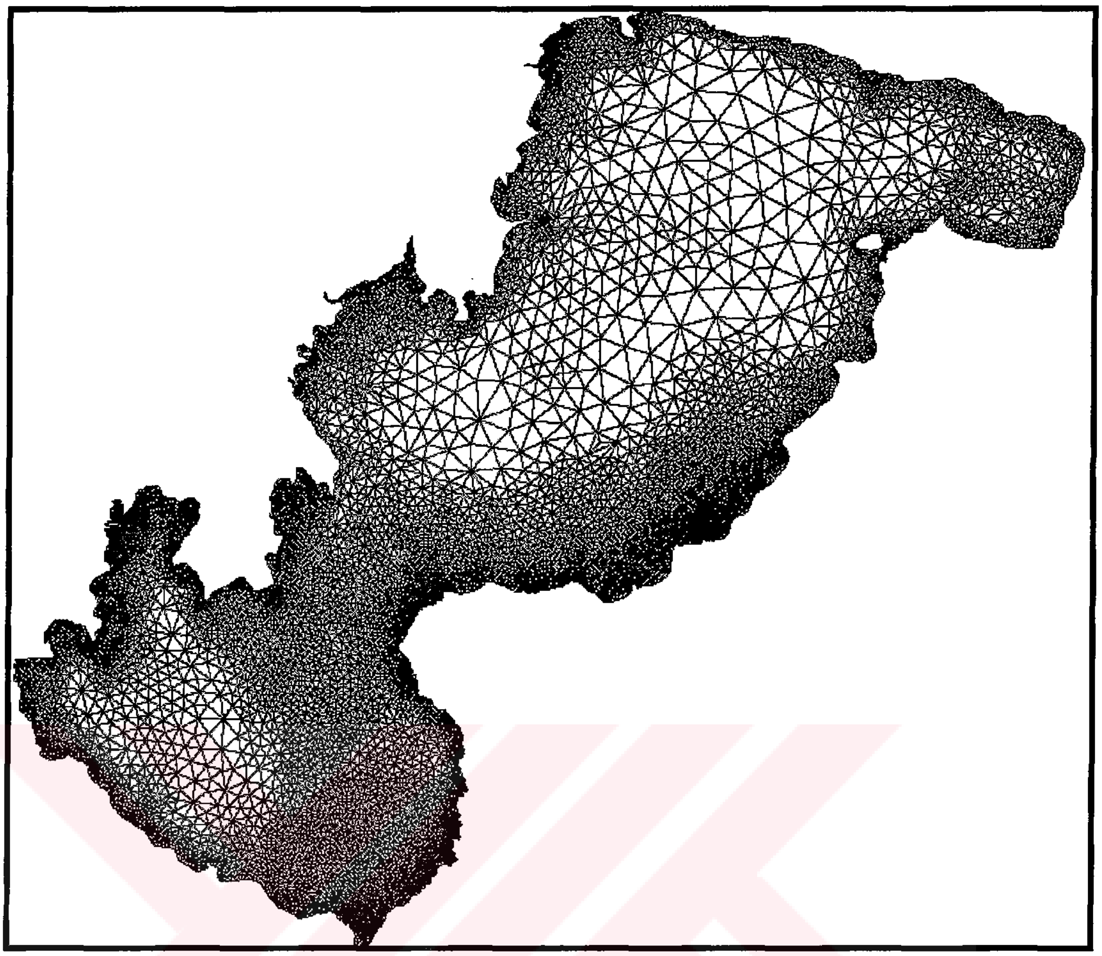

Figure 4.3 Aquadyn finite element mesh of Köyceğiz Lake with 12000 elements.

These criterias should be described briefly as:

- In order to define the bathymetry of lake, nodes must be inserted carefully. While inserting the nodes, links of element must be predicted. Unless the will be removed and new node will be inserted again.
- The hydrodynamic properties of shorelines, river mouths and channel inlet are greater at lake. Therefore condensation at these places are greater than other places. This is a stability criteria. If Pe is small enough, oscillations will not occur during the solution of advection-diffusion process.

The criterias that are described above are some of the general mesh generation and hydraulic modelling concepts. If these concepts are not taken into consideration during the mesh generation, the model may not run or the results of model may not be acceptable.

The generated mesh of Köyceğiz Lake is consist of 2017 nodes and 3656 elements (Figure 4.5).

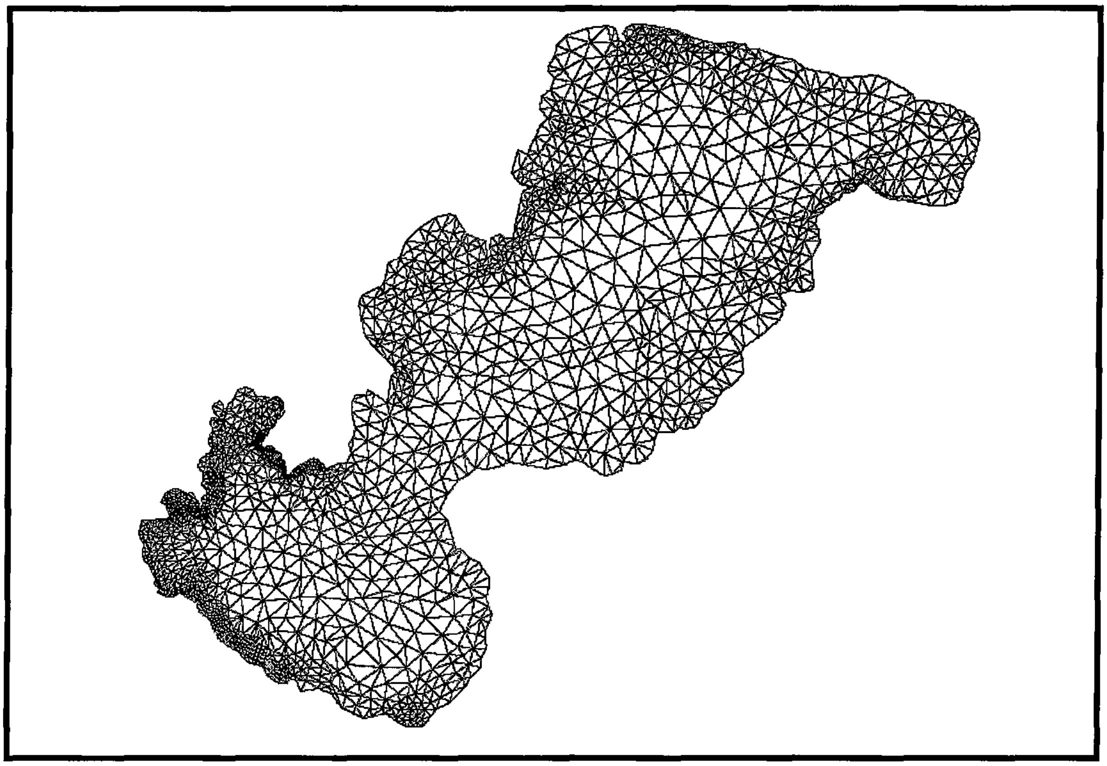

Figure 4.4 Aquasea finite element mesh of Köyceğiz Lake with 3656 elements.

Bathymetry reflects the bottom topography of lake. The water depth term at governing equations shows the importance of bathymetry values in model setup. The bathymetric map of lake was obtained from International Mediterranean Project.

The generated mesh was modified until it allowed to insert the bottom topography correctly. The interactive mesh generation property protected the data after inserting or deleting nodes.

When bathymetric corrections were completed, the contrast of mesh between the fast varied areas was obtained by inserting additional nodes. This is an smoothness criteria of mesh generation, and stability criteria of hydraulic modelling.

Fast varied bathymetry contour lines increases total node number and elements. The bathymetry lines defined at every 5 m.

Although the maximum depth of lake is about 36 m averaged value at deepest contour range was defined as 32.5 m. After the mesh generation, parameters are flow and transport model were defined. The bathymetry values over generated finite element mesh is seen in Figure 4.5.

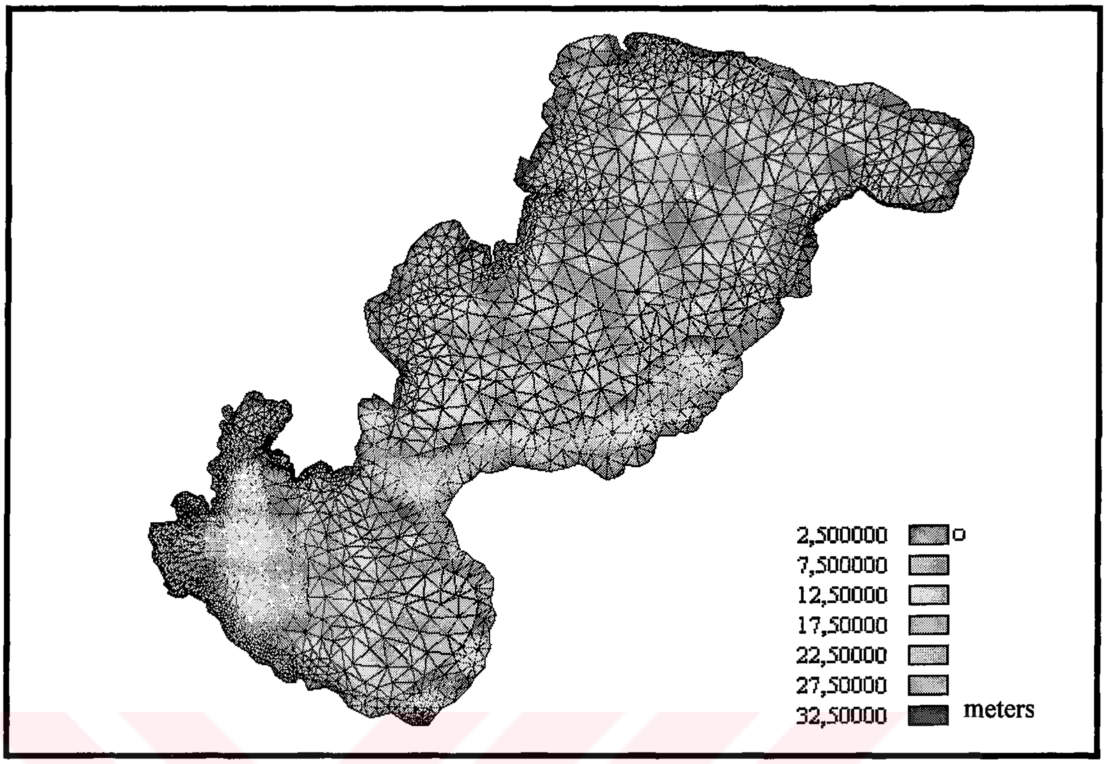


Figure 4.5 Inserted bathymetry values distribution on finite element mesh of the Köyceğiz Lake.

The refinements of fast varied sections are seen in Figure 4.6a and 4.6b.

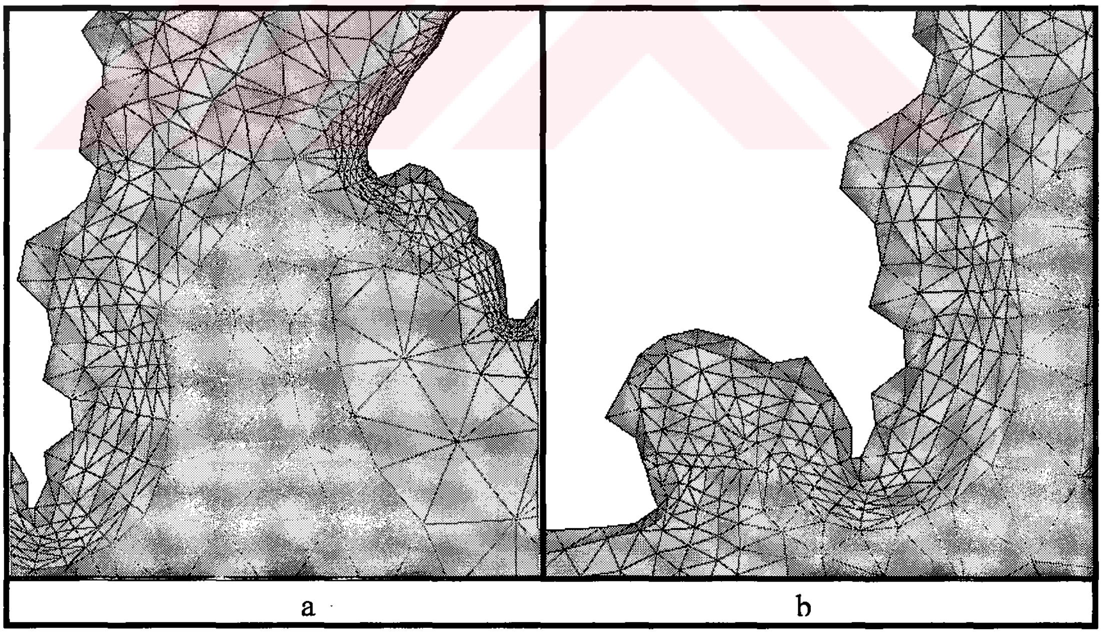


Figure 4.6a and 4.6b Refinements of bathymetry values of Köyceğiz Lake.

Model parameters adjusted with calculation and estimation of some terms.

Manning coefficient was defined as 0.025. It was converted to chezy coefficient which varies with depth values.

The iteration parameters were modified to obtain a stable solution.

Model calibration was constitude with several forces. The forces that are acting on lake are defined in 8 h run model as:

- Wind Force: The dominant wind over lake is in NE direction. The wind speed was defined as 3 m/s with $1.1*10^{-3}$ wind coefficient from field measurements (Kabdaşlı and others, 2000). This is a not a storm surge model, therefore the wind speed was defined as it.
- Tidal Wave: According to previous studies on area, it was seen that the water level changes with 0.15 m amplitude on lake due to tidal force from sea with a period of 8 h. These values are taken from previous field studies (Kabdaşlı, 2000).
- Rivers: The rivers flow parameters were defined in model with previous field measurements of DSI. From western part of lake, Namnam River was defined with 20 $m^3$/s flow quantity and from eastern part of lake Yuvarlak River was defined with 14 $m^3$/s flow quantity and from Northern part of lake Kargıcık River was defined with 8 $m^3$/s flow quantity. The salinity concentration of rivers was defined as 0 mg/l.
- Coriolis: Due to large dimension of basin the coriolis term was defined in the model. The averaged latitude for coriolis force is 36.5 degrees.

In flow process tidal wave is the boundary condition at channel inlet of lake. This time dependent flow boundary condition, so the solution of model unsteady.

In transport process the boundary condition is the salinity which was defined as 2.9 mg/l at the channel inlet of lake. Unlike flow boundary condition, it isn't time dependent.

As it is seen, the lake model depends on wind force, tidal wave, river inflows, and coriolis force. The results of model are compared with field measurements at Discussion part.

### 4.3.2 Model of Dalyan Channel

Numerical model of Dalyan Channel was developed with Aquadyn software package. The whole geometry of channel is larger than the modeled area. This is a reason of iteration process for generated finite element mesh.

While defining the external boundary, nodes were inserted in short distance. The density of some parts condensed and coarsed later.

The finite element mesh of channel was generated with automatic mesh generation property. The modelling criterias defined at lake model were also considered in channel model.

The generated finite element mesh is consist of 1632 nodes and 2541 elements Figure 4.7.

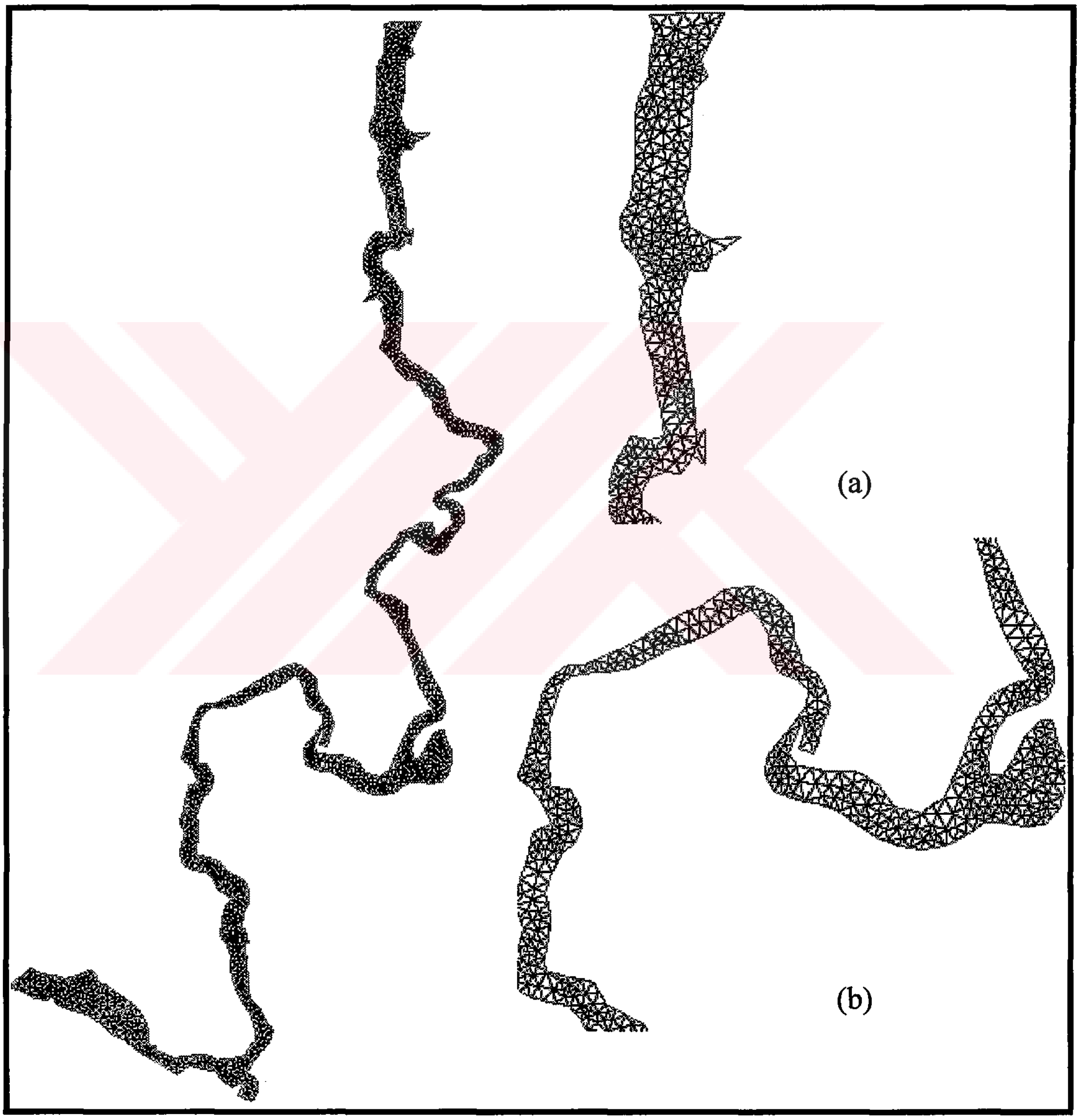


Figure 4.7 Aquadyn finite element mesh of Dalyan Channel and the refinements (a) and (b).

Model parameters adjusted with calculation and estimation of some terms.

According to the theoretical and the previous field measurements manning coefficient was defined as 0.025 at every nodes, longitudinal dispersion coefficient was defined as 20 $m^2/s$, and transversal was defined as 0 $m^2/s$.

Model calibration was constituded with several forces. The forces that are acting on channel were defined in 8 h run model as:

Tidal wave was seen that the water level changes with 0.20 ~ 0.40 m. amplitude on channel open section due to tidal force from sea with a period of 8 h (Kabdaşlı and others, 2000). In this model tidal wave with 0.2 m. amplitude at 8 h. periods was defined at downstream open section. The initial water levels at upstream and downstream sections were defined as 3.0 m. and 2.8 m. respectively as a result of flow through the channel from lake to lake while the tidal variation isn't seen.

The flow boundary conditions are free slip boundary condition (Un = 0) at left and right coasts of channel, water level at upstream open section, and time dependent water level at downstream open section (tidal wave).

In transport process the boundary conditions are the oxygen concentration which was defined as 10.68 mg/l at upstream open section and 10.15 mg/l at downstream open section. These values are taken from previous field measurements (Maktav and others, 1996). These conditions aren't time dependent.

Channel model depends on tidal wave, flow from lake to sea. The results of model are compared with field measurements at Discussions part.

# 5. DISCUSSIONS

## 5.1 Results of Köyceğiz Lake Model

The Lake Model was solved for 8 h. The time step was adjusted with courant criteria as 12 s. The results of iteration were stored at every 300 step which is equal to an hour. The flow model was solved with convective terms. This effects stability of iteration and tells us to decrease the timestep of flow model.

During the iteration process the stability criterias courant number and peclet number are under limitations. Therefore the results of numerical model are stable.

The results of water level variations, velocity vectors, and concentration values are discussed in 2nd, 4th, and 6th hours. The finite element mesh of lake is seen in Figure 5.1.

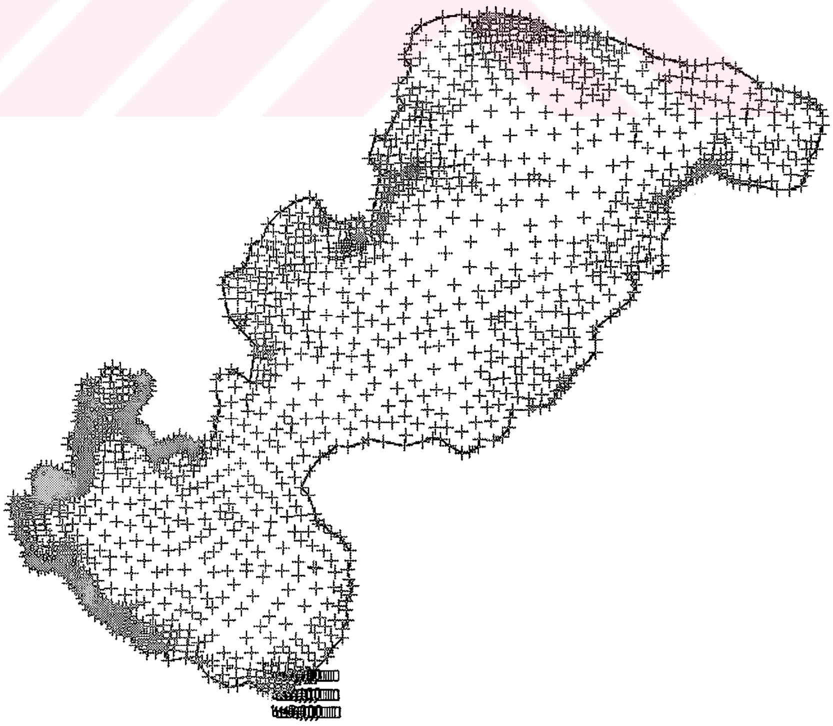

Figure 5.1 Finite Element Mesh of Köyceğiz Lake.

### 5.1.1 Water Level Variations at 2nd, 4th, and 6th Hours

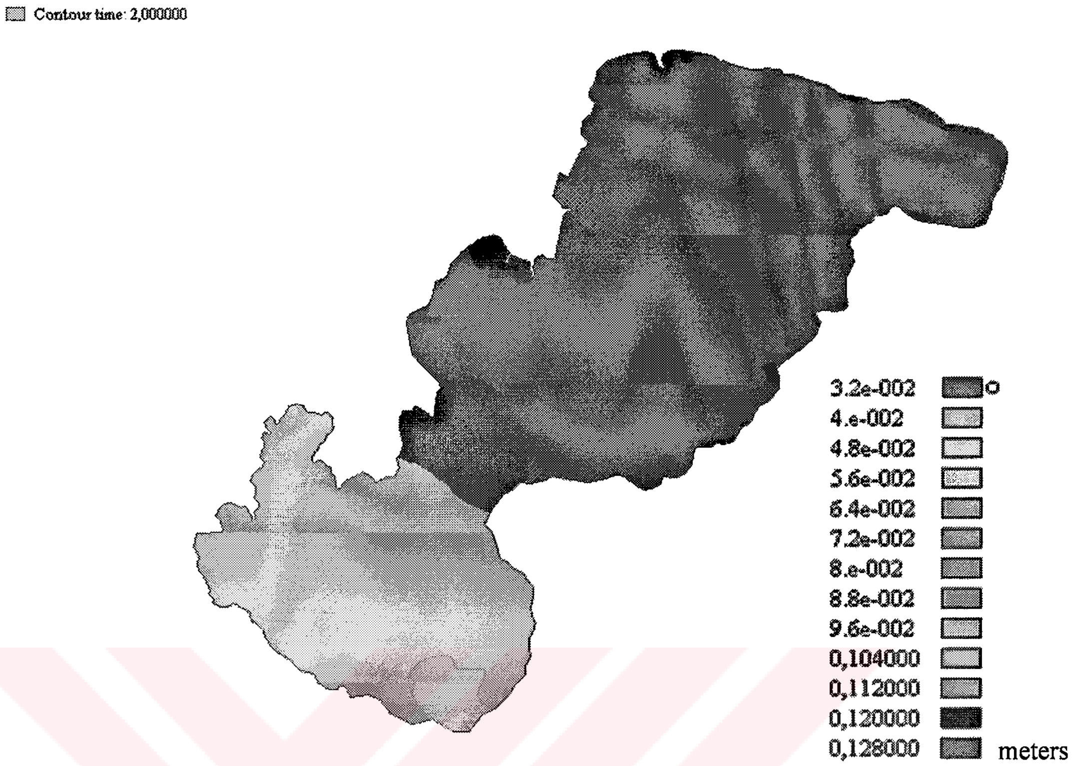




Figure 5.2 Water level variations at 2nd hour. Positive values indicate water level over mean water depth.

In the 2nd hour it is seen that water accumulates to the northeast part of the lake (Figure 5.2). This accumulation is a result of tidal wave.

As it was mentioned before period of tidal wave is 8 h and the peak value of tidal wave elevation at channel inlet occurs at 2nd hour. The results of water elevation in Figure 5.2 shows the surface elevation during the highest tidal wave elevation at channel inlet.

It is also seen that at channel inlet water level over mean value is about 0.0032 m. The wind force acting through northeast with 5 m/s reduces the accumulation at the northeast part of the lake and the slope of accumulation through channel inlet and north of lake is smaller.

The Figure 5.2 shows that the rivers at lake system with the discharges 20, 14, and 8 $m^3/s$ do not effect the water level elevation. The discharges of rivers would be effect with higher values.

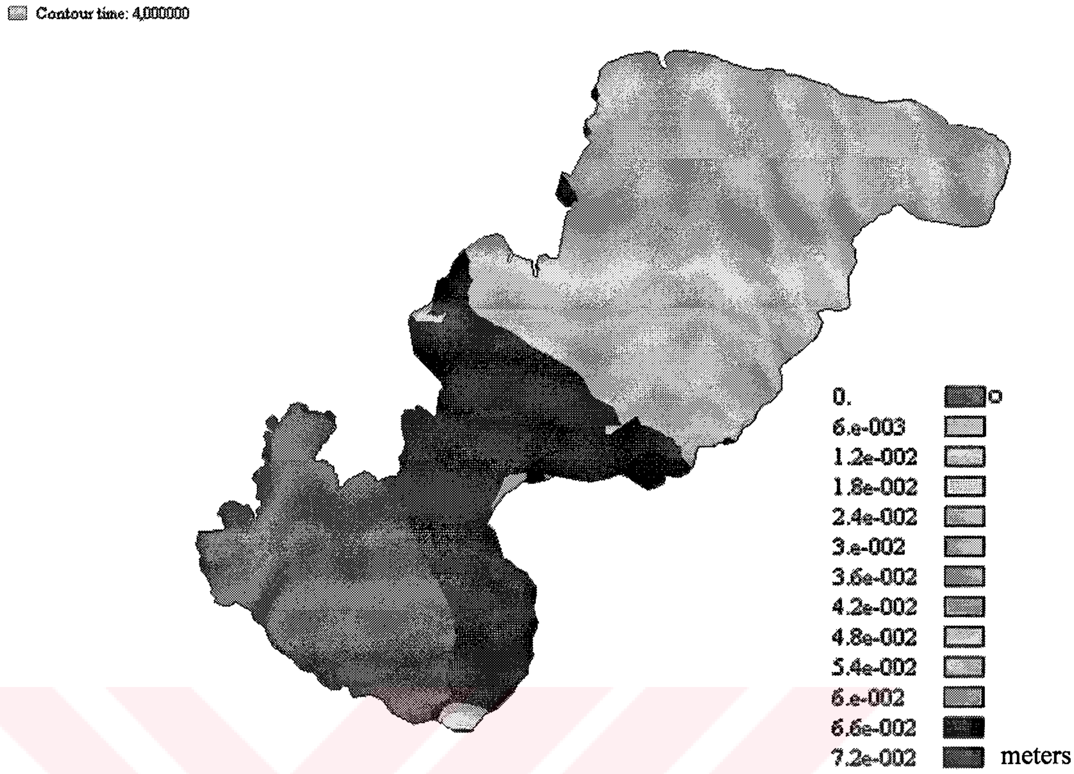


Figure 5.3 Water level variations at 4th hour.

In the 4th hour it is seen that water level elevation reduces at lake system variation are smaller than 2nd hour (Figure 5.3).

The water elevation at channel inlet is 0. As it was mentioned before period of tidal wave is 8 h and tidal wave elevation at channel inlet is zero as a result of half period.

After the 2nd hour water elevation at channel inlet begins to decrease (Figure 5.3).

As a result of reducing in tidal wave elevation at channel inlet, accumulated water at lake system begins to move through the channel inlet. By the movement of large water volume through the channel, water accumulates at south part of lake system (Figure 5.3).

The wind force acting on lake is also effective on movement of water from north to south (Figure 5.3).

The elevation values seen in Figure 5.3 are nearly mean water level. As a result of mean level lake system and movement from north to south, Kargıcak River, which drains into the lake from north coast, can be seen hardly.

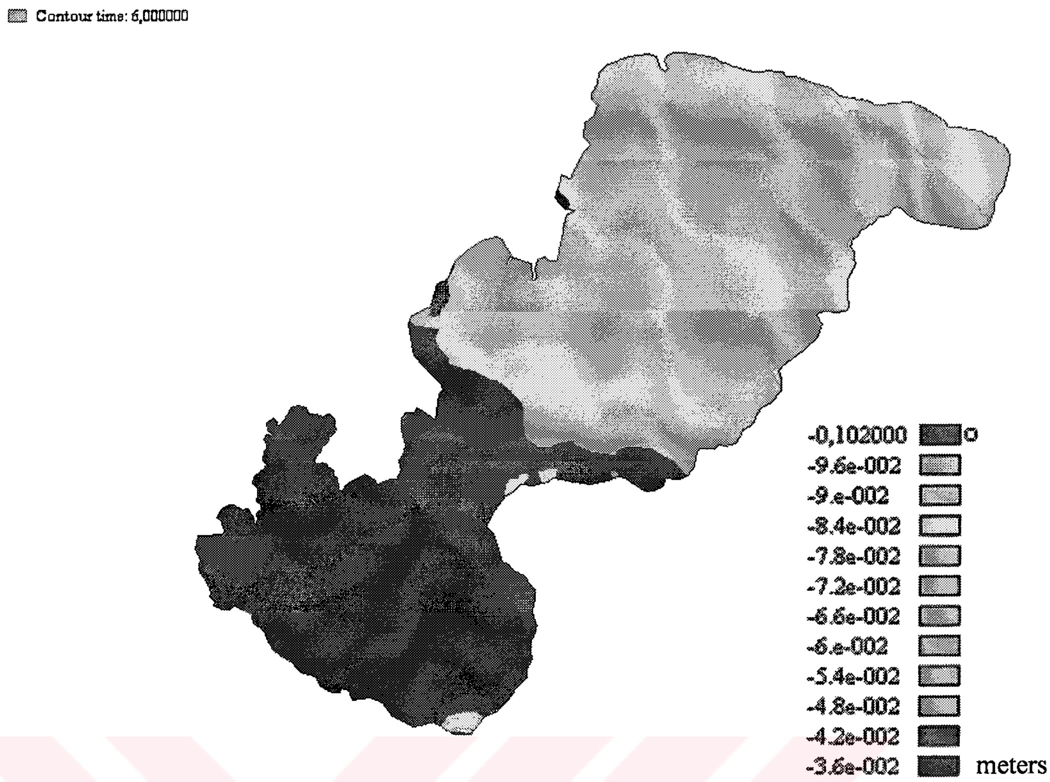


Figure 5.4 Water level variations at 6th hour. Negative values indicate the water level below the mean water depth.

In Figure 5.4 it is seen that water level elevation is below the mean water level of lake system. The water level elevation at channel inlet is -0.1 m.

At 6th is the trough of tidal wave at channel inlet. The water level elevation at channel inlet is the minimum water level of channel and lake system. The difference in water level causes water movement through the channel inlet (Figure 5.4).

As a result of accumulation in south part of lake, slope of surface is highly increasing near the channel inlet (Figure 5.4).

The wind forces are also effective in this accumulation. Therefore water level at northeast part of the lake is higher than the southeast part of the lake (Figure 5.4).

It is water movements at lake system are highly depends on tidal wave.

The cross sectional figures of lake system through southeast northeast direction at 2nd, 4th, and 6th hours are in Appendices A.

### 5.1.2 Velocity Vectors at 2nd, 4th, and 6th Hours

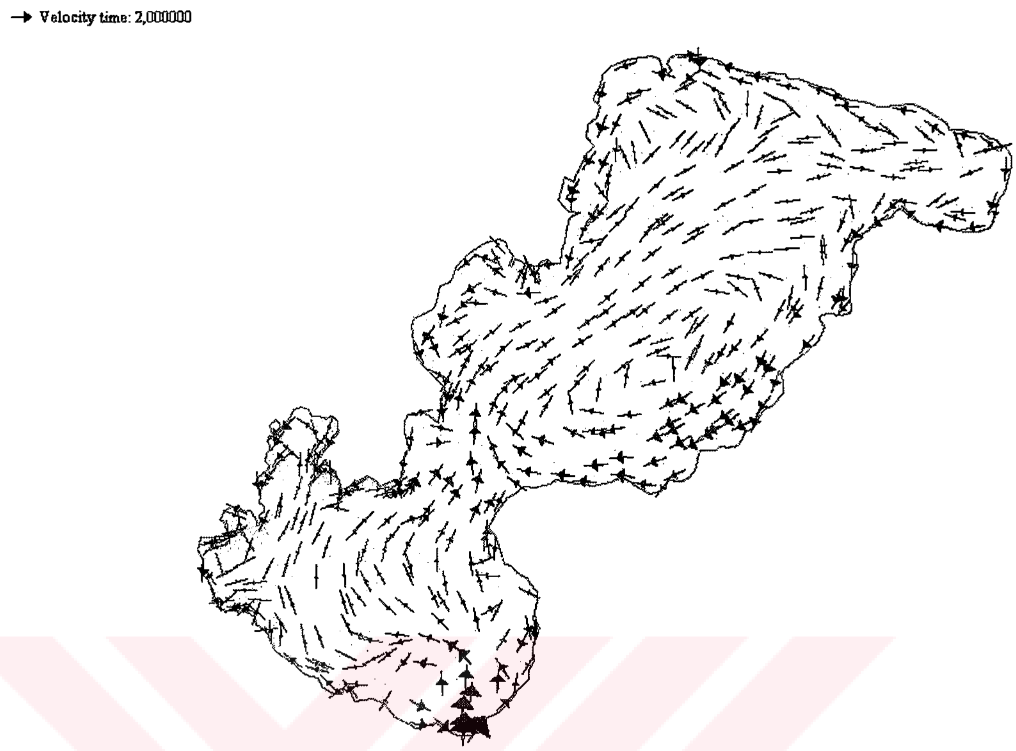


Figure 5.5 Velocity vectors at 2nd hour.

In the 2nd hour it is seen there are different current cycles in lake system with the effects of forces (Figure 5.5).

In the channel inlet it is seen that the velocity vectors are in channel lake direction. This is a result of tidal wave elevation at channel inlet (Figure 5.5). The peak water level at channel inlet explains this process. The water level at channel inlet is approximately 1 m/s.

It is also seen that currents are in two main groups in northeast trough and southeast trough. This is a result of bottom topography and geometry of lake. Additionally higher currents are seen near the coasts (Figure 5.5).

There isn't an important difference at river mouths. Flood waves might change the appearances of currents. Wind force acting through northeast is also effective at northeast parts of lake system (Figure 5.5).

At the narrow middle part of the lake velocities are higher an in direction of tidal wave currents of channel inlet (Figure 5.5).

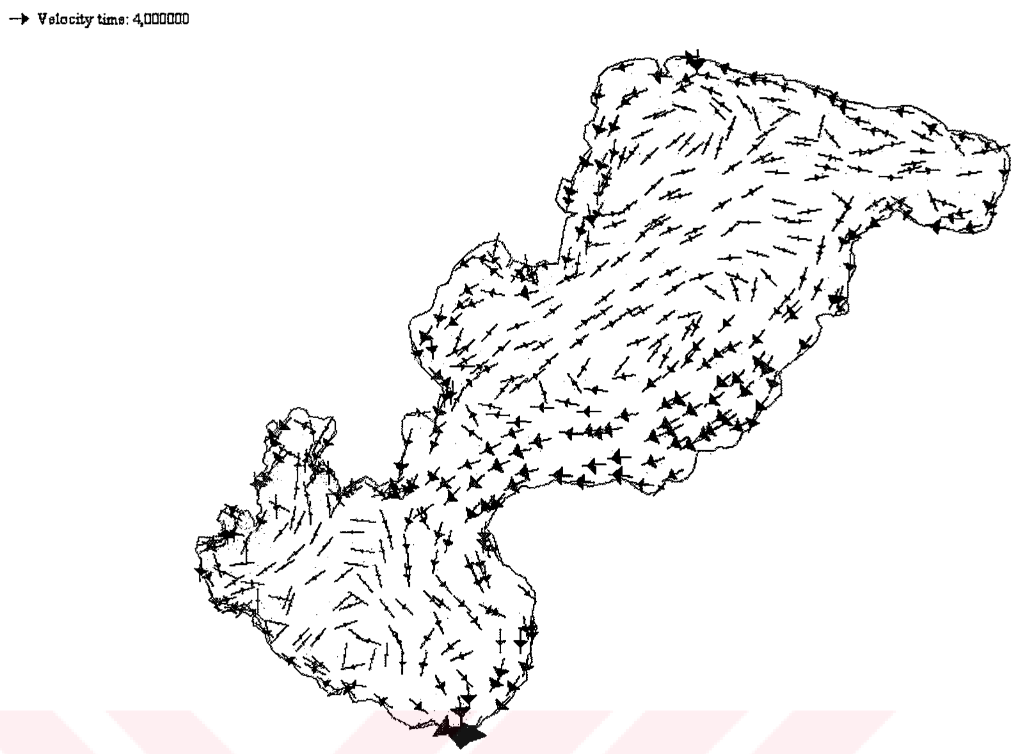


Figure 5.6 Velocity vectors at 4$^{th}$ hour.

In the 4$^{th}$ hour it is seen that currents are in direction from lake to channel at channel inlet (Figure 5.6).

As a result of tidal wave period, water moves from lake to sea after the 2$^{nd}$ hour, and therefore currents occur in north-south direction with additional wind and river discharge effects (Figure 5.6).

In Figure 5.5 it was seen that increase in tidal elevation causes currents in channel lake direction and as a result of close system circular currents occur. Two main circular currents occur in lake system as north part and south part. Bottom topography of two troughs at lake system and the narrow middle part of lake are the dominant factors of these two circular currents.

In Figure 5.6 it is seen that the tidal force change the circular currents in lake. The velocities at channel inlet, narrow middle part of lake and coasts of lake system are greater than the other parts of lake system (Figure 5.6).

The Kargıcak River's inflow can be seen clearly as a result of same direction with tidal wave currents (Figure 5.6).

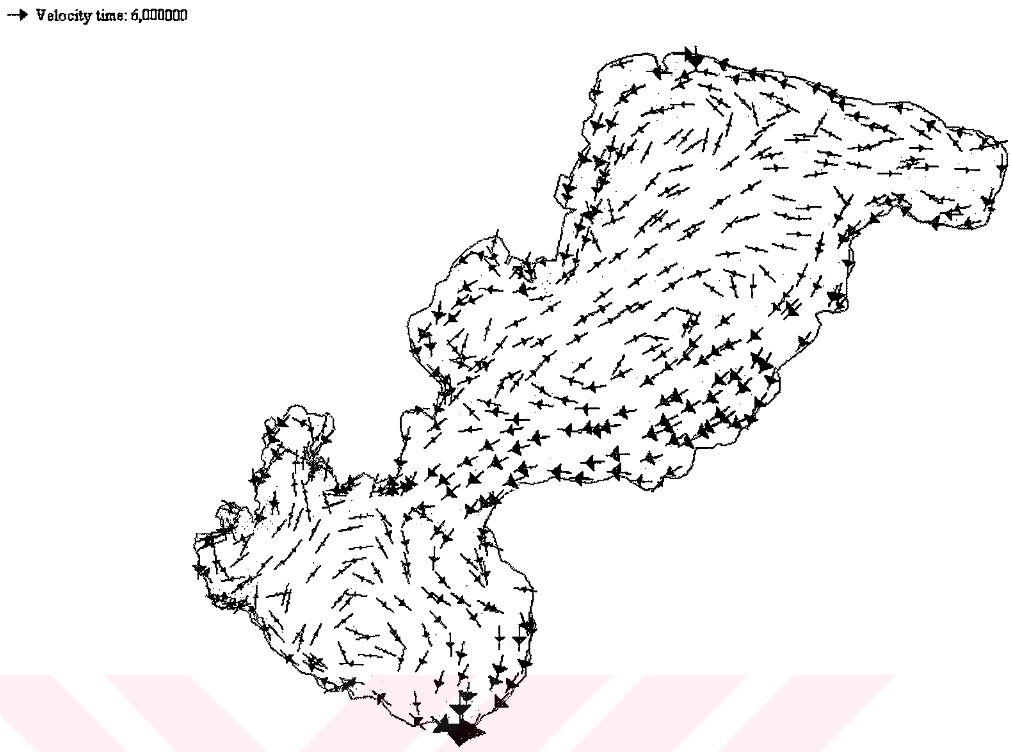


Figure 5.7 Velocity vectors at 6th.

In the 6th hour it is seen that currents are in the same with 4th hour from lake to channel (Figure 5.7).

At the 6th hour tidal wave period, water elevation at channel inlet is in minimum level. Therefore the directions of currents at 4th and 6th hour are nearly same. After the 6th hour water level begins to increase and the currents change direction to the lake.

As a result of irregular coast geometry, currents are seen in different directions at south part lake (Figure 5.7).

The current circulation is still seen at north trough this would be as a result of coriolis force acting on lake (Figure 5.7).

The velocity vectors at channel inlet cause vortexes (Figure 5.7). The vortexes at river mouths and channel inlet are seen in Appendix B.

The explanations of Figure 5.6 are also valid for the Figure 5.7. The velocity values at channel inlet and specified points are given in Appendices C.

### 5.1.3 Salinity Values at 2nd, 4th, and 6th Hours

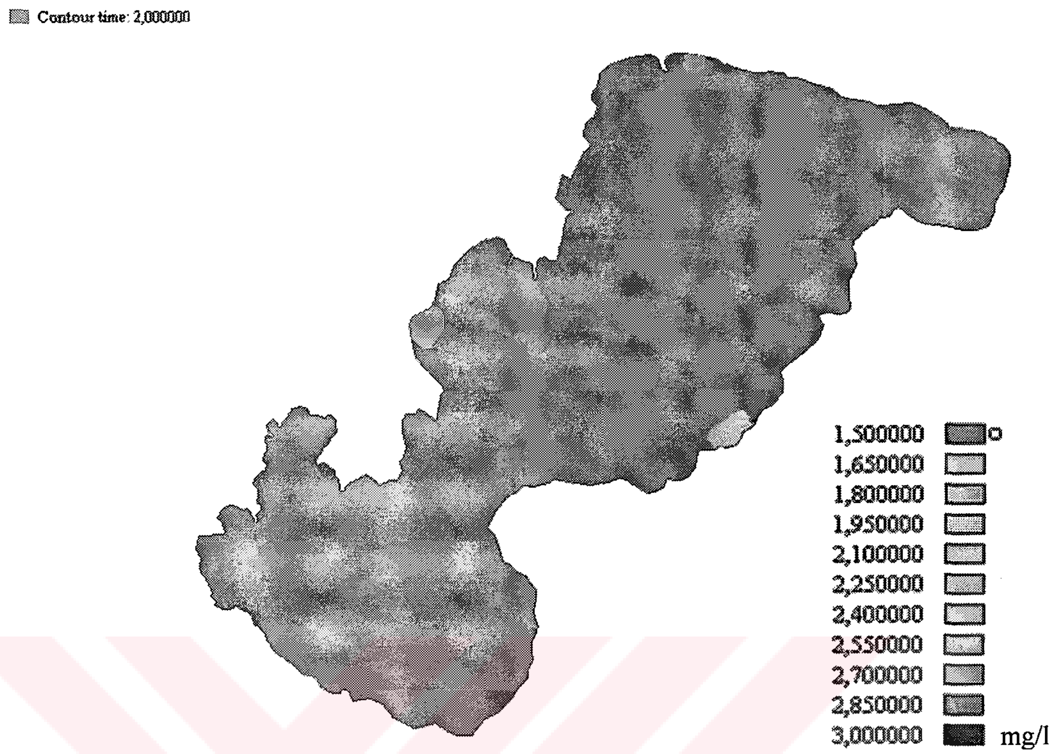


Figure 5.8 Salinity values at 2nd hour.

In the 2nd hour salinity value of lake is approximately 3.0 mg/l. The initial condition of transport model is 2.9 mg/l. The range of salinity between the zero concentrated rivers and the 2.9 mg/l lake system occurs in short distances (Figure 5.8).

The minimum concentration values are seen at river mouths with the 1.5 mg/l concentration value of salinity (Figure 5.8).

As it is seen the concentration, changes with the tidal wave variation at channel inlet and river inflow (Figure 5.8).

The higher currents at Namnam River from west and Yuvarlak River from east affect the transport process of salinity and lower concentration values are seen in wide range in river mouths. This shows that transport process highly depends on advection phenomena (Figure 5.8).

As a result of lower velocities Kargıcak River from north supports narrow lower concentration values at short distance in river mouth (Figure 5.8).

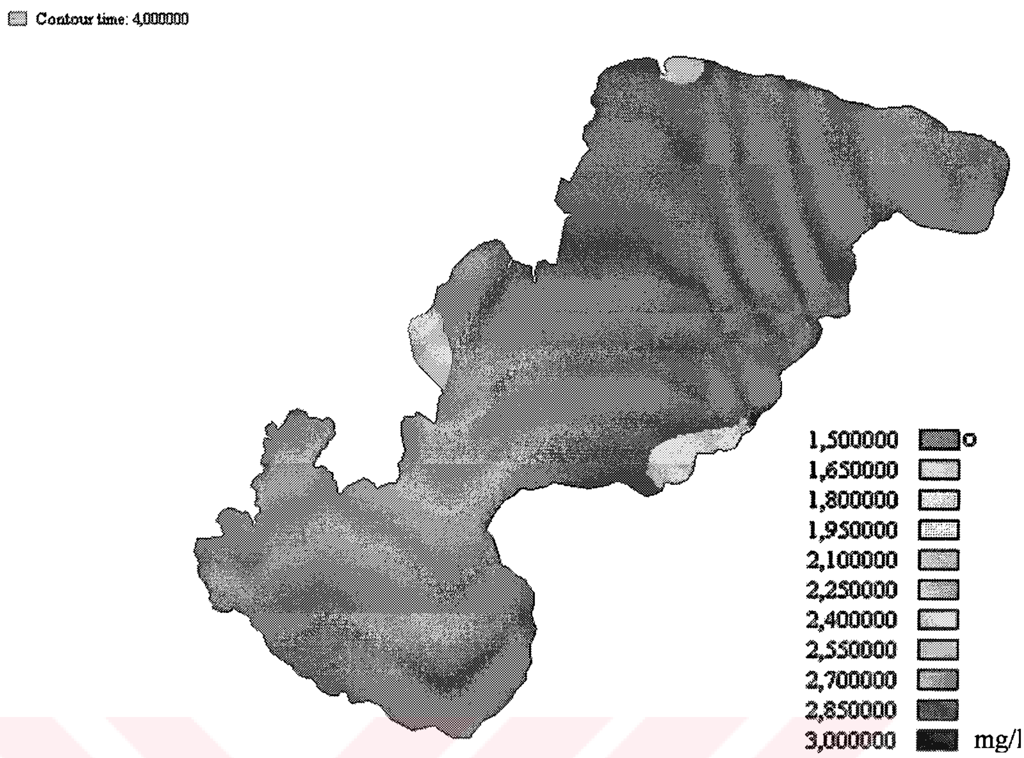


Figure 5.9 Salinity values at 4th hour.

In the 4th hour of transport model it is seen that concentration of lake reduces at places near the river mouths (Figure 5.9).

As it is seen in Figure 5.6 the currents are still in the same way from north to south. The result of current in coastal region is appeared in concentration variation at river mouths (Figure 5.9).

The concentration salinity at lake is generally same as 3.0 mg/l, and the concentration of river mouths are also the same as 1.5 mg/l (Figure 5.9).

The difference between the 2nd and 4th hours is the transition distance of concentration at river mouths. It is seen that the distance of transition is greater in than in the 4th hour (Figure 5.9).

Due to currents direction in coastal region (Figure 5.6 and 5.7) the concentration salinity is transported in northeast southwest direction (Figure 5.9).

It again shows that transport process at lake highly depends on advection phenomena (Figure 5.9).

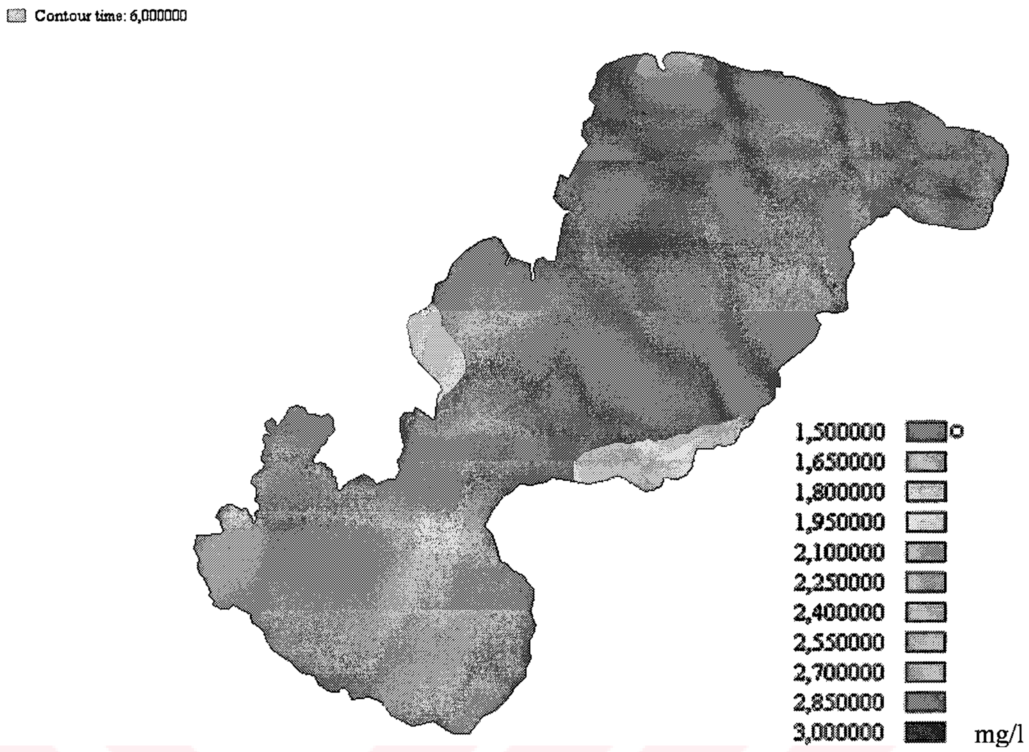


Figure 5.10 Salinity values at 6th hour.

In the 6th hour of transport model it is seen that the concentration of lake and river mouth have the same values as 3.0 mg/l and 1.5 mg/l, respectively (Figure 5.10).

The difference between 4th and 6th hours is wide transition distance of concentration (Figure 5.10). Transition of concentration is again in northeast southwest direction due to high current values at coastal region of lake.

It is also seen that the transition of concentration at Kargıcak River at north part of lake occurs through the west coasts of lake as a result of currents direction.

It is seen that concentration at lake depends on advective phenomena. The initial value of iteration and boundary conditions of channel inlet and rivers are defined with the previous field measurements. Field measurements at lake and channel is as 2.9~3.0 mg/l and 1.1 mg/l, respectively. The numerical results obtained with 8th run are 2.9~3.0 mg/l and 1.5 mg/l. As it is seen the results of numerical model and field measurements are similar.

### 5.1.4 Channel Inlet

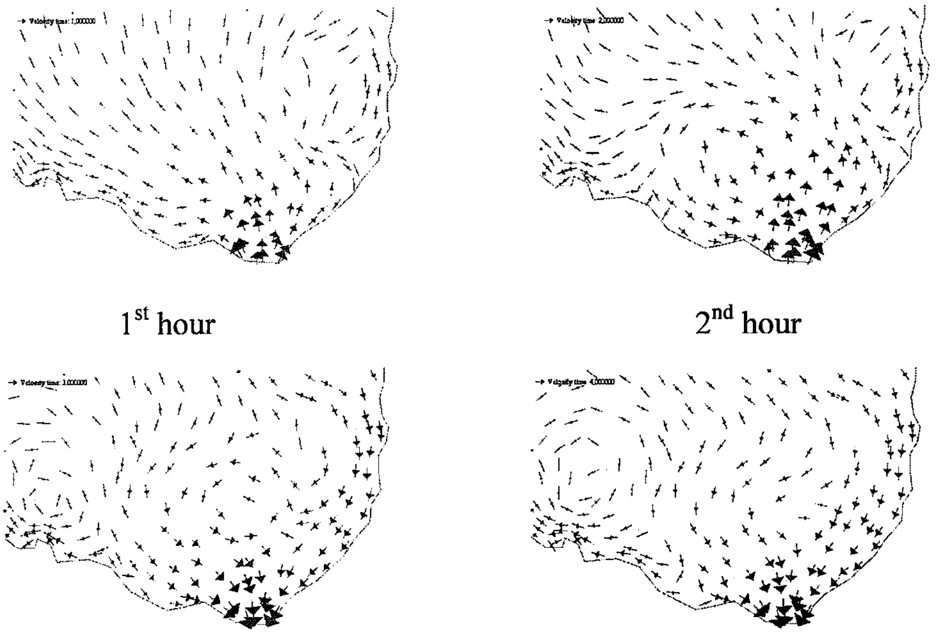

1st hour 2nd hour

3rd hour 4th hour

Figure 5.11 Velocity vectors variation at channel inlet due to tidal wave period.

The velocity vectors at channel inlet in half period of tidal wave are seen in Figure 5.11. It is seen that as a result of tidal wave elevation at channel inlet, velocity vectors change at 3rd hour to the opposite direction (Figure 5.11).

It is also seen that the streamlines are not parallel and vortexes are seen in different places (Figure 5.11).

In order to relate the results of tidal wave with hydrodynamic properties, one of the nodes at channel inlet was selected and the location of selected node is seen in Figure 5.12.

The velocity values in y direction at 1626th node are seen in Figure 5.13. The Figure 5.13 shows that velocity in y direction is greater during the first quarter of tidal wave. The maximum velocity in y direction is about 0.8 m/s.

The elevation values in y direction at 1626th node are seen in Figure 5.14. The figure shows the elevation of water at different time. According to the Figure 5.14 elevation in y is greater as a result of tidal wave elevation in channel inlet.

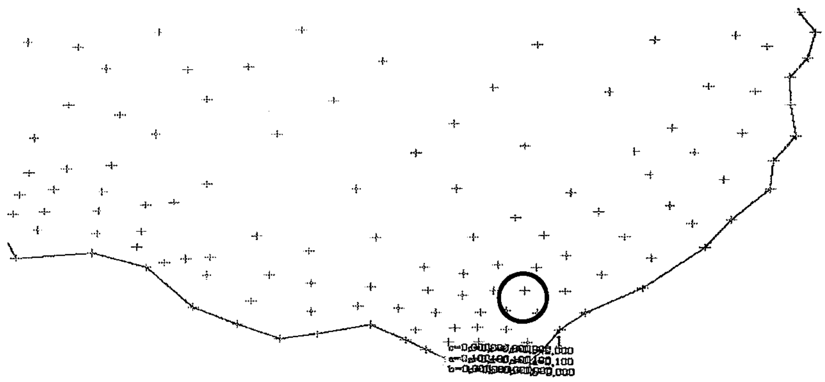

Figure 5.12 Location of 1626th node at channel inlet.

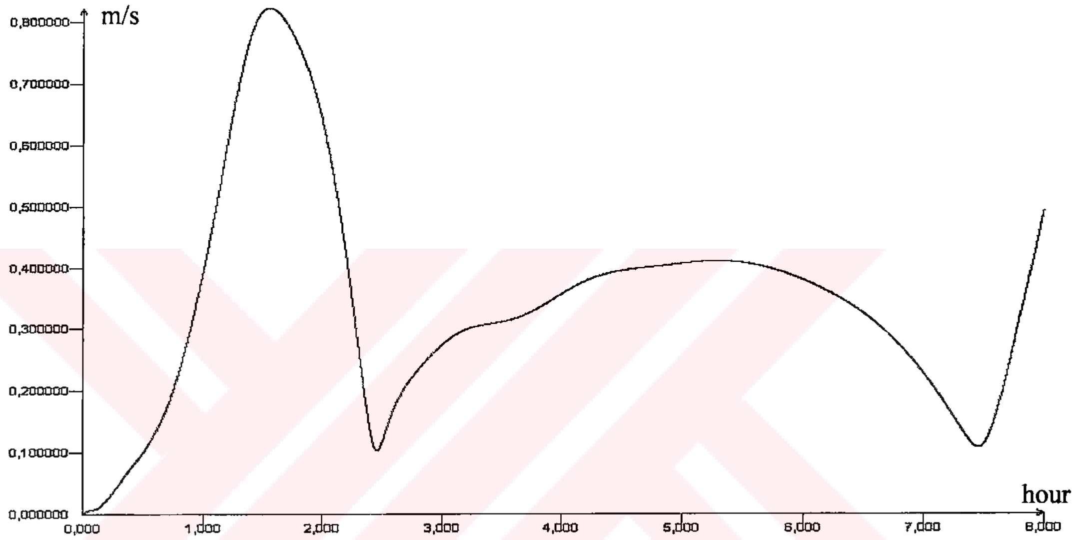


Figure 5.13 Velocities of 1626th in y direction (y axis) in 8 h period (x axis).

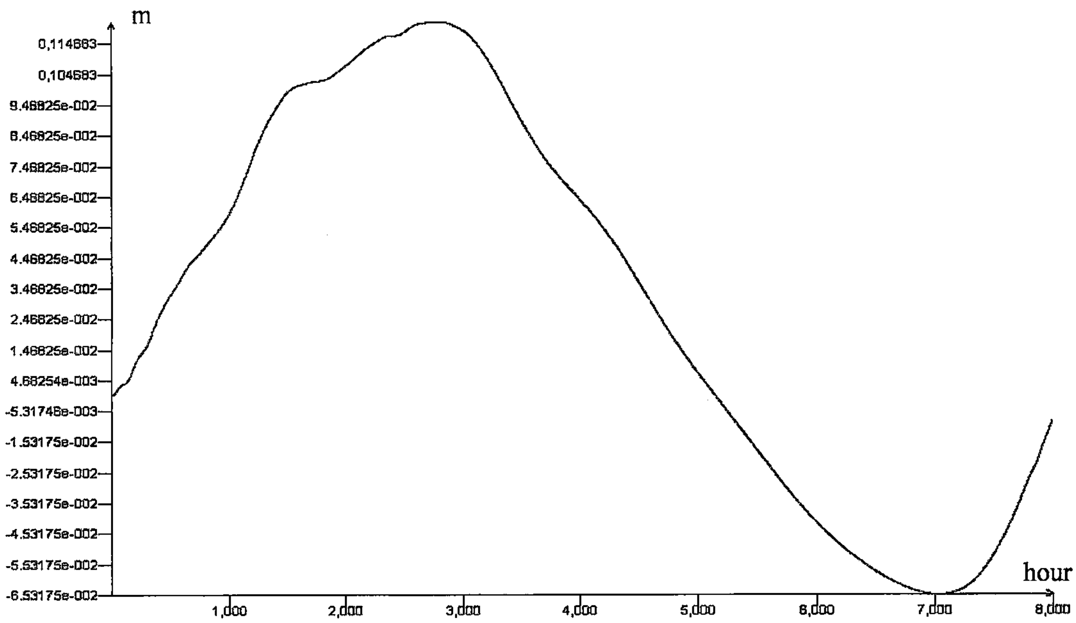


Figure 5.14 Elevations of 1626th node in y direction (y axis) in 8 h period (x axis).

## 5.2 Results of Dalyan Channel Model

Dalyan Channel was modeled with Aquadyn software package on triangular mesh elements (Figure 5.15). The Channel Model was solved flow and transport process for 8 h. The flow model was solved with flow from lake to sea and tidal wave elevation from sea to lake. The velocity vectors were change directions in iteration period. This shows the interaction of sea and lake during the tidal force period. The transport model was calibrated with oxygen concentration of channel inlet and sea. The dispersion parameters are calculated with the equations and the field measurements as. During the iteration process the stability criteria's courant number and peclet number are under limitations. Therefore the results of numerical model are stable. The results of water level values, velocity vectors, velocity values, and concentration values are discussed in 1$^{st}$, 2$^{nd}$, 4$^{th}$ and 6$^{th}$ hours.

Figure 5.15 Finite element mesh of Dalyan Channel.

### 5.2.1 Water Level Variations at 1st, 2nd, 4th, and 6th Hours

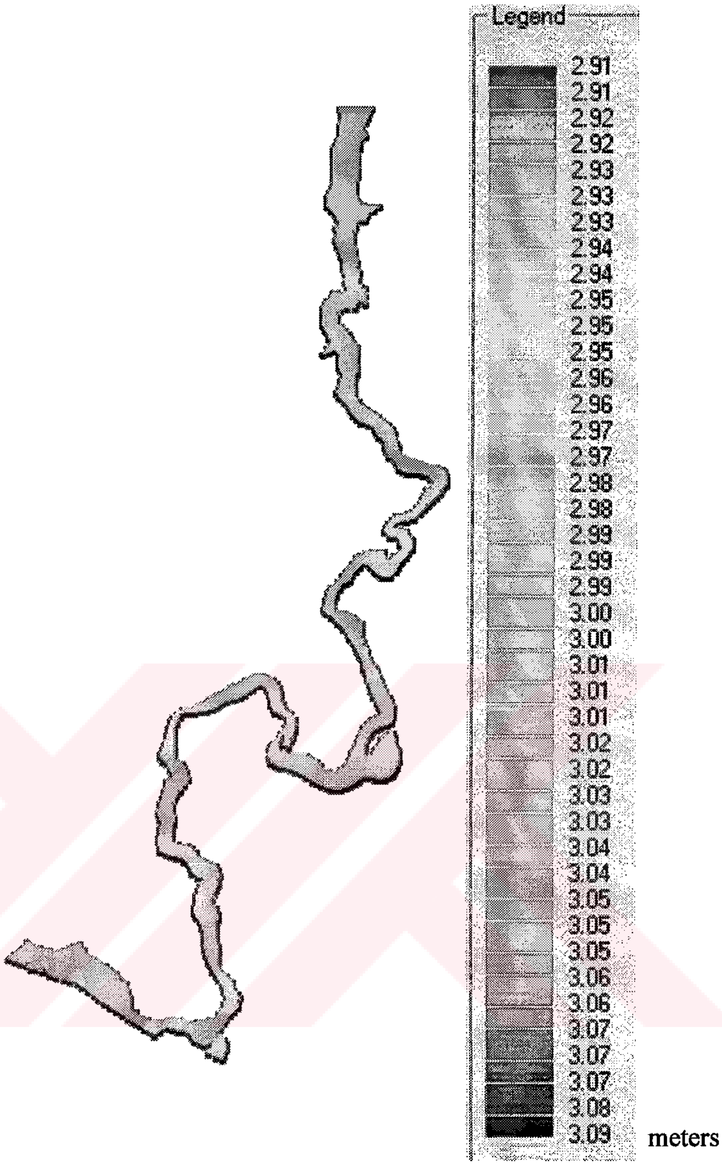


Figure 5.16 Water level variations at 1st hour. Values indicate the water depth.

In Figure 5.16 it is seen that water depth varies between 2.90 and 3.10 m. It is almost 3.0 m at every part. At narrow parts of the channel the depth of water will be higher if contraction slowly occurs. At some parts water level at narrow parts is smaller than the closer parts. This is a reason of tidal wave and lake sea interaction.

There are some parts with 3.10 m water depth at downstream of channel. The reason for this depth is the interaction of currents from sea and lake at this part.

In Figure 5.16 it is clearly seen that water level is same as 3.0 m at each the part of the channel.

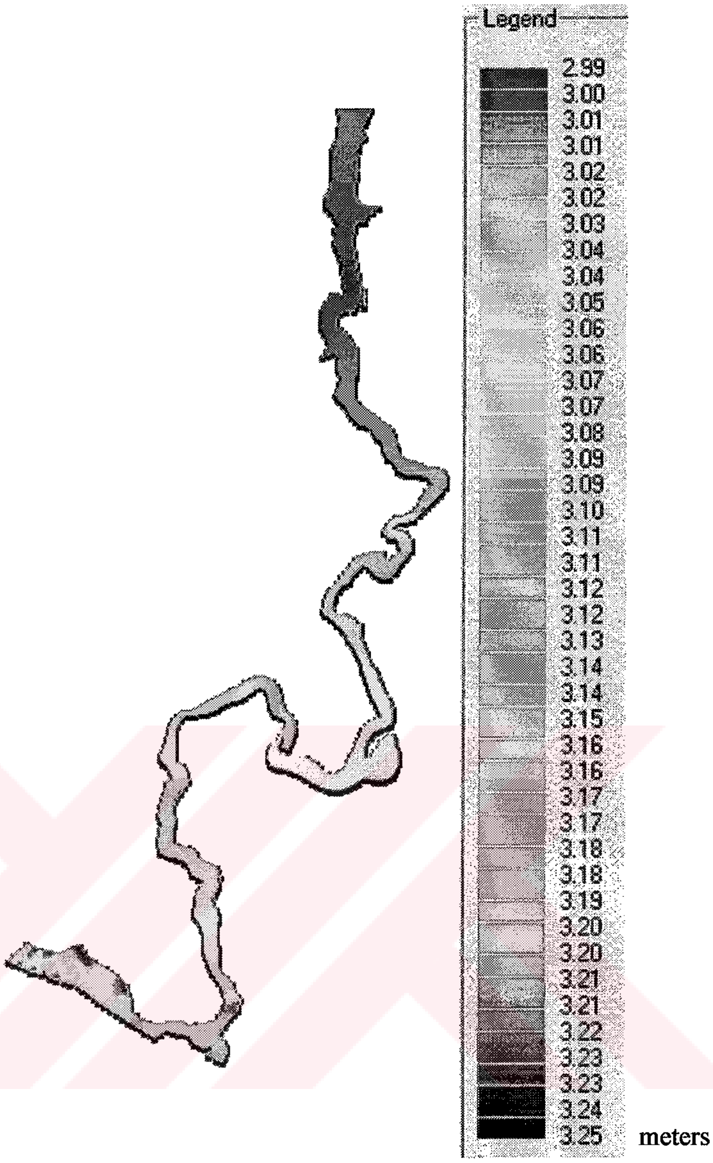


Figure 5.17 Water level variations at 2nd hour. Values indicate the water depth.

In Figure 5.17 it is seen that water level varies between 3.0 m and 3.25 m. The difference between the 1st and 2nd hours is the slope of water surface. As a result of tidal wave at sea open section the water moves from sea to lake and cause water depth increase at channel.

Tidal wave period is 8 hour. At the 2nd hour the wave reaches to its highest elevation as 3.25 m. Therefore the water depth at 2nd hour at channel are the higher values (Figure 5.17). Although the highest water elevation was defined as 3.2 m at open section, the depth of water at some parts is higher than 3.2 m as a result of channel geometry.

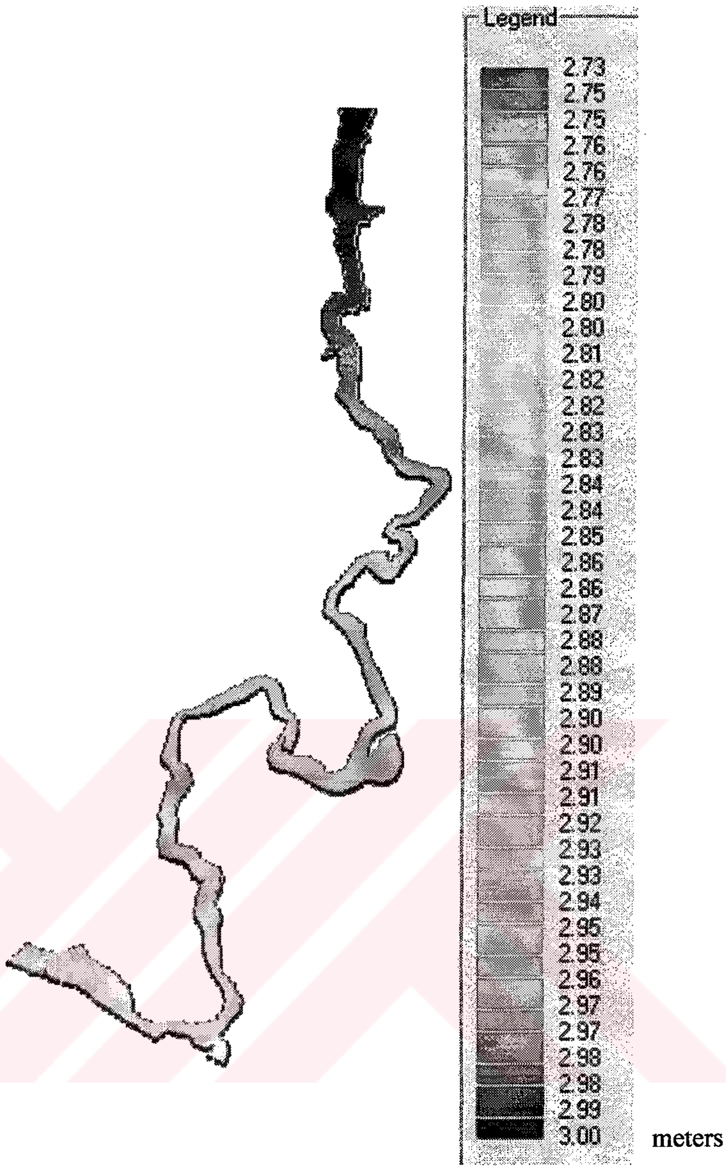


Figure 5.18 Water level variations at 4th hour. Values indicate the water depth.

In Figure 5.18 it is seen that depth of water again reduces and it is almost 3.0 m at sea and lake open sections.

At the same parts of downstream section water level is smaller than the others. The reason for this water level variation is the geometry of channel as it was mentioned before (Figure 5.18).

At the upstream section of channel water level is nearly same as 2.98 m between the middle of channel and lake open section (Figure 5.18).

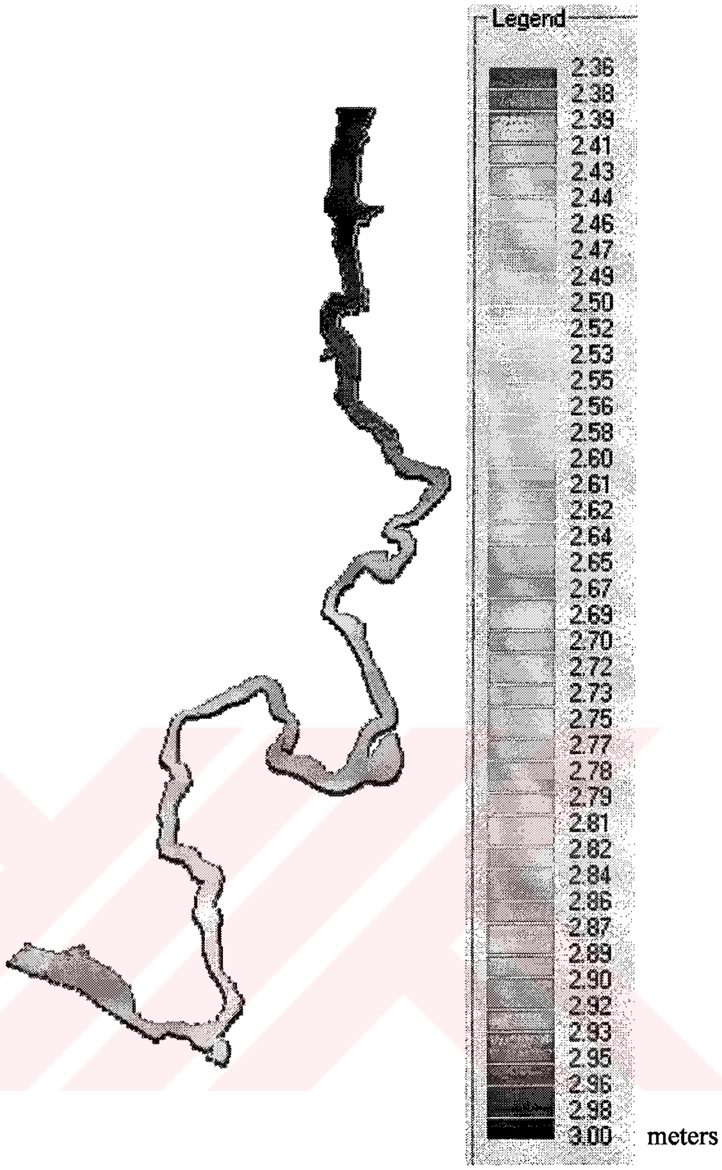




Figure 5.19 Water level variations at 6th hour. Values indicate the water depth.

In Figure 5.19 it is seen that water level varies between 2.35 m and 3 m. The tidal wave elevation at 6th hour is the trough. Therefore the values at this time are the lowest values of tidal wave period.

At the sea open section the water depth was defined as 2.4 m as boundary conditions. The reason for lower value than boundary section at closer parts is the channel geometry (Figure 5.19).

It is also seen that slope of water surface is regular at this time (Figure 5.19).

### 5.2.2 Velocity Vectors at 1st and 2nd Hours

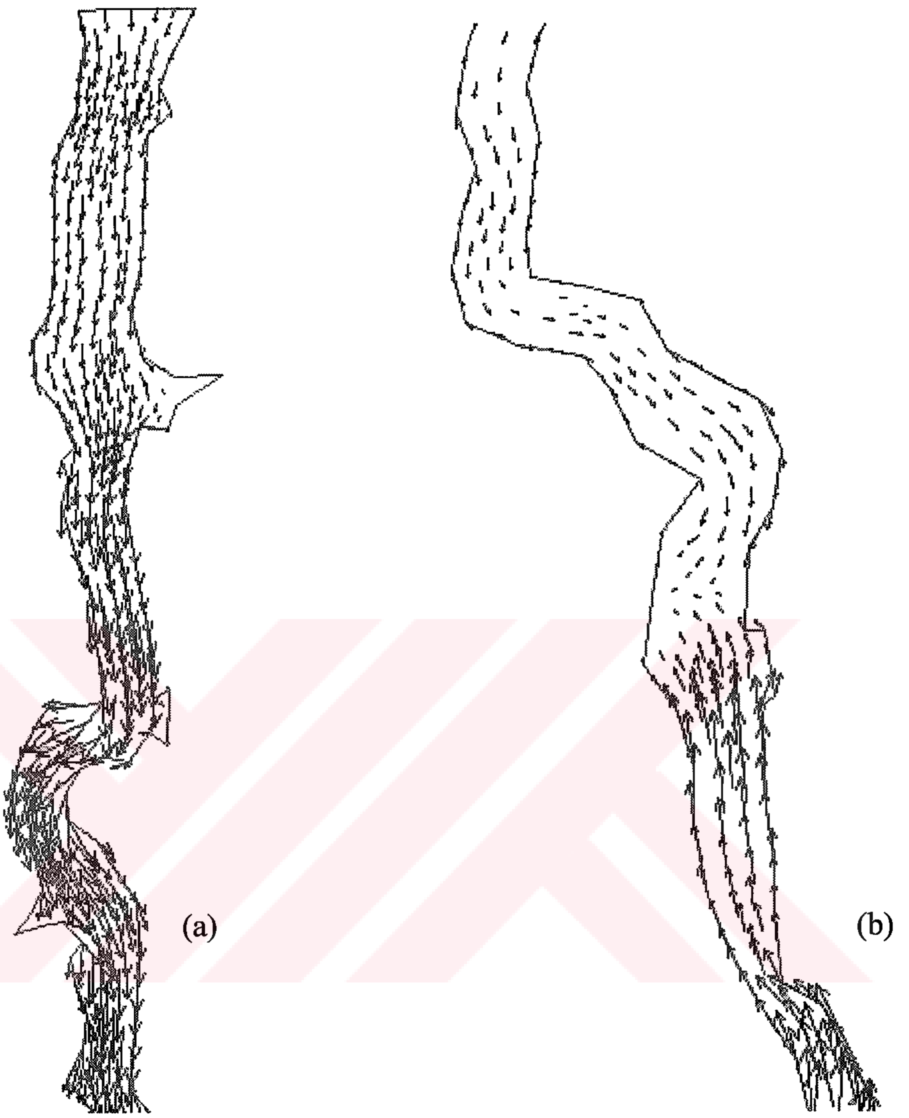


Figure 5.20a and 5.20b Velocity vectors of lake open section (a) and sea open section (b) at 1st hour.

Figure 5.20a shows the currents at the lake open section in the 1st hour. The currents from lake to sea occur as a result of channel slope and higher water elevation of lake. The currents from sea to lake occur as a result of tidal wave elevation at open sea.

In Figure 5.20a and 5.20b the sea and lake interaction is seen clearly. The water level at downstream slowly increases to the 3.2 m. During this increase the currents from downstream to lake begins (Figure 5.20b).

Interaction of the currents from lake and sea are seen in Figure 5.20b. When the currents from lake and sea meet, they were deflected to the external boundary of channel (Figure 5.20).

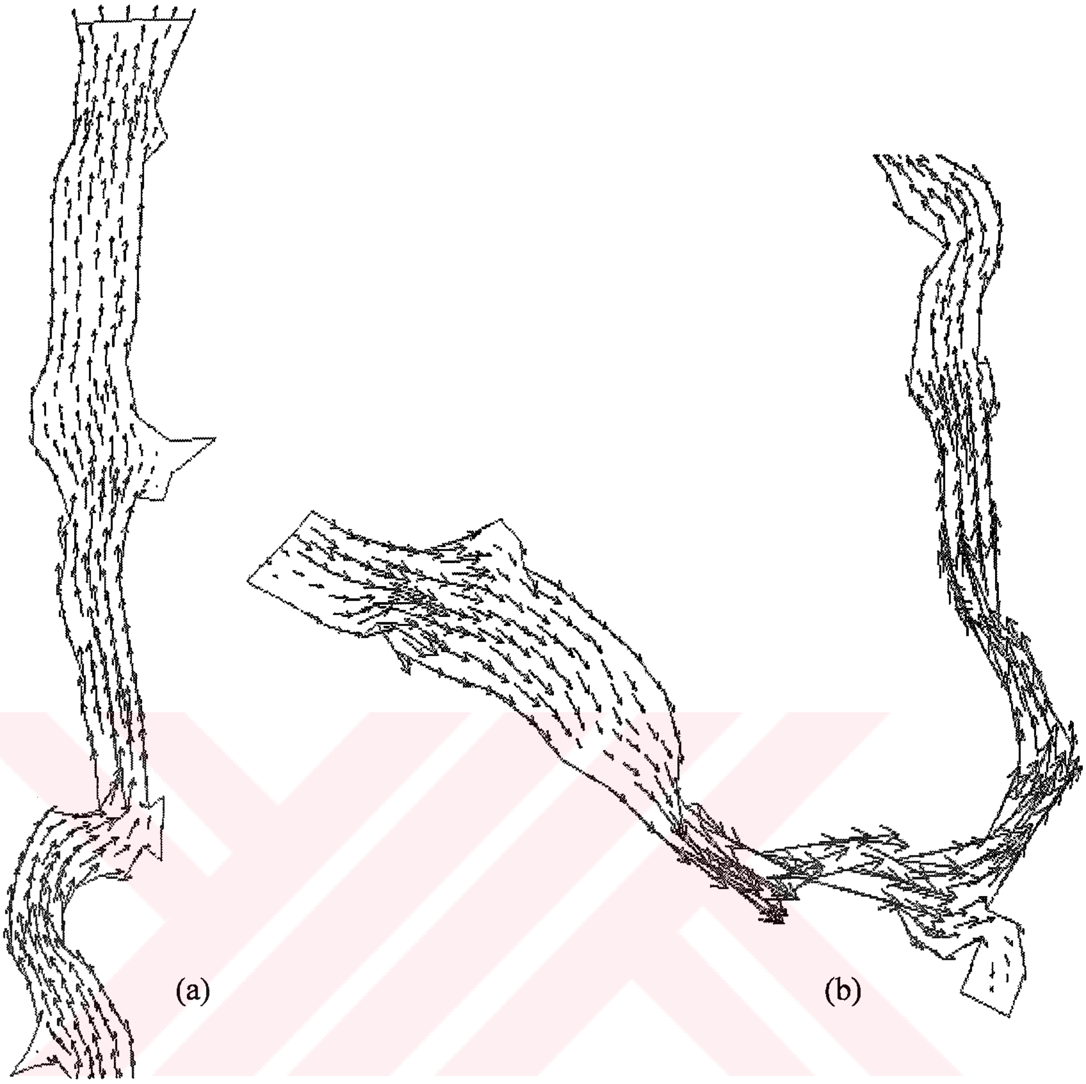


Figure 5.21a and 5.21b Velocity vectors of lake open section (a) and sea open section (b) at 2nd hour.

In Figure 5.21 it is seen that velocity vectors are in channel are completely in direction from sea to lake. The tidal wave elevation at 2nd hour is the highest value of water level as 3.20 m at open section of sea. The water level was defined as 3.0 m at the lake open section. In Figure 5.21b the water values are higher as over 1.0 m/s at narrow sections than the wide sections.

As a result of wall boundary condition, Un = 0, velocity vectors at external boundaries are parallel to the external boundary.

Velocity vectors don't effect the indentation of channel. The inner parts of channel only affected by currents when the interaction of currents from lake and sea occurs near the mouth of these indentations. As a result of sea-lake interaction, currents were deflected to these inner regions.

### 5.2.3 Velocity Values at 4th and 6th Hours

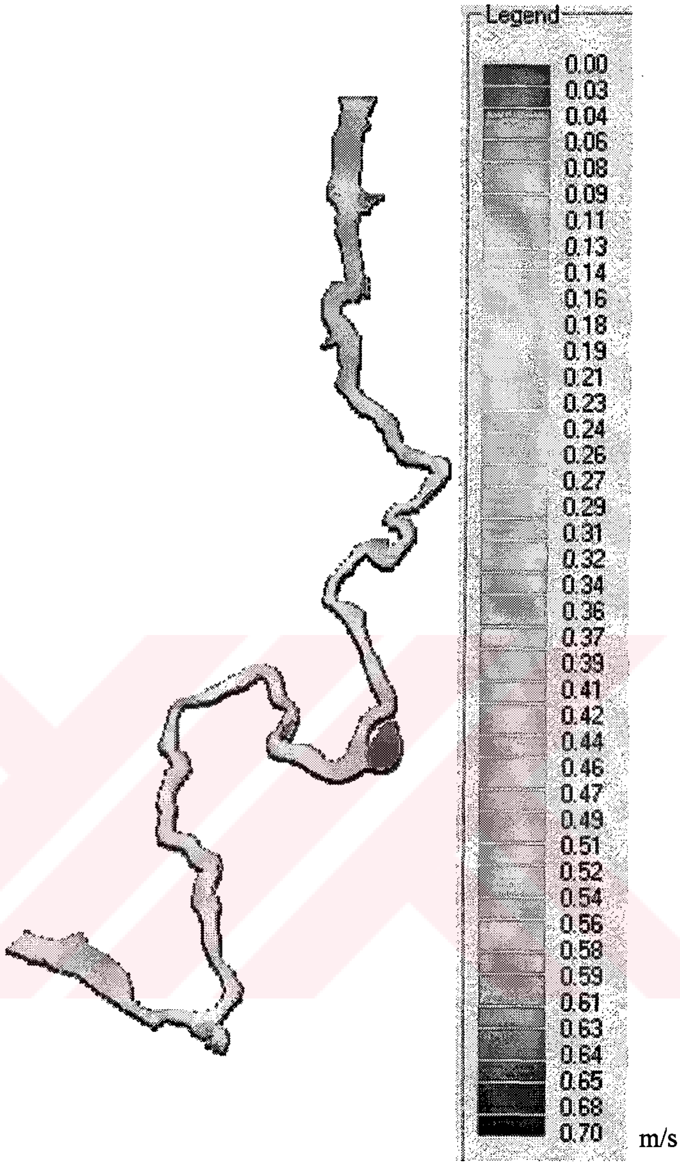


Figure 5.22 Velocity values at 4th hour.

In Figure 5.22 it is seen that water velocity varies between 0.04 m/s and 0.7 m/s.

The highest velocities are seen at narrow sections of channel. The lowest velocities are seen at inner parts of channel and indentations.

Due to tidal period the water level at channel is almost same as 3.0 m, and the currents at this time is smaller as a result of same water level at downstream and upstream sections (Figure 5.22). The zero velocities seen at upstream open boundary is the result of same water level.

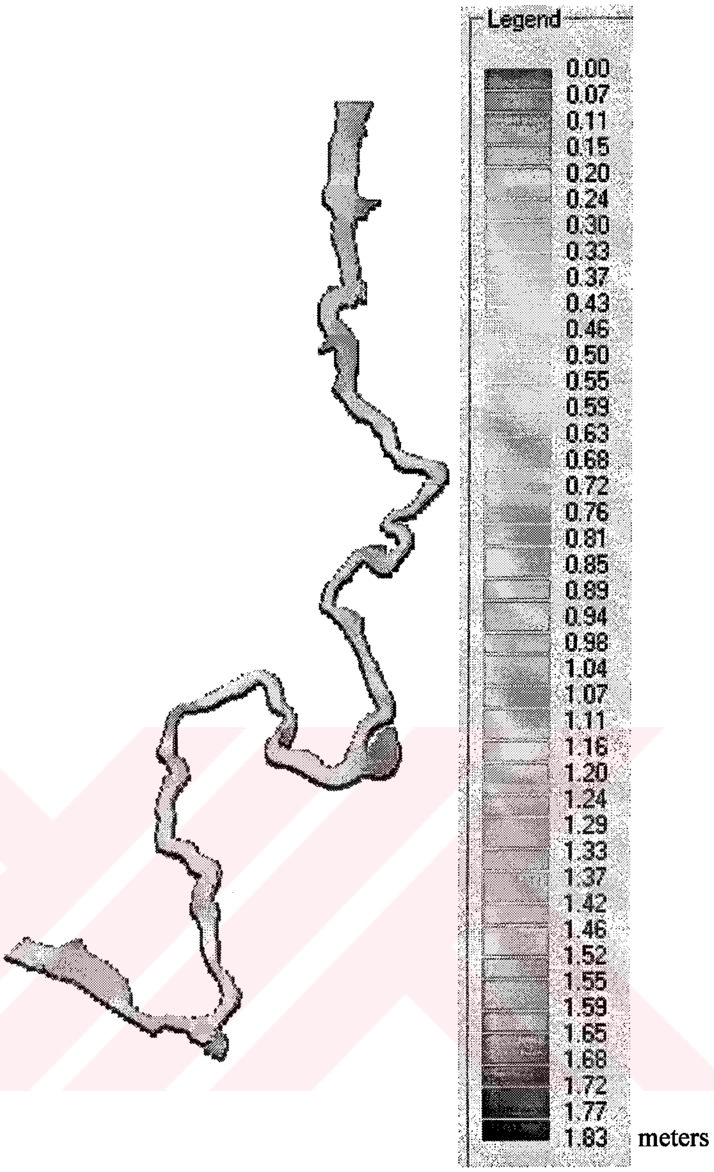


Figure 5.23 Velocity values at 6th hour.

In Figure 5.23 it is seen that water velocity varies between 0 and 1.83 m/s at 6th hour.

During the tidal wave period at the 6th hour is the minimum water elevation as 2.40 m is seen at downstream open section. As a result of surface water slope, water moves with higher velocities at this time (Figure 5.23).

The highest velocities at channel are seen at narrow sections and lowest at wide and inner regions (Figure 5.23).

### 5.2.4 Oxygen Values at 2nd and 4th Hours

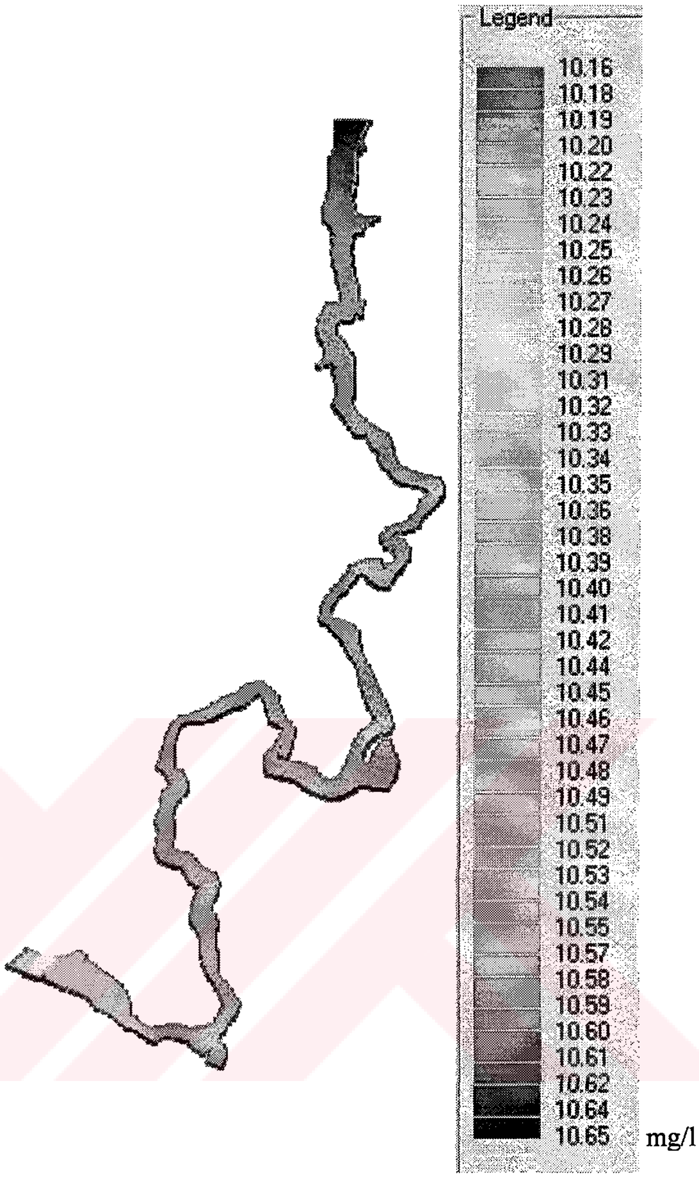


Figure 5.24 Concentration of oxygen at 2nd hour.

In Figure 5.24 it is seen that concentration at 2nd hour varies rapidly at downstream part of channel.

The initial concentration value at channel is 10.65 mg/l, and the boundary conditions of oxygen concentration at upstream and downstream is 10.65 mg/l, 10.18 mg/l, respectively.

The concentration of oxygen can't reach to the middle region of channel. There are several reasons for this such as tidal wave period, wave elevation, dispersion coefficients, and geometry of channel.

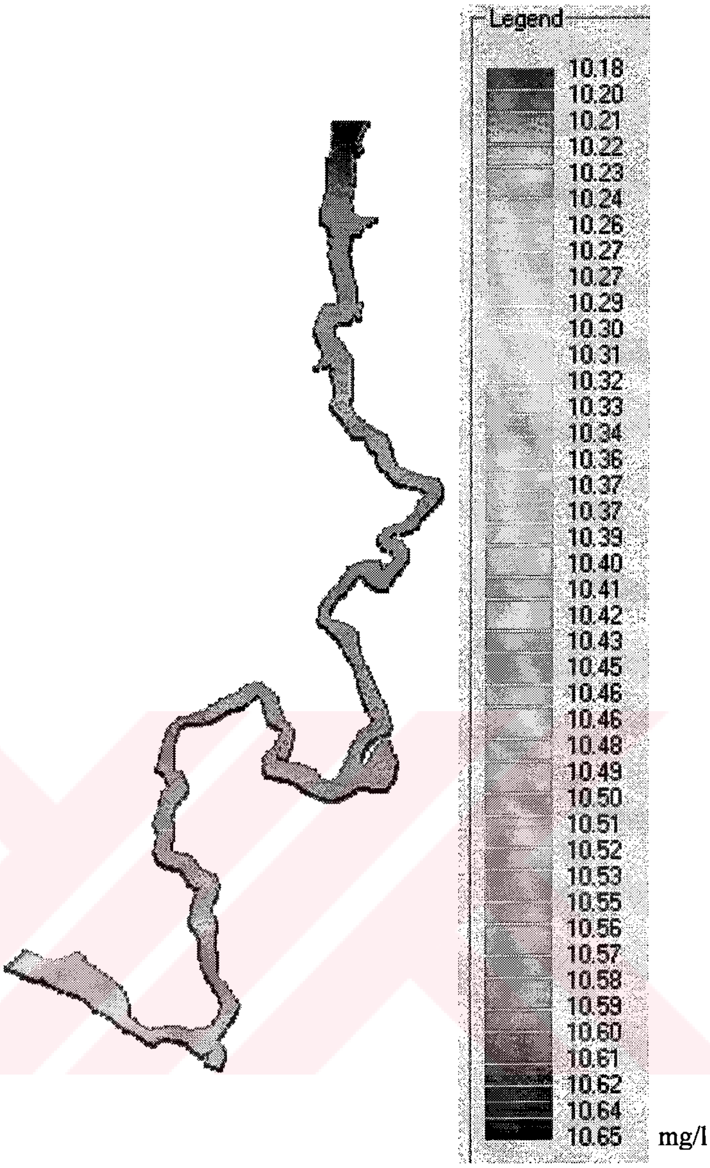


Figure 5.25 Concentration of oxygen at 4$^{th}$ hour.

In Figure 5.25 it is seen that there isn't an important change in concentration of oxygen.

The range is still the same as seen in Figure 5.25. It is seen that there is transition at a part of downstream region (Figure 5.25).

The results of transport model of channel show that oxygen concentration increases coming closer to the lake. The reason for this areal distribution is the interaction of freshwater of lake and seawater.

It is also seen that transport on channel highly depends on diffusion. As a result of this discussion the dispersion parameters should be effect in longer iteration solutions.

## 5.3 Comparing The Numerical Results with Field Measurements

The lake model results show that there velocity vectors depend on the tidal period. The confirmation of lake model was done with transport process. The concentration values of salinity at lake were obtained from previous field measurements (ESA, 2000). According to these measurements the salinity of lake system is approximately 3.0 mg/l and at river mouths the value decreases to 1.3 mg/l due to freshwater inflow to the lake system. The numerical results given above in Figure 5.8, 5.9, and 5.10 show similar concentration of salinities at river mouths and lake system as 1.5 mg/l and 3.0 mg/l. The previous field measurements stations at lake system are given in Figure 5.26 and the water quality values are given in Table 5.1 (Maktav and others, 1996).

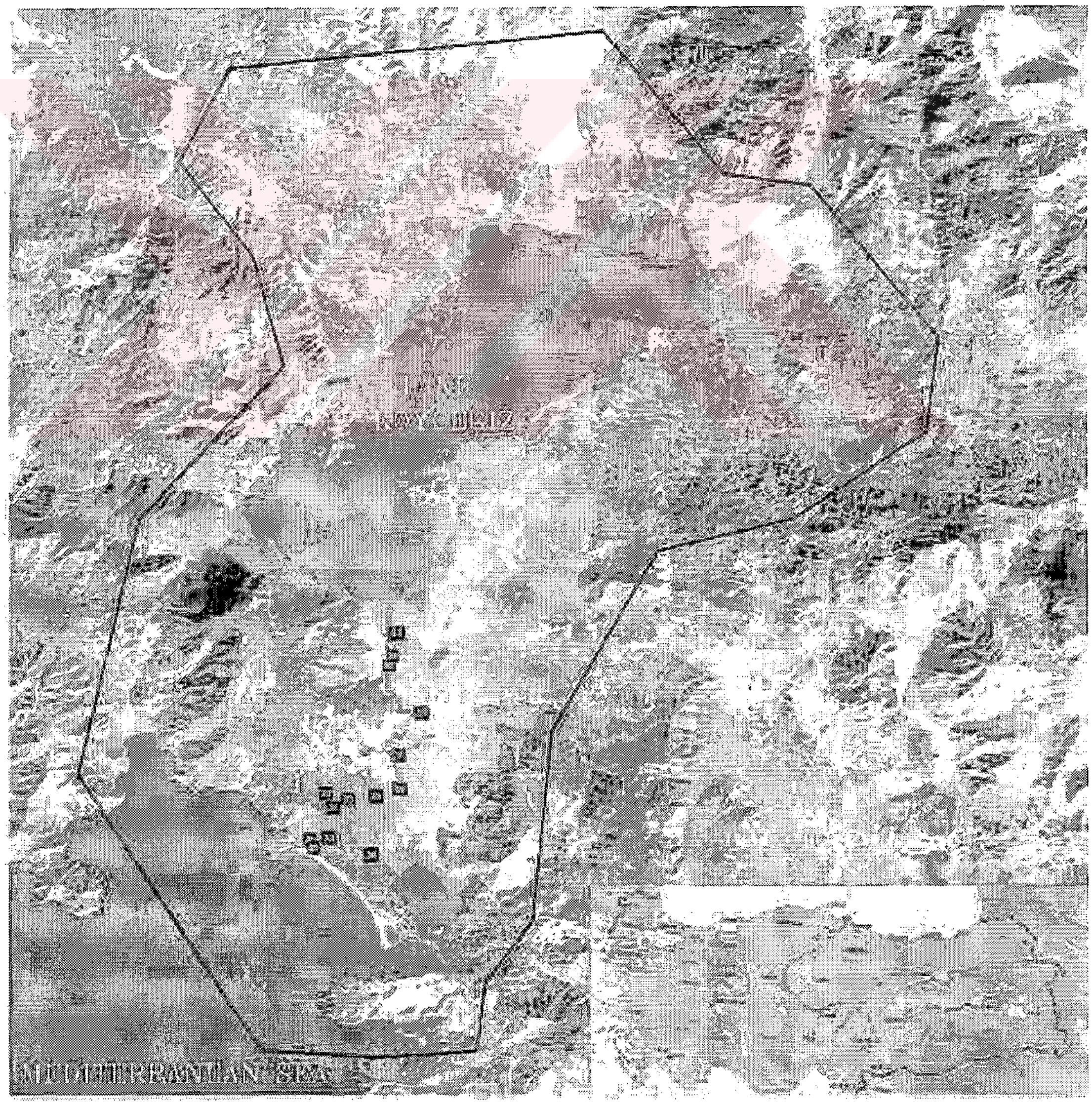

Figure 5.26 Field measurements stations at lake and channel (Maktav and others, 1996).

Table 5.1 Water quality measurements of lake at stations (Maktav and others, 1996).

| Station | Latitude | Longitude | Salinity (mg/lt) | Temp. (C°) | O (mg/lt) | Depth (m) | Time | Explanations |
|---|---|---|---|---|---|---|---|---|
| 1 | 3657.40 | 2841.21 | 2.9 | 17.4 | 9.1 | 4.2 | 13.35 | |
| 2 | 57.35 | 40.6 | 2.9 | 17.2 | 8.7 | 5.0 | 13.5 | |
| 3 | 57.23 | 39.94 | 2.9 | .17,0 | 8.6 | 5.4 | 14.05 | Reeds |
| 4 | 56.48 | 39.6 | 2.9 | 16.9 | 8.5 | 4.9 | 14.23 | |
| 5 | 55.95 | 39.25 | 3.0 | 17.2 | 8.8 | 1.9 | 14.31 | Reeds |
| 6 | 55.62 | 38.81 | 2.9 | 16.6 | 8.6 | 5.3 | 14.4 | Turbid Bay |
| 7 | 55.27 | 37.77 | 3.0 | 17.2 | 8.5 | 3.9 | 14.56 | In the river mouth |
| 8 | 55.32 | 37.69 | 1.1 | 13.9 | 9.5 | 2.0 | 15.00 | In the river mouth |
| 9 | 54.26 | 37.61 | 3.0 | 17.2 | 9.5 | 3.3 | 15.15 | |
| 10 | 53.80 | 37.11 | 3.1 | 17.5 | 9.5 | - | 15.25 | No currents |
| 11 | 53.04 | 36.56 | 3.1 | 17.2 | 9.6 | 31.6 | 15.45 | |
| 12 | 53.90 | 38.50 | 3.0 | 16.9 | 9.9 | 2.0 | 16.12 | |
| 13 | 57.30 | 41.76 | 2.9 | 16.5 | 10.0 | 11.1 | 16.21 | |
| 14 | 56.89 | 41.69 | 2.9 | 16.6 | 9.8 | 20.0 | 9.58 | |
| 15 | 56.32 | 41.18 | 3.0 | 16.9 | 9.1 | 25.0 | 10.07 | |
| 16 | 55.41 | 40.31 | 3.0 | 16.8 | 9.0 | 22.9 | 10.26 | |
| 17 | 54.25 | 39.07 | 3.0 | 16.4 | 10.4 | 5.2 | 10.46 | |
| 18 | 53.78 | 38.54 | 3.0 | 16.4 | 10.4 | 2.5 | 10.46 | Reeds |
| 19 | 53.00 | 38.25 | 3.0 | 16.5 | 9.3 | 5.3 | 11.14 | |
| 20 | 52.23 | 38.12 | 2.9 | 15.7 | 9.4 | 4.3 | 11.25 | Backside of the channel |

In channel model the currents due to tidal wave elevation are given at previous field studies (Kabdaşlı and others, 2000). According to these measurements the tidal elevation at sea open section was defined as a greater value in order to model a tidal wave effect with higher amplitude. The model shows the velocity currents successfully and the changes of vector directions in channel with the sea-lake interaction (Figure 5.20a, 5.20b, 5.21a, and 5.21b).

The oxygen transport model at channel shows the similar values with the previous studies at lake, which are given in Appendix D. The only differences are seen at upper parts of channel due to vegetation of channel.

Both of the models are solved the flow and transport process in 8$^{th}$ hour period. Although the iteration period isn't long like the other similar models, the results are acceptable with the field measurements. In 24-hour iteration time, the flow and transport model should be changed in a very little percentage.

The result of comparing the numerical model and field measurements for both models shows similar results at lake and channel.

# 6. CONCLUSIONS

In this study hydrodynamic properties of Köyceğiz-Dalyan Lagoon System investigated with numerical codes. The lagoon system was modeled in two parts with two different numerical codes. Water elevation, velocity vectors, salinity, and oxygen values were simulated by these codes. The simulated data were compared to available field measurements. It was seen that the numerical model results were similar to field measurements.

Lake model was calibrated with 1.) Tidal wave with 0.15 m amplitude and 8 h period, 2.) Wind force acting on lake with 3 m/s speed and $1.1*10^{-3}$ wind coefficient, 3.) River inflows of Namnam River, Kargıcak River, Yuvarlak River with flow quantities 20, 14, 8 $m^3/s$, respectively. The concentration values of salinity at river waters were defined as zero. The concentration of salinity at channel inlet was defined as 2.9 mg/l (Maktav and others, 1996).

The flow model results show that the main force acting on lake is the periodic tidal wave. Different wind speed, and tide parameters calibration show that wind force acting on lake is the second important effect on current directions. The wind forces acting from northeast cause higher currents at coastal region of lake. The tidal variation acting from channel inlet causes currents between lake and channel. But it is seen that the currents are not regular and at some places vortexes are seen clearly. Additionally vortexes at river mouths show that the rivers inflows change the currents in a small area. In general flow pattern of lake shows two main circular motions at north trough and at south trough. This is a typical flow circulation seen at lakes. It is seen that velocities at coastal region of lake are higher than the deep parts of lake.

The transport model results show that the salinity transport highly depends on tidal force. As a result of increase in channel inlet during the tidal wave period, the concentration at like increases from 2.9 to 3.0 mg/l at lake. Only at river mouths there is a transition region of concentration. The concentration of salinity at river mouth and lake is very similar to the previous field measurements (Maktav and others, 1996). The transition region is also affected with the high velocity vectors acting parallel to coastline.

Channel model was calibrated with 1.) Tidal wave with 0.40 m amplitude and 8 h period, 2.) Steady flow from lake to sea with a 0.20 m of flow table difference. Concentration of oxygen was defined as 10.68 mg/l at upstream (lake open section) and 10.15 mg/l at downstream (sea open section). These values were obtained from field studies (ESA, 2000).

The flow model results of channel model shows the sea and lake interaction successfully. At the beginning of the tidal wave period, the currents in channel are in direction from lake to sea. At the end of the 1st hour, water level at downstream (sea open section) rises up to the same level with the upstream (lake open section). This cause reduces in currents. After the 2nd hour water level reaches the highest level as 3.2 m at downstream of channel and as a result of it currents are seen direction from sea to lake.

Both of the models reflect the hydrodynamic properties of lake and channel with defined forces. Different scenarios with different parameters and conditions would improve the purpose of this study.

Generally numerical models results show that Köyceğiz-Dalyan Lagoon System depends on inflow and outflow balance. The connection to the sea has very dominant role on controlling the minimum and maximum water levels of system.

It can be concluded that the numerical methods with field measurements can provide valuable information about the hydrodynamic properties of complex systems.

## REFERENCES


**Bradford, S.F. and Katopodes, N.D.,** 2000. The Anti-Dissipative, Non-Monotone Behaviour of Petrov-Galerkin Upwinding, *International Journal For Numerical Methods in Fluids*, **33**, 583-608.

**Dalziel, S.B., Holford, J.M. and Hunt, G.R.**, 1999. Enviromental Fluid Dynamics, Department of Applied Mathematics Theoretical Physics, *The University of Cambridge*, Cambridge, England.

**Durst, F.**, 2000. Fluid Mechanics Developments and Advancements in the 20th Century, Institude of Fluid Mechanics, *University of Erlangen-Nuremberg*, Erlangen.

**El Kadi AI, Ling G**. 1993. The Courant and Peclet number criteria for the numerical solution of the Richard's equation, *Water Resources Research*, 29. 3485–3494.

**ESA**, 2000. International Mediterranean Project, Project code: MM.XXSF, Yıldız Technical University Press Publication, İstanbul, Turkey.

**Gresho, P.M., Sani, R.L.,** 2000. Incompressible Flow and The Finite Element Method, Volume I-II, John Wiley & Sons Ltd.

**Güney, M.Ş.**, 1995. Akışkanlar Mekaniği, İzmir Dokuz Eylül University Engineering Faculty Publications No: 204, İzmir.

**Hydrosoft,** 1999. Aquadyn Software Manual Book, Hydrosoft Energie, Canada.

**İTÜ,** 2000. Türkiye'nin Akdeniz Kıyılarında Köyceğiz Dalyan Koruma Alanında Yersel Veriler ve Uydu Verileri Entegrasyonu İle Bir Kıyı Bilgi Sistemi Oluşturma Pilot Projesi, Proje No 779, İstanbul Teknik Üniversitesi Araştırma Fonu, İstanbul.

**Kabdaşlı, S., Oğuz, B., Ünal, E., Aydıngakko, A., Kırdağlı, M., and Mercan D.E.,** 2000. Köyceğiz Gölü Su Seviyelerinin İzlenmesi Projesi, İstanbul Teknik Üniversitesi Hidrolik Anabilim Dalı, İstanbul.

**Maktav, D., Sunar, F., Kabdaşlı, S., and Musaoğlu, N.,** 1996. Use of Remote Sensing for Monitoring The Lagoon Köyceğiz And Its Enviroment in Turkey, *NATO/AGARD Meeting*,Toulouse, France.

**Olsen, N.R.B,** 1999. Computational Fluid Dynamics in Hydraulic and Sedimentation Engineering, The Norwegian University of Science and Technology, Department of Hydraulic and Enviromental Engineering, ISBN 82 7598-041-0.

**Olsen, N.R.B,** 2000. CFD Algorithms for Hydraulic Engineering, The Norwegian University of Science and Technology, Department of Hydraulic and Enviromental Engineering, ISBN 82 7598-044-5.

**Olsen, N.R.B,** 2001. Hydroinformatics Fluvial Hydraulics and Limnology, The Norwegian University of Science and Technology, Department of Hydraulic and Enviromental Engineering, ISBN 82 7598-046-1.

**Orkwis, P.D., Wolff, J.M.,** 2001. Numerical Methods in Transport Phenomenon, Computational Fluid Dynamics, WSU.

**Sander, J.**, 1998. Dynamical Equations and Turbulent Closures in Geophysics, *Continuum Mech. Termodyn.,* **10,** 1-28.

**Stewart, R.H.,** 1998. Introduction to Physical Oceanography, Department of Oceanography, Texas A& M University, Texas.

**Umgiesser, G. and Zampato, L.,**1998. *Modeling The Channel Network of the City of Venice*, ISDGM-CNR, Italy.

**U.S. Army Corps of Engineers**, 1991. Tidal Hydraulics Engineer Manual No. 1110-2-1607, Department of Army U.S. Army Corps and Engineers, Washington.

**Vatnaskil,** 1998. Aquasea Manual Book, Vatnaskil Consulting Engineers, Island.

**Wright, N.G.,** 2001. Conveyance Implifications for 2-D and 3-D Modelling, HR Wallingford and the Enviromental Agency.

**APPENDIX A:** The cross sectional water level elevation figures of lake system.

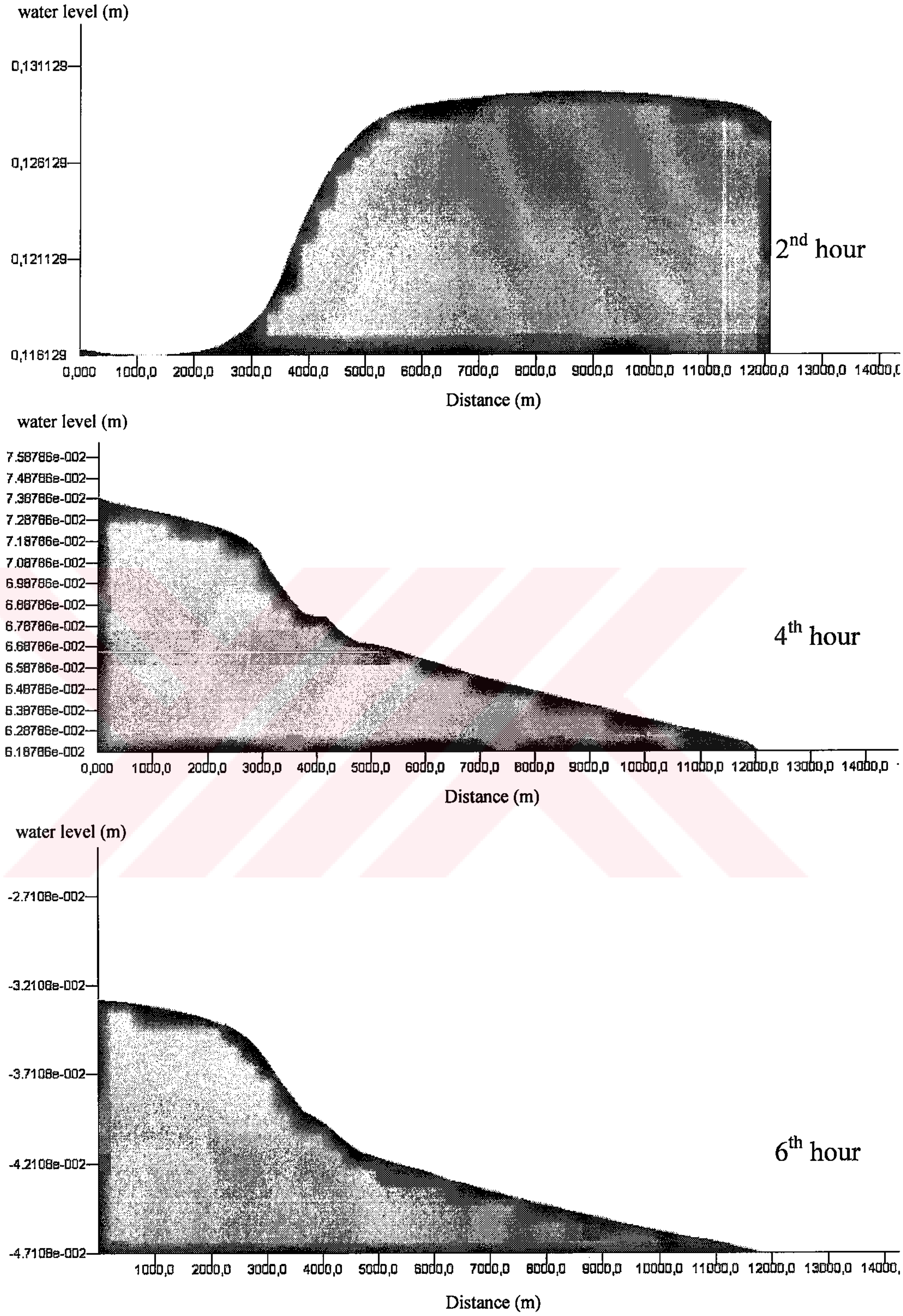


Figure A.1 The cross sectional figures of lake system through southeast northeast direction at 2nd, 4th, and 6th hours.

**APPENDIX B:** The currents and vortexes at Namnam River and Dalyan Channel


(a) Namnam River mouth

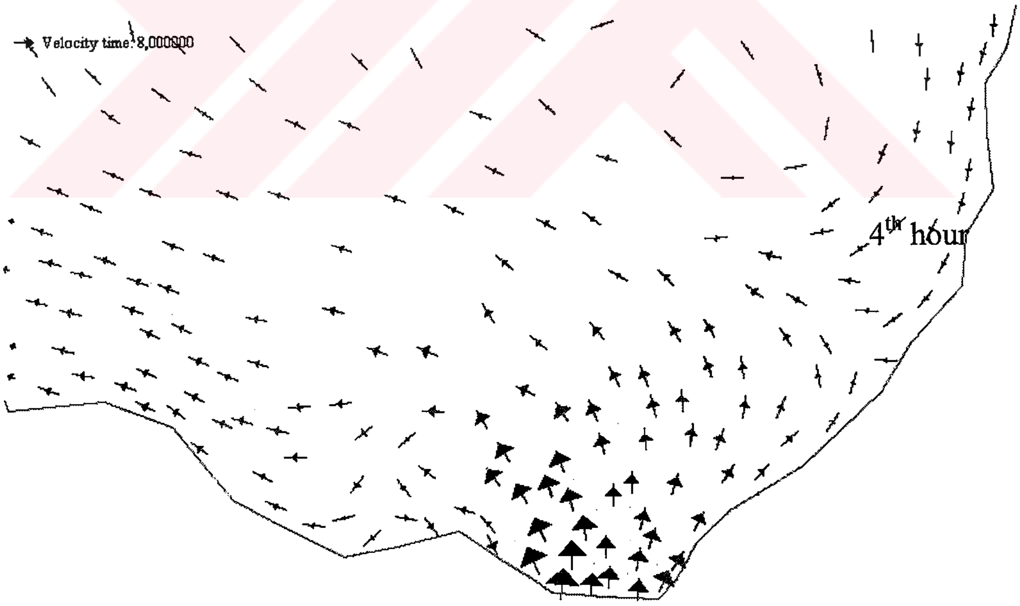


(b) Dalyan Channel Inlet

Figure B.1 The currents and vortexes at Namnam River mouth (a) and Dalyan Channel Inlet (b).

**APPENDIX C:** The velocity variation in y direction with time at specified points.

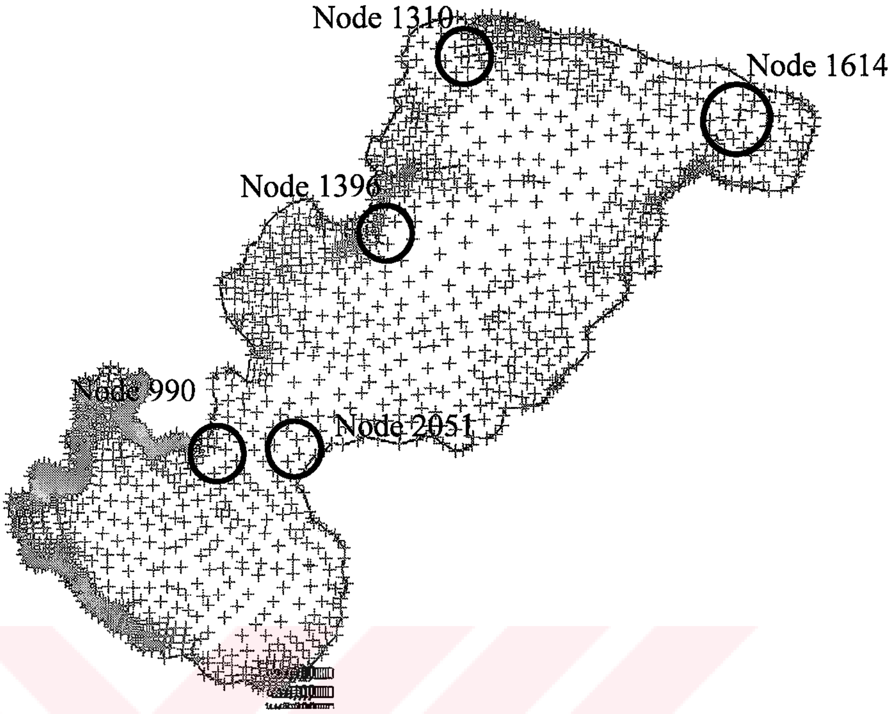


Figure C.1: The specified nodes locations at lake surface.

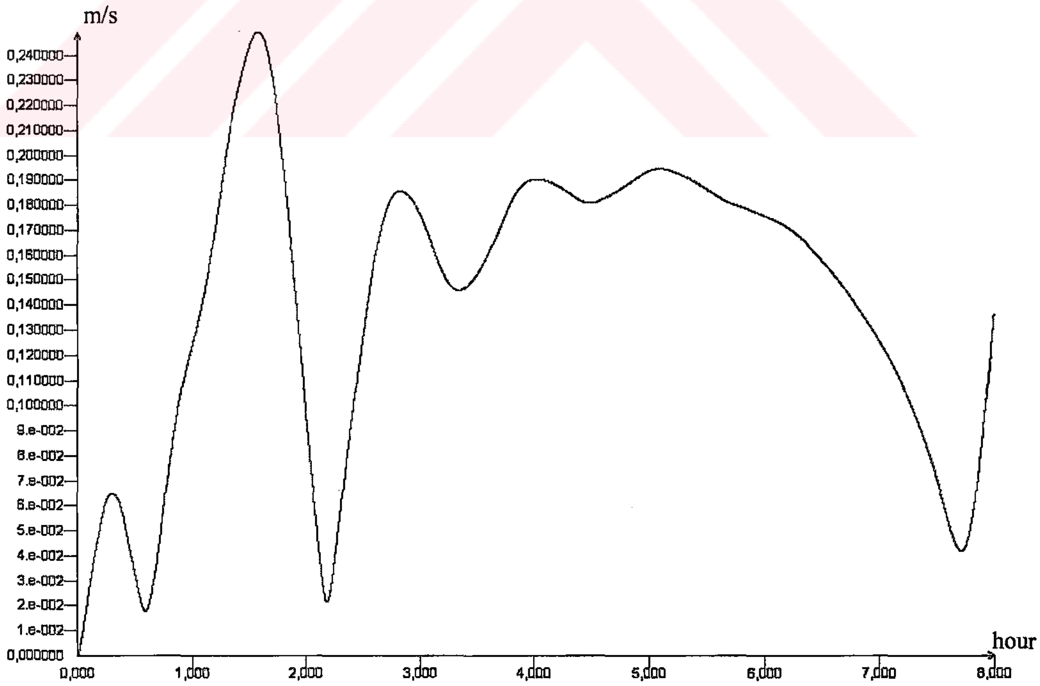


Figure C.2 Velocity values at node 2051 in y direction for $8^{th}$ hour.

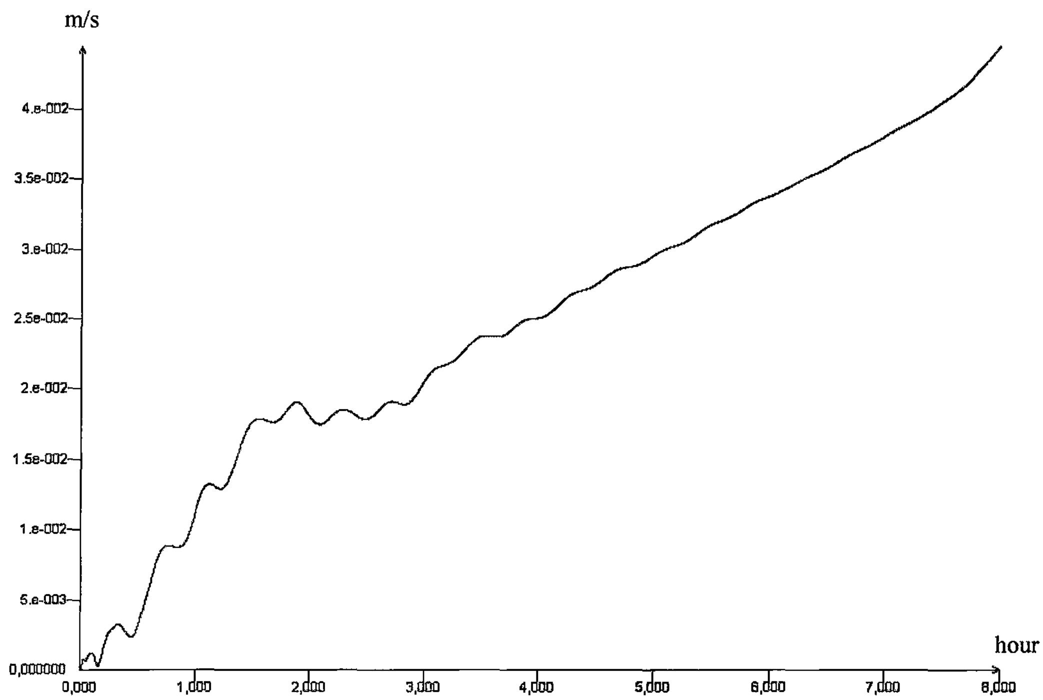


Figure C.3 Velocity values at node 1614 in y direction for 8th hour.

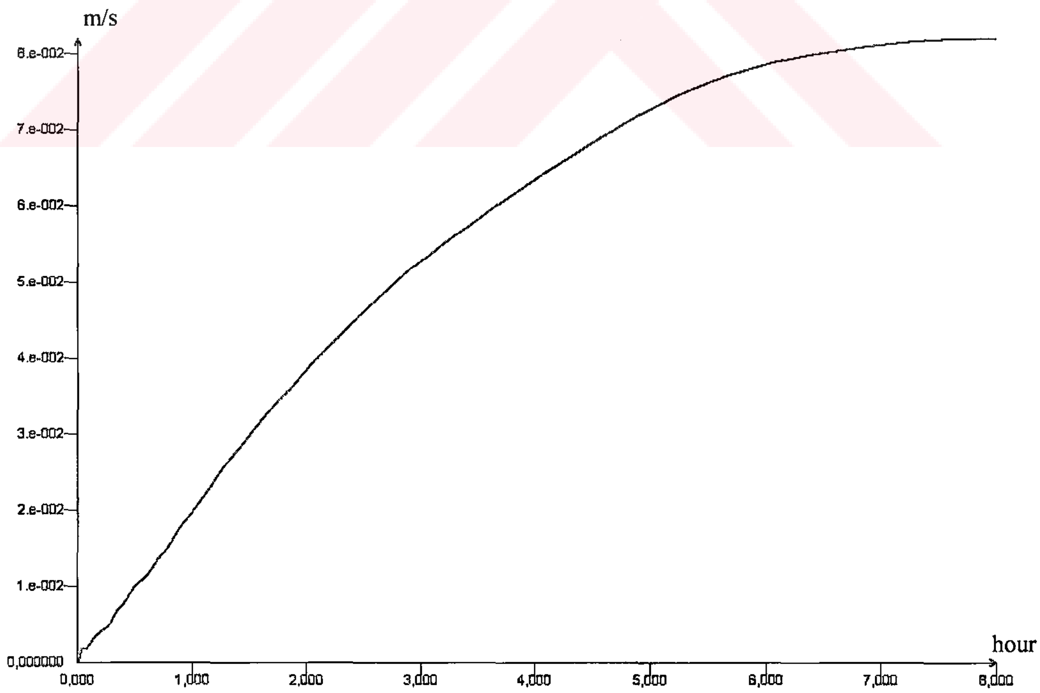


Figure C.4 Velocity values at node 1310 in y direction for 8th hour.

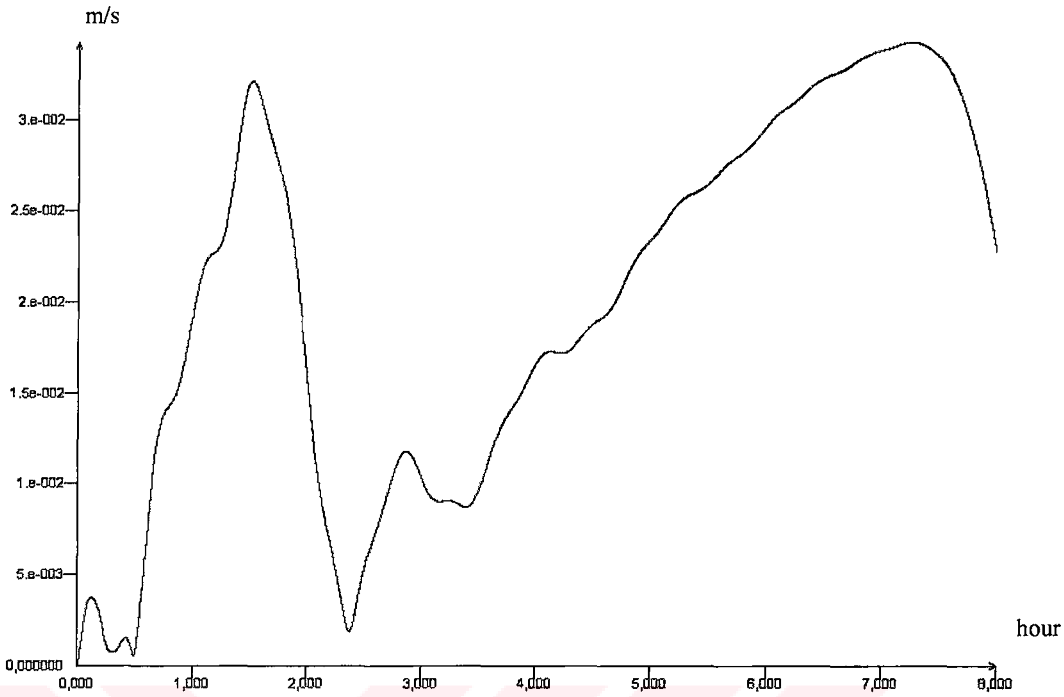


Figure C.5 Velocity values at node 1396 in y direction for 8th hour.

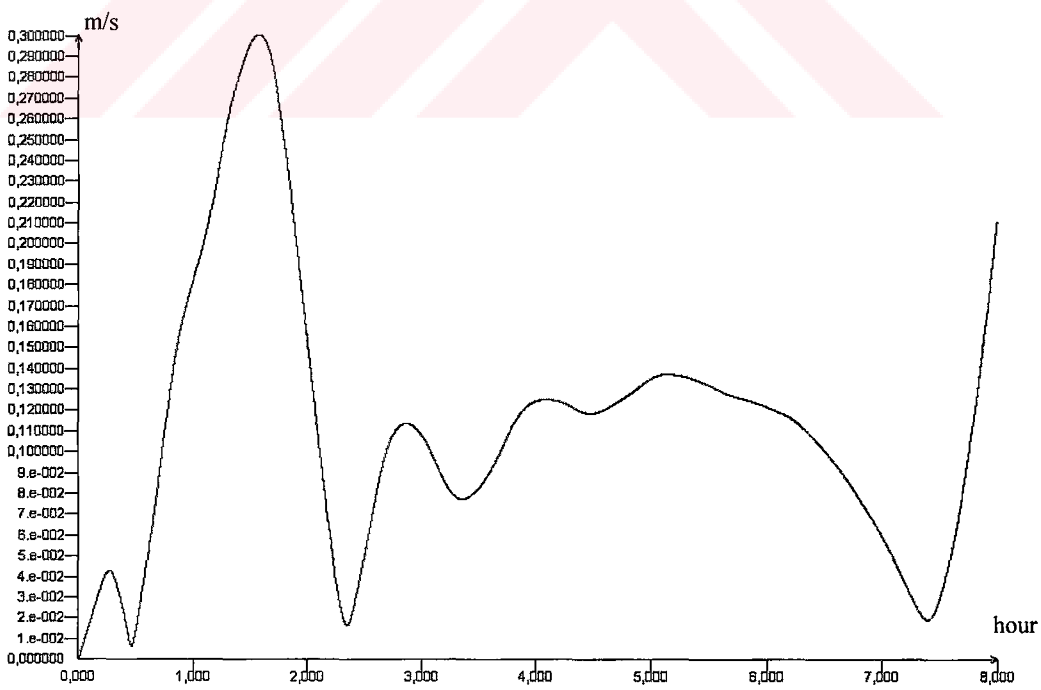


Figure C.6 Velocity values at node 990 in y direction for 8th hour.

**APPENDIX D:** Water quality measurements in 14-15 February 1997.

Table D.1 Water quality measurements in 14-15 February 97 (ESA, 2000).

| Station | Depth (m) | Latitude | Longitude | Date | Hour | Temp (C) | Ph (units) | SpCond | TDS | DO (%Sat) | DO (mg/l) | Redox (mV) | Turbidity NTU |
|---|---|---|---|---|---|---|---|---|---|---|---|---|---|
| 1 | 0 | 6490 | 4091 | 15.02.97 | 15:27 | 12.26 | 8.5 | 4475 | 2.86 | 95.4 | 10.04 | -106 | 24 |
| 2 | 0 | 6510 | 4091 | 15.02.97 | 16:30 | 12.49 | 8.48 | 4476 | 2.86 | 97.7 | 10.24 | -52 | 24.8 |
| 3 | 0 | 6480 | 4090 | 15.02.97 | 15:06 | 12.44 | 8.48 | 4384 | 2.81 | 94.4 | 9.9 | -96 | 22.7 |
| 4 | 0 | 6500 | 4090 | 15.02.97 | 18:08 | 12.3 | 8.49 | 4507 | 2.88 | 95.1 | 10.01 | -105 | 28.1 |
| 5 | 0 | 6520 | 4090 | 15.02.97 | 16:50 | 12.48 | 8.46 | 4427 | 2.83 | 90.7 | 9.51 | -95 | 24.7 |
| 6 | 0 | 6540 | 4090 | 15.02.97 | 17:19 | 12.82 | 8.27 | 4241 | 2.71 | 76.5 | 7.97 | -83 | 23.6 |
| 7 | 0 | 6490 | 4089 | 15.02.97 | 14:30 | 12.13 | 8.51 | 4546 | 2.91 | 94.3 | 9.96 | -109 | 23 |
| 8 | 0 | 6510 | 4089 | 15.02.97 | 17:43 | 12.37 | 8.48 | 4507 | 2.88 | 94.9 | 9.98 | -53 | 26.3 |
| 9 | 0 | 6460 | 4088 | 15.02.97 | 13:30 | 12.07 | 8.51 | 4407 | 2.82 | 94.1 | 9.96 | -112 | 23.2 |
| 10 | 0 | 6480 | 4088 | 15.02.97 | 14:00 | 12.15 | 8.49 | 4338 | 2.78 | 92.3 | 9.76 | -57 | 22.3 |
| 11 | 0 | 6500 | 4088 | 15.02.97 | 18:38 | 12.54 | 8.45 | 3776 | 2.42 | 90.1 | 9.46 | -108 | 25.3 |
| 12 | 0 | 6470 | 4087 | 15.02.97 | 13:09 | 11.71 | 8.53 | 4488 | 2.87 | 96.1 | 10.25 | -68 | 33.7 |
| 13 | 0 | 6490 | 4087 | 15.02.97 | 18:59 | 12.18 | 8.48 | 4316 | 2.76 | 91.3 | 9.64 | -108 | 25.4 |
| 15 | 0 | 6460 | 4086 | 15.02.97 | 12:02 | 12.18 | 8.54 | 4265 | 2.73 | 95.8 | 10.12 | -83 | 23.8 |
| 16 | 0 | 6480 | 4086 | 15.02.97 | 12:28 | 12.32 | 8.51 | 4424 | 2.83 | 99.4 | 10.45 | -64 | 2.7 |
| 18 | 0 | 6430 | 4085 | 15.02.97 | 10:10 | 11.57 | 8.59 | 4440 | 2.84 | 95 | 10.17 | -128 | 20.6 |
| 20 | 0 | 6450 | 4085 | 15.02.97 | 11:40 | 11.89 | 8.54 | 4079 | 2.61 | 93.7 | 9.97 | -115 | 21.5 |
| 21 | 0 | 6420 | 4084 | 15.02.97 | 9:06 | 11.25 | 8.6 | 4390 | 2.81 | 96.4 | 10.4 | 78 | 25.1 |
| 22 | 0 | 6430 | 4084 | 15.02.97 | 9:40 | 11.28 | 8.57 | 4240 | 2.71 | 93.2 | 10.04 | -126 | 27.3 |
| 23 | 0 | 6440 | 4084 | 15.02.97 | 10:49 | 11.1 | 8.6 | 4498 | 2.88 | 98.5 | 10.65 | -104 | 22.7 |
| 24 | 0 | 6450 | 4084 | 15.02.97 | 11:20 | 11.35 | 8.6 | 2317 | 1.48 | 96 | 10.4 | -127 | 21.7 |
| 26 | 0 | 6430 | 4083 | 14.02.97 | 16:30 | 11.35 | 8.57 | 4435 | 2.84 | 91.3 | 9.82 | -47 | 16 |
| 27 | 0 | 6440 | 4083 | 14.02.97 | 15:44 | 11.23 | 8.58 | 4524 | 2.9 | 93.5 | 10.08 | -88 | 21.3 |
| 28 | 0 | 6450 | 4083 | 14.02.97 | 14:33 | 11.2 | 8.59 | 4586 | 2.93 | 97.2 | 10.49 | 189 | 19.8 |
| 30 | 0 | 6440 | 4082 | 14.02.97 | 15:23 | 11.36 | 8.57 | 4466 | 2.86 | 94.8 | 10.2 | 56 | 29.9 |
| 31 | 0 | 6450 | 4082 | 14.02.97 | 15:06 | 11.24 | 8.58 | 4513 | 2.89 | 94.4 | 10.18 | 25 | 18 |
| 32 | 0 | 6460 | 4082 | 14.02.97 | 14:12 | 11.17 | 8.58 | 4547 | 2.91 | 94.5 | 10.21 | 190 | 3 |

**Davut KOCA**

Davut KOCA was born in Kağızman, Kars in 1978. Between 1989 and 1995 he had studied at İstanbul Kartal Burak Bora Anatolian High School. In 1996 he began to study civil engineering at İzmir Dokuz Eylül University and graduated from Engineering Faculty in 2000. In 2000 he began to study at Istanbul Technical University Civil Engineering Faculty Hydraulic Master Programme. He has got knowledge on foreign languages and softwares. By this study he improved his knowledge and experiences on hydraulic modelling.